Combined Model Reference Adaptive Control Design as a Load Control System on a Marine Diesel Engine

Ioannis Papadonikolakis

Diploma Thesis

School of Naval Architecture and Marine Engineering
National Technical University of Athens

Thesis Supervisor: Dr. G. Papalambrou, Lecturer
Committee Member: Professor N. Kyrtatos
Committee Member: Professor C. Frangopoulos

April 2014

Acknowledgements

This work has been carried out at the Laboratory of Marine Engineering (LME) at the School of Naval Architecture and Marine Engineering of the National Technical University of Athens under the supervision of Dr. George Papalambrou, Lecturer in Control Systems.

I would like to thank to Professor Nikolaos Kyrtatos for providing the opportunity to work with a full-scale marine propulsion facility of LME for the implementation of the final experimental evaluation control trials. I would also like to thank him for allowing to use the control systems room in LME facilities, where a big percentage of this work was performed using the laboratory device of heat exchanger.

I would like to show my greatest appreciation to my supervisor Dr. George Papalambrou for giving me the opportunity to work on this topic as well as for his unceasing guidance, helpful discussions and comments.

I would also like to thank Professor Christos Frangopoulos for being a member of my supervisors committee.

I am deeply grateful to the PhD student Sotirios Topaloglou for handling the whole experimental setup of the CAT marine diesel engine test bench and for his precious help during the conduction of the final experimental control trials.

I owe a very important debt to my sister Georgia Papadonikolaki, PhD student in the Department of Water Resources and Environmental Engineering of the School of Civil Engineering of the National Technical University of Athens, for her general guidance and comments. I also owe my deepest gratitude to my parents for their unceasing encouragement.

Abstract

The main purpose of this diploma Thesis was the design of an adaptive load control system on a marine diesel engine, in the powertrain facilities in LME. Control was applied on the outlet analog water valve of a 1.2 MW water brake dyno, coupled to a 448 kW marine diesel engine, during transient low load operation. Control of water brake's fill level results in control of applied torque (load) to the engine shaft. The type of adaptive controller chosen for the implementation of load controller was Combined Model Reference Adaptive Control (CMRAC), a combination of direct and indirect MRAC (Model Reference Adaptive Control). Gradient system identification algorithm was used for water brake system plant parameters estimations. Both plant parameters and controller parameters estimations were used for the construction of the control command to the analog valve.

Results from experimental evaluation of MRAC and CMRAC proved that both controllers were unstable in the presence of nonlinearities and measurement noise of a complex process like that of the water brake. System response to control command was oscillatory and control error did not converge to zero. System identification algorithm overestimated water brake plant parameters leading to overestimation of controller parameters. Finally, the use of dead-zone robustness technique, so as to eliminate response oscillations, and of proportional gain, so as to decrease control law values, led the final experimental test of a MRAC load control system to successful performance with good stability and generated control error converging to zero. Experimental evaluation of controllers and system identification algorithms' stability and convergence properties were also carried out using a laboratory device and computer simulation. All of the experimental and computer simulation trials were implemented using MATLAB/Simulink and dSPACE Rapid Prototyping Environment.

Contents

Nomenclature

α	Constant used for the creation of the adjustment gain γ_{sl}
β	Constant used for the creation of the adjustment gain γ_{sl}
Δ	Size of the dead-zone
ϵ	Identification error (used in recursive algorithms presentation)
γ	Adaptation gain
γ_{sl}	Adjustment gain used for sequential learning algorithm implementation
$\hat{\epsilon}$	Identification error
$\hat{\theta}$	Vector of estimated model parameters using recursive least squares algorithm
$\hat{\theta}_0$	Initial value of estimated parameters vector
$\hat{\theta}_{iv}$	Vector of estimated model parameters using instrumental variable algorithm
$\hat{b}_p$	Plant parameter estimation
$\hat{y}$	System's output signal estimation
Λ	Controller design constant
λ	Forgetting factor
ω_1	Control sensitivity vector
ω_2	Control sensitivity vector
$\overline{\omega}_1$	Filtered control sensitivity vector
$\overline{\omega}_2$	Filtered control sensitivity vector
$\overline{\theta}$	Unknown parameters vector

$\overline{\overline{\varpi}}$	Filtered internal signals vector
$\overline{e}$	Noise vector
$\overline{u}_c$	Filtered control law signal
$\overline{x}$	Data vector
$\overline{y}_p$	Filtered response of the plant
ϕ_{θ_0}	Controller parameter error
ϕ_{θ_1}	Controller parameter error
ϕ_{θ_2}	Controller parameter error
ϕ_θ	Controller parameter error
ϕ_k	Controller parameter error
θ	Controller parameter
θ_0	Controller parameter
θ_1	Controller parameter
θ_2	Controller parameter
ϖ	Internal signals vector
ϑ	Controller parameters vector
A	Output signal polynomial
a_m	First order reference model parameter
a_p	First order plant parameter
a_{m1}	Second order reference model parameter
a_{m2}	Second order reference model parameter
a_{p1}	Second order plant parameter
a_{p2}	Second order plant parameter
B	Input signal polynomial
b_m	First order reference model parameter

b_p First order plant parameter

b_{m0} Second order reference model parameter

b_{p0} Second order plant parameter

C Noise polynomial

e System's random noise signal

e_c Control error

e_i Identification error

e_k Closed loop estimation error

e_{θ_0} Closed loop estimation error

e_{θ_1} Closed loop estimation error

e_{θ_2} Closed loop estimation error

e_θ Closed loop estimation error

h Controller design constant

I_2 Unitary diagonal matrix $2x2$

I_3 Unitary diagonal matrix $3x3$

I_{21} Unitary column matrix with two rows

I_{31} Unitary column matrix with three rows

I_{41} Unitary column matrix with four rows

J Sum of squares of identification errors

k Controller parameter

k_p Second order plant parameter

k_m Second order reference model parameter

n Total number of estimated parameters

n_b Plant parameter error

N_c Normalization factor

N_i	Normalization factor
$n_{\alpha 1}$	Plant parameter error
n_α	Plant parameter error
n_β	Plant parameter error
n_a	Plant parameter error
n_{kp}	Plant parameter error
na	Output signal polynomial's order
nb	Input signal polynomial's order
P	Covariance matrix
P_0	Initial value of covariance matrix P
Q	Polynomial used to generate the instrumental variable
R	Polynomial used to generate the instrumental variable
r	Reference input signal
u	System's input signal
u_c	Control law signal
V	Instrumental matrix
v	Instrumental variables vector
X	Data matrix
y	System's output signal
y_i	Estimated plant's response
y_m	Response of the reference model
y_p	Plant's response signal
z	Instrumental variable
Z_{41}	Zero column matrix with four rows
$\overline{x}_0$	Initial value of data vector

v_0 Initial value of instrumental variable vector

Z_{21} Zero column matrix with two rows

Chapter 1

Introduction

1.1 Problem Description

The main purpose of this diploma Thesis is the design of a Combined Model Reference Adaptive Controller (CMRAC), as a load control system of a marine diesel engine in the powertrain facilities in LME. The CMRAC is applied on the outlet analog water-valve of a Froude-type water brake, a device used for testing of engine under rapid speed and torque transients. Control command is supplied to the outlet analog water valve, through an electronic-pneumatic transducer, which converts the electric signal to proportional air quantity as supply to the valve. The control problem is to achieve the application of requested torque (loading) to the powertrain. The desired engine's torque is adjusted by the tuning of water flow through water brake, using a closed-loop control system with torque reference input. Water brake controller has to operate as a servo for tracking torque changes. This simulates a propeller along a propeller curve, with the torque being proportional to the square of speed.

Combined Model Reference Adaptive Controller (CMRAC) is a combination of direct Model Reference Adaptive Controller (direct MRAC) and indirect Model Reference Adaptive Controller (indirect MRAC). The innovative characteristic of CMRAC algorithm is that control law creation is dependent both on control parameter estimations, as in direct MRAC, and on plant parameter estimations, as in indirect MRAC. Coupling between direct and indirect schemes is done by the creation and use of the so-called closed loop estimation errors, which are additionally used for the creation of the control law. It is considered that if both direct and indirect MRAC are used together, the response of closed loop control system is improved in terms of speed, accuracy and robustness.

The indirect part of the CMRAC designed can be implemented by any system identification algorithm appropriate for the identification of the system plant to be con-

trolled. This is one of the biggest advantages of CMRAC. Three different identification algorithms were used for the purposes of this diploma Thesis, least squares algorithm, instrumental variables algorithm and sequential learning algorithm. So, three different versions of CMRAC were designed

- CMRAC using recursive least squares identification algorithm (CMRAC-RLS)
- CMRAC using recursive instrumental variables algorithm (CMRAC-RIV)
- CMRAC using sequential learning algorithm (CMRAC-SL)

Performance of system identification and control algorithms designed was evaluated using a heat exchanger experimental device at LME. The main purpose of these experimental trials was to control the air temperature inside a plastic tube close to the reference value. Many experiments were performed so as to analyze the advantages and disadvantages of the controllers designed, as heat exchanger device is a good simulator of a real process with features like nonlinearities, external disturbances, measurement noise, etc. In addition, experience related with data acquisition and tuning of control algorithms was gained.

System plant output signal and reference input signal, which is either equal to the reference signal of the closed-loop control system or to an external reference signal, in open loop, are the required by the system identification algorithm data to estimate system plant parameters. Plant parameters estimations and the difference between the system's real output signal and system's estimated output signal (identification error) are the identification algorithm "products" required for the implementation of CMRAC.

Heating and cooling the airstream, processes taking place during the operation of heat exchanger, can be mathematically modelled by a first order differential equation with acceptable accuracy. Therefore, heat exchanger CMRAC algorithm was setup for a first order plant. Air heater provided a safe environment prior applying control and identification algorithms on a 450 kW engine powertrain. Water brake plant was mathematically modelled by a second order differential equation giving adequate accuracy for controller design. In turn, water brake CMRAC algorithm was setup for a second order plant. With this information and trying to keep the CMRAC algorithm simple enough, only system plant and reference model of unity relative degree were used. As a result, both system identification and control algorithms were designed in order to identify and control a system plant of unity relative degree, respectively. Obviously, better performance can be achieved using non-linear model based controllers as the actual plant may be infinite dimensional, nonlinear and its measured input and output

may be corrupted by noise and external disturbances. The aim of this Thesis, though, is to detect the capabilities and limitations of CMRAC in order to define its range of applicability and orient a further development for applications in powertrains.

Adaptation gain is one of the most important design parameters for adaptive controllers performance. It is the design parameter most difficult to tune and even a very small change in its value may turn a control system from stable to unstable.

Input signal of a system identification algorithm, used for the estimation of system plant parameters, is the most important design parameter for its satisfactory performance. Frequency, amplitude and rate of change are the basic tuning characteristics of the input signal which must be adjusted so as not to excite system dynamics of higher order and keep the latter close to linear operating ranges. Moreover, input signals used by identification algorithms must be persistently exciting, a property essential for the robustness of the estimator and for the convergence of plant parameters to their nominal values.

As most of the control systems designed for real processes applications, a discrete time version of CMRAC was designed for the purposes of this diploma Thesis as it is more suitable for implementation in practice than are the corresponding continuous time algorithms. In discrete time versions of CMRAC, plant parameters estimations and controller parameters estimations are continuously adjusted through difference equations. This avoids algebraic problems arising from the inversion of matrices containing parameter estimations.

Robustness of an adaptive controller is a requirement for the satisfactory performance of an adaptive control system when applied on a real process. Persistent excitation, of the signals used by the control algorithm to estimate control parameters (reference input signal and system's output signal), is required for a robust CMRAC. When these signals are not persistently exciting and measurement noise is present, control parameters cannot converge and the control system can be led to sudden instability and failure. Dead-zone robustness technique is used so as to eliminate degradation of CMRAC performance whenever the signals used for producing control parameter estimations are losing their persistently exciting properties.

1.2 Literature Search

Information related with computer simulations and experimental performance of water brake under closed-loop control mode, as part of an internal combustion engine test bench, is referred to [6], [11], [14], [9] and [10].

Information required for the design of all the system identification algorithms used

was found in [16] and [12]. Important information relevant to tuning and troubleshooting of system identification algorithms was also found in [16].

A Combined Model Reference Adaptive Control scheme was firstly developed by M. Duarte and K. Narendra and is presented in [3]. Basic mathematical equations used for the design of CMRAC presented in this diploma Thesis were drawn from [3]. Further development and applications of CMRAC are presented in [2], [4] and [5].

Basic features of adaptive control theory and its stability were found in [13], [12], [7] and [1]. Application of a simple feedforward adaptive controller for temperature control of a heat exchanger is presented in [17].

1.3 Water Brake Facility at LME

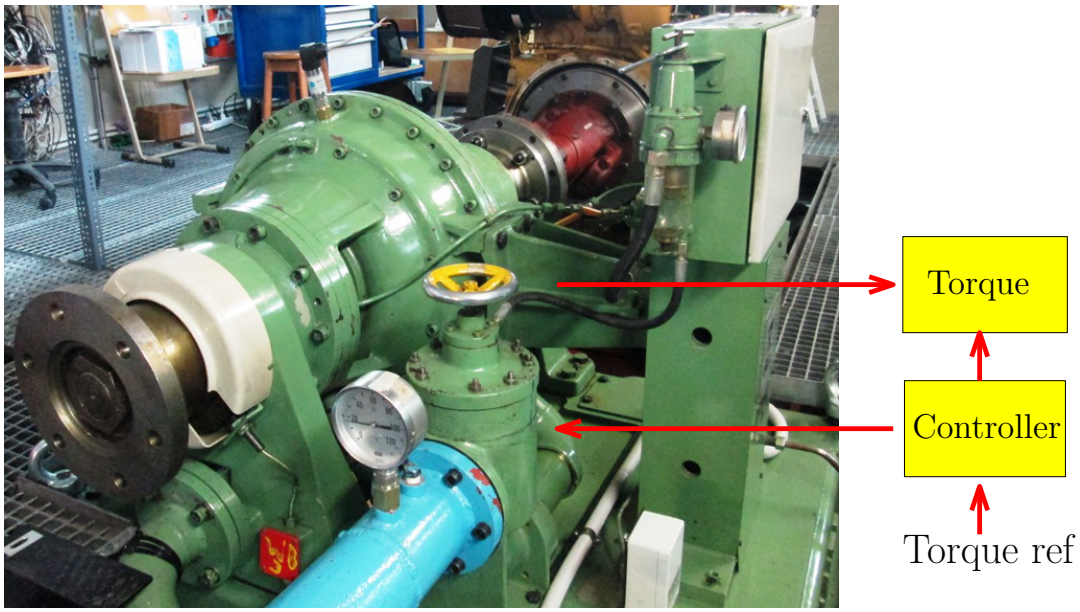

Figure 1.1: Water Brake at LME

Hydraulic dynamometers [6], [11], [14], [9], [10] have been for a long time the preferred device for testing of engines under rapid speed and torque transients, particularly in the area of high power internal combustion engine testing, due to their high torque absorption capacity per unit rotational inertia. The typical setup of an internal combustion engine test bench equipped with a water brake consists of an IC engine as the device under test and the brake simulating the load. The engine speed n_E, the dynamometer speed n_D and the dynamometer torque T_D can be measured. The desired engine speed and torque set points constitute the inputs of the test bed.

The water brake at LME (Figure 1.1), type 9n 38F, is manufactured by AVL Zoellner GmbH and has a load capacity of 1200 kW, with maximum speed 4000 rpm. It is coupled to a CATERPILLAR 3176B marine diesel engine, with power 448 kW at 2300 rpm. A pump supplies water to the water brake whose fill level and consequently load is controlled by a water outlet valve, operated under a closed loop control electro-hydraulic servo system. Applied torque by the water brake is measured by a load cell installed on the arm of the dynamometer. The load cell signal is transmitted to a load cell amplifier, with a 0-10 V signal range for 0 - 5000 Nm. Control command is supplied to the outlet analog water valve, through a electronic/pneumatic transducer, which converts the electric signal to proportional air quantity as supply to the valve. A simplified diagram of water brake's controller setup is shown in Figure 1.2.

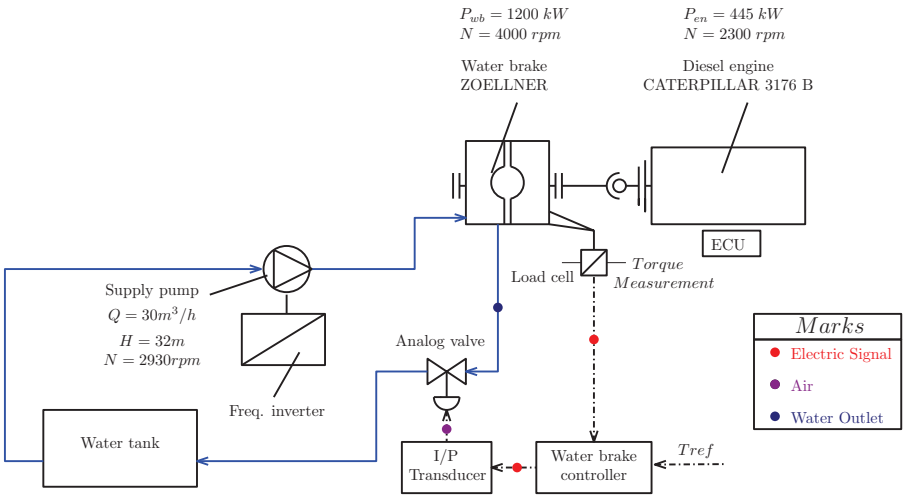

Figure 1.2: The complete control setup at the powertrain Facility in LME

The water brake can be divided into two essential parts, as presented in [14] the rotor driven by the engine to be tested, consisting of the turbine wheel and shaft, and the stator unit composed of the housing and the supply. In contrast to torque converters and clutches (they are based on the same working principle), a water brake has only one rotating part, resulting in 100% slip between the two units and thus a large thermal impact on the working fluid.

The hydraulic dynamometer working compartment consists of special semi-circular shaped vanes cast into stainless steel rotor and stators. Water flowing in a toroidal vortex pattern around these vanes creates a torque reaction through the dynamometer casing which is measured by a precision load cell. The power absorbed by the dynamometer is carried away by the water in the form of heat.

Cross sections of water brake and water output valve are presented in Figure 1.3

and in Figure 1.4 respectively.

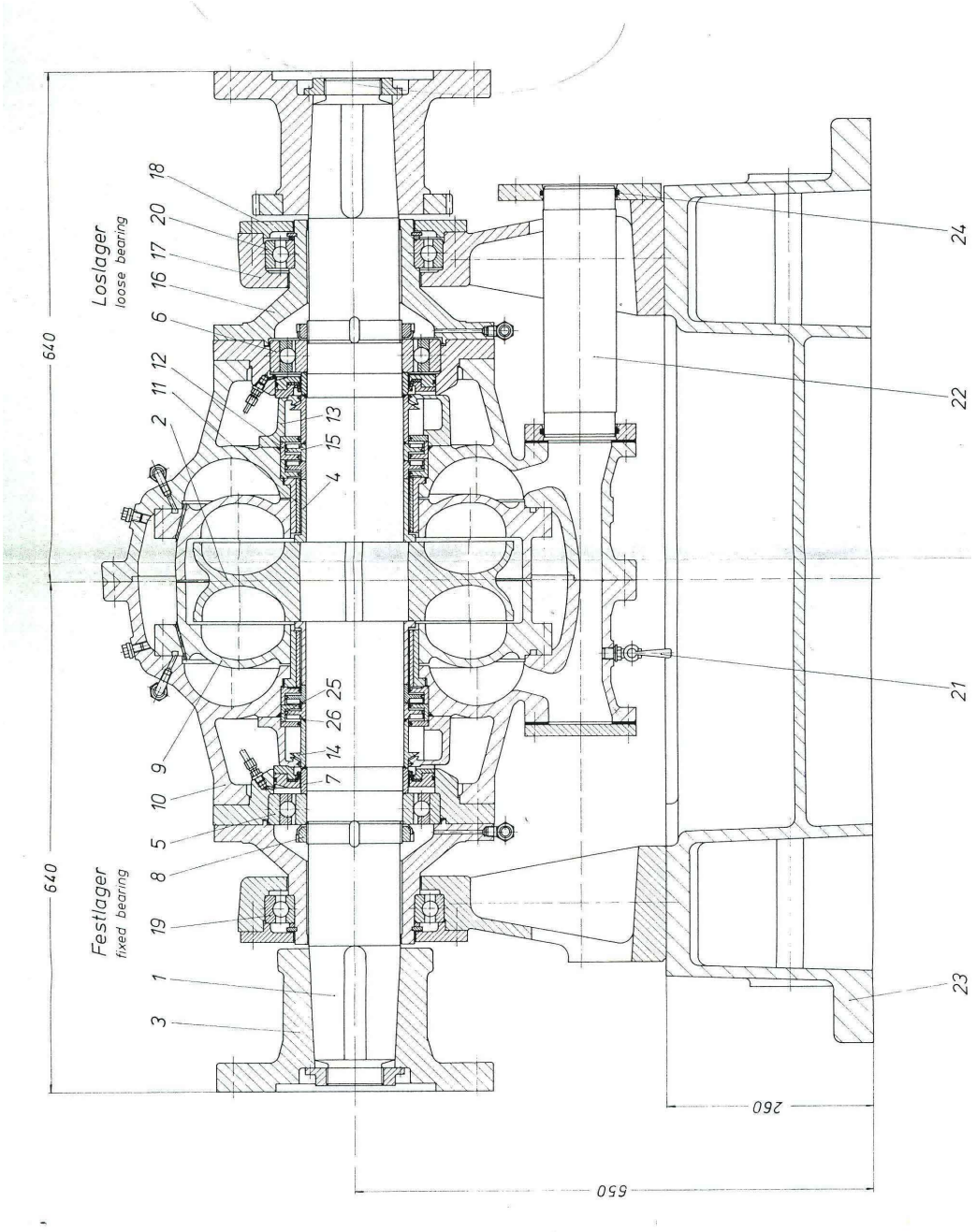

Figure 1.3: Cross section of water brake

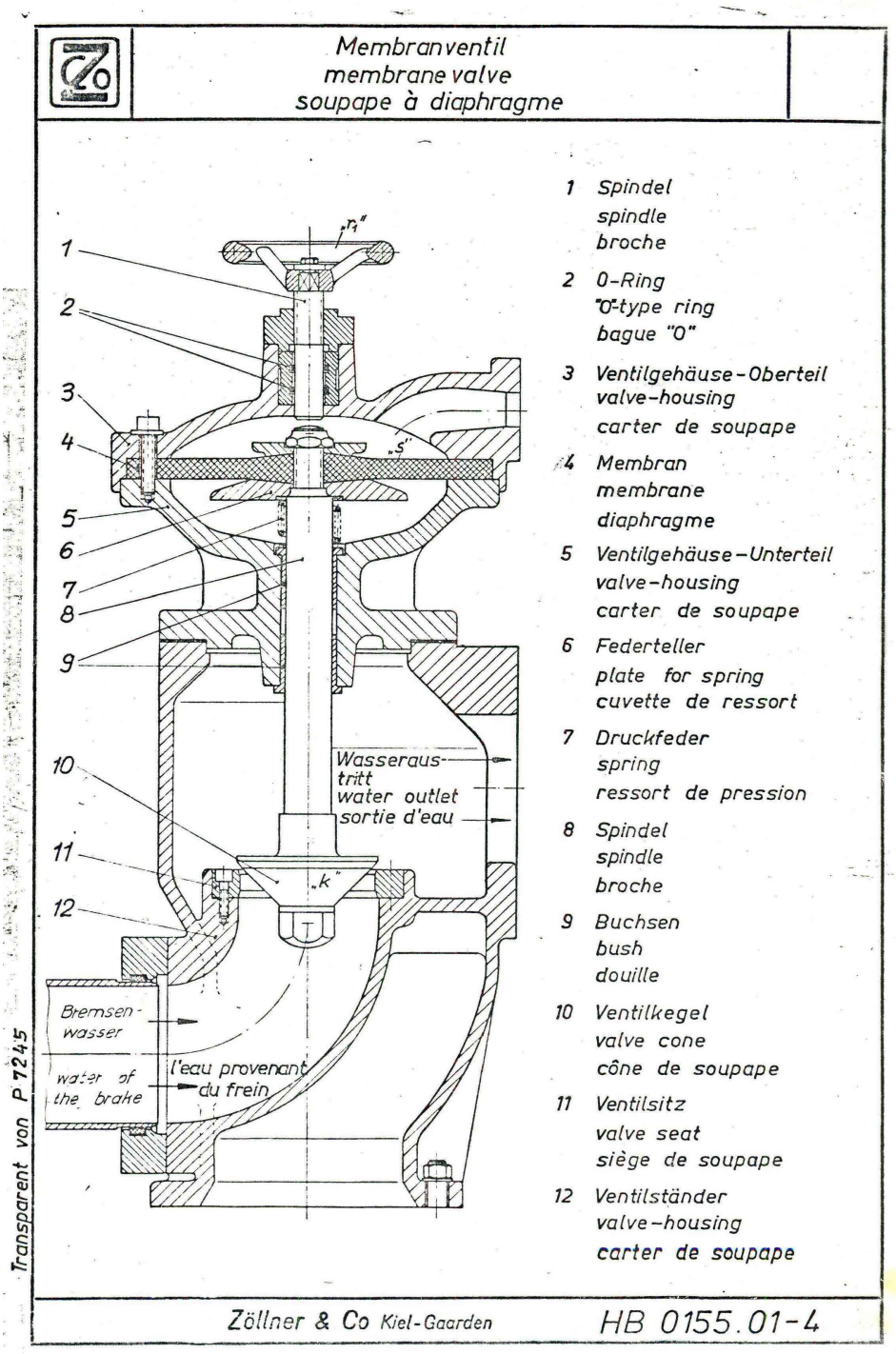

Figure 1.4: Cross section of water output valve

1.4 Heat Exchanger Experimental Device

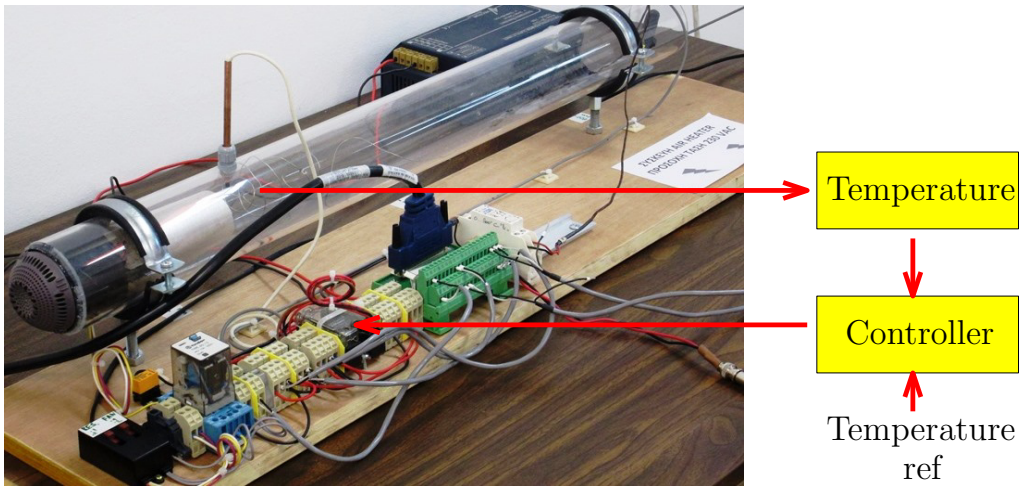

Figure 1.5: Heat Exchanger Experimental Device at LME

The heat exchanger experimental device at LME is an airstream heating system that consists of

- A blower which operates at a constant speed and circulates an airstream along a plastic tube.
- A heating electrical resistance, with power 2000 W.
- An actuator consisting of power electronics which heats the airstream by applying voltage across the resistance.
- Two thermocouple sensors, placed close to and far from the heating resistance.
- A third thermocouple placed at an adjustable distance from the resistance, thus allowing to investigate time delays in temperature measurements.
- A data acquisition card model PCI-6221 from NATIONAL INSTRUMENTS, placed in the PCI bus of the control computer, used for the implementation of the control system experimental tests.

Data processing and digital control system implementation were performed using MATLAB/Simulink.

The heat exchanger experimental device was used both for system identification algorithms' performance evaluation and for performance trials implementation on the various controllers designed. The device was designed and implemented by Dr. G. Papalambrou at LME and is shown in Figure 1.5.

Chapter 2

Adaptive Control and System Identification Theory

In this chapter both adaptive control and system identification theory basics, used for the purposes of this Thesis, are being presented. Mathematical equations of control and identification algorithms are also provided. Furthermore, the main objectives of adaptive control are presented so as the choice of this type of control can be justified.

2.1 Adaptive Control

The word adapt means *to change (oneself) so that one's behaviour will conform to new or changed circumstances.* Adaptive control is a control technique designed to continually adjust the changing controller parameters in the presence of uncertain variations in plant parameters. It differs from an ordinary controller in that the controller parameters are variable and there is a mechanism for adjusting these parameters on-line based on signals in the system. Its basic objective is to find the feedback control law that changes the structure and the dynamics of the system so as to maintain stable performance despite the changes occurring at its functional characteristics during its operation.

The way the parameter estimator (adaptive law) is combined with the control law gives rise to two different approaches, direct and indirect adaptive control. The type of adaptive controller designed as a result of this Thesis is *Combined Model Reference Adaptive Control (CMRAC)* [3] which is a combination of *Direct Model Reference Adaptive Control (MRAC)* [13], one of the most popular approaches for designing adaptive controllers, and *Indirect Model Reference Adaptive Control* [12] .

2.1.1 Model Reference Adaptive Control

A Model Reference Adaptive Control system (Figure 2.1) is composed of four parts

- a *plant* which parameters are usually unknown
- a *reference model* for specifying the desired output of the control system
- a *controller* (Figure 2.2) which provides a *control law* containing adjustable parameters and
- an *adaptation mechanism* for the update of adjustable parameters

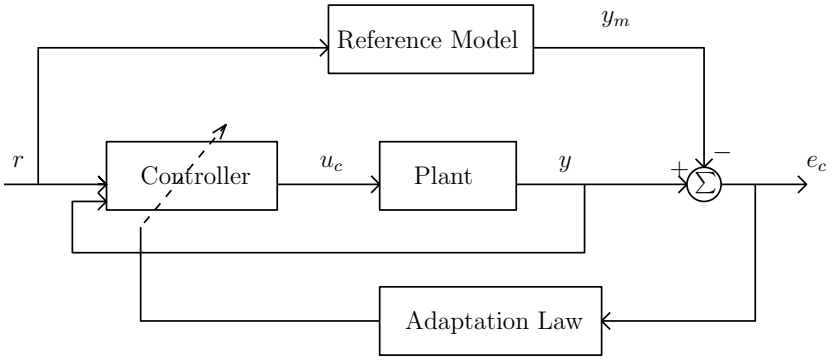

Figure 2.1: A Model Reference Adaptive Control system

The plant is assumed to have a known structure but its parameters are unknown. For linear plants, as those this Thesis deals with, this means that the number of poles and zeros are known but that the location of these poles and zeros are not.

A reference model is used to produce the ideal response of the adaptive control system to the input signal. It is necessary in order for the adaptation mechanism to adjust controller parameters in the proper direction. Choice of the reference model is part of the adaptive control system design.

The adaptation law created by the controller searches for parameters such that the response of the plant under adaptive control becomes the same as that of the reference model, i.e, the aim of the adaptation mechanism is to make the tracking error converge to zero.

The objective of MRAC is to create the feedback control law that changes the structure and dynamics of the plant so that its input/output properties are exactly the same as those of the reference model. Matching between plant and reference model responses guarantees that for any given reference input signal, the tracking error, which represents the deviation of plant's response from the desired one, converges to zero with time. There are two well-known versions [7], [12] of Model Reference Adaptive Control

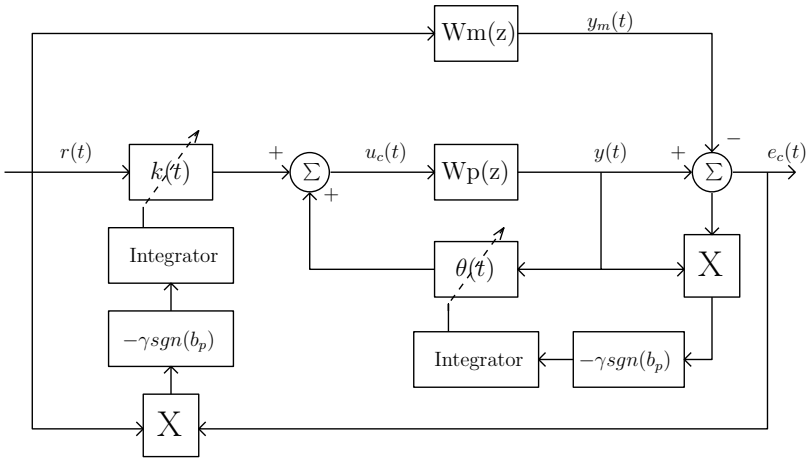

Figure 2.2: Structure of Model Reference Adaptive Controller

- Direct Model Reference Adaptive Control (direct MRAC)
- Indirect Model Reference Adaptive Control (indirect MRAC)

In *direct MRAC* the plant model is parameterized in terms of the unknown controller parameters that are estimated directly using all the information available from the plant at a certain moment without intermediate calculations involving plant parameter estimates. Control parameters are directly adjusted from on-line measurements to minimize the deviation between the plant output and the reference model output (control error). A direct MRAC system is shown in Figure 2.3.

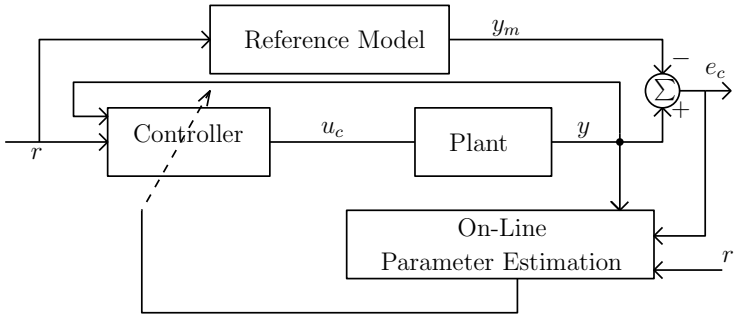

Figure 2.3: A Direct MRAC system

In *indirect MRAC* the parameters of the plant model are estimated dynamically on-line using measured plant input-output information from the system. At every instant of time, assuming that the estimates represent the true values of the plant parameters, the control parameters are computed by solving certain algebraic equations to achieve desired overall system characteristics. The form of the control law and algebraic equations is chosen to be the same as the respective ones that could be used

to meet the performance requirements for the plant if its parameters were known. An indirect MRAC system is shown in Figure 2.4.

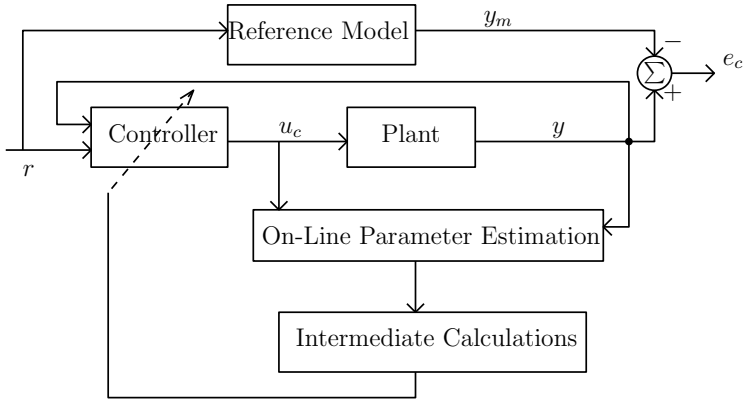

Figure 2.4: An Indirect MRAC system

The principle behind the design of direct and indirect model reference adaptive control is that the design of the controller treats the estimates of the controller parameters (direct MRAC) or of the plant parameters (indirect MRAC) as if they were the true parameters. This design approach is called *certainty equivalence* [7]. The idea behind the certainty equivalence approach is that as the parameter estimates converge to the true ones, the performance of the adaptive controller tends to that achieved by the respective one in the case of known parameters.

2.1.2 Combined Model Reference Adaptive Control

Combined MRAC is an approach to model reference adaptive control based on a combination of direct and indirect MRAC. The controller structure is identical to that used in the direct method, but the algorithm used to update the controller parameters depends both on the control error as in *direct MRAC* and on the plant's model parameter estimations as in *indirect MRAC*. The concept behind this approach is that faster and more accurate control may be possible when more information about the process under control is available. Furthermore, it is possible to improve the transient behaviour in terms of robustness if both techniques are used together. The combined MRAC method was first introduced by Duarte and Narendra [3], [2].

Mathematical equations for direct MRAC and Combined MRAC, for both first and second order systems, are presented below as these are the control techniques used for the implementation of this Thesis.

2.1.3 Mathematical Equations

Direct Model Reference Adaptive Control of First Order Systems

The discretized direct MRAC for a first order plant is implemented as below.
Input

- $y_p(t)$, the response of the plant
- $r(t)$, the reference signal
- $e_c(t) = y_p(t) - y_m(t)$, the control error.

Output

- $u_c(t)$, the control law signal.

Internal signals

- $y_m(t)$, the response of the reference model.
- $\theta(t)$, $k(t)$, the controller parameters.

Design Parameters

- $\gamma > 0$, the adaptation gain which regulates the rate of change for $\theta(t)$ and $k(t)$.

Plant model

$$y_p(t) = \frac{b_p}{z + a_p} u_c(t) \tag{2.1}$$

where a_p and b_p are the unknown plant parameters.
Reference model

$$y_m(t) = \frac{b_m}{z + a_m} r(t) \tag{2.2}$$

where a_m and b_m are known constants.
Control law

$$u_c(t) = \theta(t) y_p(t) + k(t) r(t) \tag{2.3}$$

where $\theta(t)$, $k(t)$ are adjustable controller parameters.
Adaptive laws for control parameters

$$\dot{\theta}(t) = -\gamma sgn(b_p) e_c(t) y_p(t) \tag{2.4}$$

$$\dot{k}(t) = -\gamma sgn(b_p) e_c(t) r(t) \tag{2.5}$$

The aim of direct MRAC is the determination of a bounded control law so that

$$\lim_{t \to \infty} e_c(t) = 0 \tag{2.6}$$

Hence, the adaptive control problem can be equivalently stated as the determination of adaptive laws (2.4) and (2.5) so that condition (2.6) is satisfied.

Direct Model Reference Adaptive Control of Second Order Systems

The discretized direct MRAC for a second order plant is implemented as below (Figure 2.5).

Input

- $y_p(t)$, the response of the plant
- $r(t)$, the reference signal
- $e_c(t) = y_p(t) - y_m(t)$, the control error.

Output

- $u_c(t)$, the control law signal.

Internal signals

- $y_m(t)$, the response of the reference model
- $k(t)$, $\theta_1(t)$, $\theta_2(t)$, $\theta_0(t)$, the controller parameters.
- $\dot{\omega}_1(t) = \Lambda\omega_1(t) + hu_c(t)$, the control sensitivity signal.
- $\dot{\omega}_2(t) = \Lambda\omega_2(t) + hy_p(t)$, the control sensitivity signal.

Design Parameters

- $\gamma > 0$, the adaptation gain which regulates the rate of change for $k(t)$, $\theta_1(t)$, $\theta_2(t)$ and $\theta_0(t)$.
- $\Lambda = -b_m$.
- $h = 1$.

Plant model

$$y_p(t) = \frac{k_p(z + b_{p0})}{z^2 + a_{p1}z + a_{p2}}u_c(t) \tag{2.7}$$

where a_{p1}, a_{p2}, b_{p0} and k_p are the unknown plant parameters.

Reference model

$$y_m(t) = \frac{k_m(z + b_{m0})}{z^2 + a_{m1}z + a_{m2}}r(t) \tag{2.8}$$

where a_{m1}, a_{m2}, b_{m0} and k_m are known constants.

Control law

$$u_c(t) = \vartheta^\top(t)\varpi(t) \tag{2.9}$$

where

$\vartheta(t) = [k(t)\ \ \theta_1(t)\ \ \theta_2(t)\ \ \theta_0(t)]^\top$, the controller parameters vector.

$\varpi(t) = [r(t)\ \ \omega_1(t)\ \ \omega_2(t)\ \ y_p(t)]^\top$, the internal signals vector.
Adaptive laws for control parameters

$$\dot{k}(t) = -\gamma sgn(k_p) e_c(t) r(t) \tag{2.10}$$

$$\dot{\theta}_1(t) = -\gamma sgn(k_p) e_c(t) \omega_1(t) \tag{2.11}$$

$$\dot{\theta}_2(t) = -\gamma sgn(k_p) e_c(t) \omega_2(t) \tag{2.12}$$

$$\dot{\theta}_0(t) = -\gamma sgn(k_p) e_c(t) y_p(t) \tag{2.13}$$

The aim of direct MRAC is the determination of a bounded control law so that

$$\lim_{t\to\infty} e_c(t) = 0 \tag{2.14}$$

Hence, the adaptive control problem can be equivalently stated as the determination of adaptive laws (2.10), (2.11), (2.12) and (2.13) so that condition (2.14) is satisfied.

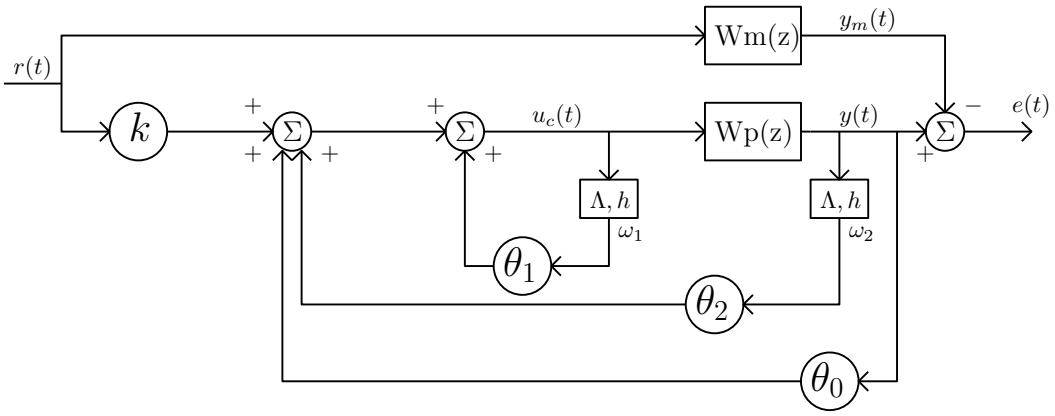

Figure 2.5: Structure of Model Reference Adaptive Controller for second order systems

Combined Model Reference Adaptive Control of First Order Systems

The discretized combined MRAC for a first order plant is implemented below.
Input

- $y_p(t)$, the response of the plant.
- $r(t)$, the reference signal.
- $e_c(t) = y_p(t) - y_m(t)$, the control error.

Output

- $u_c(t)$, the control law signal.

Internal signals

- $y_m(t)$, the response of the reference model.
- $\theta(t)$, $k(t)$, the controller parameters.
- $n_a(t)$, $n_b(t)$, the plant parameter errors.
- $e_\theta(t)$, $e_k(t)$, the closed loop estimation errors.
- $y_i(t)$, the estimated by the identification algorithm response of the plant used for validation with the real response $y_p(t)$.

Design Parameters

- $\gamma > 0$, the adaptation gain which regulates the rate of change for $\theta(t)$ and $k(t)$.

Plant model

$$y_p(t) = \frac{b_p}{z + a_p} u_c(t) \tag{2.15}$$

where a_p and b_p are the unknown plant parameters.
Reference model

$$y_m(t) = \frac{b_m}{z + a_m} r(t) \tag{2.16}$$

where a_m and b_m are known constants.
Control law

$$u_c(t) = \theta(t) y_p(t) + k(t) r(t) \tag{2.17}$$

where $\theta(t)$, $k(t)$ are adjustable controller parameters.
The error equations

$$e_c(t) = y_p(t) - y_m(t) \tag{2.18}$$

$$e_i(t) = y_i(t) - y_p(t) \tag{2.19}$$

where e_c is the control error and e_i is the identification error.

Closed-loop estimation errors

$$e_\theta(t) = -n_a(t) + \theta(t)n_b(t) + b_p\phi_\theta(t) \tag{2.20}$$

$$e_k(t) = k(t)n_b(t) + b_p\phi_k(t) \tag{2.21}$$

where e_θ, e_k are the closed loop estimation errors and ϕ_θ, ϕ_k are the controller parameter errors.

Plant parameter errors

$$\dot{n}_a(t) = e_i(t)y_p(t) + e_\theta(t) \tag{2.22}$$

$$\dot{n}_b(t) = -e_i(t)u_c(t) - \theta(t)e_\theta(t) - k(t)e_k(t) \tag{2.23}$$

Adaptive laws for control parameters

$$\dot{\phi}_\theta(t) = \dot{\theta}(t) = -\gamma sgn(b_p)[e_c(t)y_p(t) + e_\theta(t)] \tag{2.24}$$

$$\dot{\phi}_k(t) = \dot{k}(t) = -\gamma sgn(b_p)[e_c(t)r(t) + e_k(t)] \tag{2.25}$$

The combined method presented above uses the errors (2.18), (2.19), (2.20), and (2.21) for adjusting the parameters (2.24) and (2.25) which in turn create the control law (2.17). The problem may now be stated as follows. Given the identification error $e_i(t)$, defining the evolution of $e_c(t)$ and the closed-loop estimation errors $e_\theta(t)$ and $e_k(t)$, determine adaptive laws for adjusting control parameters $\theta(t)$ and $k(t)$ so that

$$\lim_{t\to\infty} e_c(t) = 0 \tag{2.26}$$

Based on the plant parameters estimations and the controller parameter values at any instant t, closed-loop estimation errors $e_\theta(t)$ and $e_k(t)$ are defined which denote the deviation of the estimated coefficients of the closed-loop transfer function from those of the reference model. Closed-loop estimation errors $e_\theta(t)$ and $e_k(t)$ are used to *carry* information from both plant parameter and control parameter estimations at time step t through to the calculation of the control law u_c at time step $t+1$. This is implemented using plant parameter errors n_a and n_b, control parameters θ and k and plant parameter estimation $\hat{b}_p$ (instead of the unknown plant parameter b_p) for their calculation. Closed-loop estimation errors are, therefore, the feature of combined model reference adaptive control algorithm which provides the connection between direct and indirect MRAC. Furthermore, control law u_c at time step $t+1$ contains information from control law at time step t, as the last is used for the calculation of plant parameter error n_b. Figure 2.6 depicts the structure of a combined model reference adaptive controller as the one designed for the purposes of this Thesis.

Combined Model Reference Adaptive Control of Second Order Systems

The discretized combined MRAC for a second order plant is implemented below.
Input

- $y_p(t)$, the response of the plant.
- $r(t)$, the reference signal.
- $e_c(t) = y_p(t) - y_m(t)$, the control error.

Output

- $u_c(t)$, the control law signal.

Internal signals

- $y_m(t)$, the response of the reference model.
- $k(t)$, $\theta_1(t)$, $\theta_2(t)$, $\theta_0(t)$, the controller parameters.
- $\dot{\omega}_1(t) = \Lambda\omega_1(t) + hu_c(t)$, the control sensitivity signal.
- $\dot{\omega}_2(t) = \Lambda\omega_2(t) + hy_p(t)$, the control sensitivity signal.
- $n_{kp}(t)$, $n_\beta(t)$, $n_\alpha(t)$, $n_{\alpha 1}(t)$, the plant parameter errors.
- $e_k(t)$, $e_{\theta 1}(t)$, $e_{\theta 2}(t)$, $e_{\theta 0}(t)$, the closed loop estimation errors.
- $y_i(t)$, the estimated by the identification algorithm response of the plant used for validation with the real response $y_p(t)$.

Design Parameters

- $\gamma > 0$, the adaptation gain which regulates the rate of change $k(t)$, $\theta_1(t)$, $\theta_2(t)$ and $\theta_0(t)$.
- $\Lambda = -b_m$.
- $h = 1$.

Plant model

$$y_p(t) = \frac{k_p(z + b_{p0})}{z^2 + a_{p1}z + a_{p2}}u_c(t) = W_p(z)u_c(t) \tag{2.27}$$

where a_{p1}, a_{p2}, b_{p0} and k_p are the unknown plant parameters.
Reference model

$$y_m(t) = \frac{k_m(z + b_{m0})}{z^2 + a_{m1}z + a_{m2}}r(t) = W_m(z)r(t) \tag{2.28}$$

where a_{m1}, a_{m2}, b_{m0} and k_m are known constants.
Control law

$$u_c(t) = \vartheta^\top(t)\varpi(t) \tag{2.29}$$

where
$\vartheta(t) = [k(t)\ \ \theta_1(t)\ \ \theta_2(t)\ \ \theta_0(t)]^\top$, the controller parameters vector.
$\varpi(t) = [r(t)\ \ \omega_1(t)\ \ \omega_2(t)\ \ y_p(t)]^\top$, the internal signals vector.
The error equations

$$e_c(t) = y_p(t) - y_m(t) \tag{2.30}$$

$$e_i(t) = y_i(t) - y_p(t) \tag{2.31}$$

where e_c is the control error, e_i is the identification error.
Closed-loop estimation errors

$$e_k(t) = k_p\phi_k(t) + k(t)n_{kp}(t) \tag{2.32}$$

$$e_{\theta_1}(t) = \phi_{\theta_1}(t) + n_\beta(t) \tag{2.33}$$

$$e_{\theta_2}(t) = k_p\phi_{\theta_2}(t) + \theta_2(t)n_{kp}(t) + k_m n_\alpha(t) \tag{2.34}$$

$$e_{\theta_0}(t) = k_p\phi_{\theta_0}(t) + \theta_0(t)n_{kp}(t) + k_m n_{\alpha 1}(t) \tag{2.35}$$

where e_k, e_{θ_1}, e_{θ_2}, e_{θ_0} are the closed loop estimation errors and ϕ_k, ϕ_{θ_1}, ϕ_{θ_2}, ϕ_{θ_0} are the controller parameters errors.
Plant parameter errors

$$\dot{n}_{kp}(t) = -e_i(t)\frac{\beta(t)\overline{\omega}_1(t) + \overline{u}_c(t)}{k_m N_i(t)} - [k(t)e_k(t) + \theta_2(t)e_{\theta_2}(t) + \theta_0(t)e_{\theta_0}(t)] \tag{2.36}$$

$$\dot{n}_\beta(t) = -sgn(k_p)e_i(t)\frac{\overline{\omega}_1(t)}{k_m N_i(t)} - e_{\theta_1}(t) \tag{2.37}$$

$$\dot{n}_\alpha(t) = -e_i(t)\frac{\overline{\omega}_2(t)}{N_i(t)} - k_m e_{\theta_2}(t) \tag{2.38}$$

$$\dot{n}_{\alpha 1}(t) = -e_i(t)\frac{\overline{y}_p(t)}{N_i(t)} - k_m e_{\theta_0}(t) \tag{2.39}$$

where
$\beta(t) = \hat{b}_p(t)$.
$\overline{u}_c(t) = W_m(z)u_c(t)$.
$\overline{\omega}_1(t) = W_m(z)\omega_1(t)$.
$\overline{\omega}_2(t) = W_m(z)\omega_2(t)$.
$\overline{y}_p(t) = W_m(z)y_p(t)$.

$N_i(t) = 1 + (\beta\overline{\omega}_1(t) + \overline{u}_c(t))^2 + \overline{\omega}_1^2(t) + \overline{y}_p^2(t) + \overline{\omega}_2^2(t)$.

Adaptive laws for control parameters

$$\dot{\phi}_k(t) = \dot{k}(t) = -[\gamma sgn(k_p)e_c(t)]\frac{y_m(t)}{k_m N_c(t)} - [\gamma sgn(k_p)]e_k(t) \tag{2.40}$$

$$\dot{\phi}_{\theta_1}(t) = \dot{\theta}_1(t) = -[\gamma sgn(k_p)e_c(t)]\frac{\overline{\omega}_1(t)}{k_m N_c(t)} - [\gamma]e_{\theta_1}(t) \tag{2.41}$$

$$\dot{\phi}_{\theta_2}(t) = \dot{\theta}_2(t) = -[\gamma sgn(k_p)e_c(t)]\frac{\overline{\omega}_2(t)}{k_m N_c(t)} - [\gamma sgn(k_p)]e_{\theta_2}(t) \tag{2.42}$$

$$\dot{\phi}_{\theta_0}(t) = \dot{\theta}_0(t) = -[\gamma sgn(k_p)e_c(t)]\frac{\overline{y}_p(t)}{k_m N_c(t)} - [\gamma sgn(k_p)]e_{\theta_0}(t) \tag{2.43}$$

where

$N_c(t) = 1 + \overline{\varpi}^\top(t)\overline{\varpi}(t)$.

$\overline{\varpi}(t) = [y_m(t)\ \ \overline{\omega}_1(t)\ \ \overline{\omega}_2(t)\ \ \overline{y}_p(t)]^\top$, the filtered internal signals vector.

The combined method presented above uses the errors (2.30), (2.31), (2.32), (2.35), (2.33) and (2.34) for adjusting controller parameters (2.40), (2.43), (2.41) and (2.42) which in turn create the control law (2.29). The problem may now be stated as follows. Given the identification error $e_i(t)$, defining the evolution of $e_c(t)$ and the closed-loop estimation errors $e_k(t)$, $e_{\theta 1}(t)$, $e_{\theta 2}(t)$ and $e_{\theta 0}(t)$, determine adaptive laws for adjusting control parameters $k(t)$, $\theta_1(t)$, $\theta_2(t)$ and $\theta_0(t)$ so that

$$\lim_{t\to\infty} e_c(t) = 0 \tag{2.44}$$

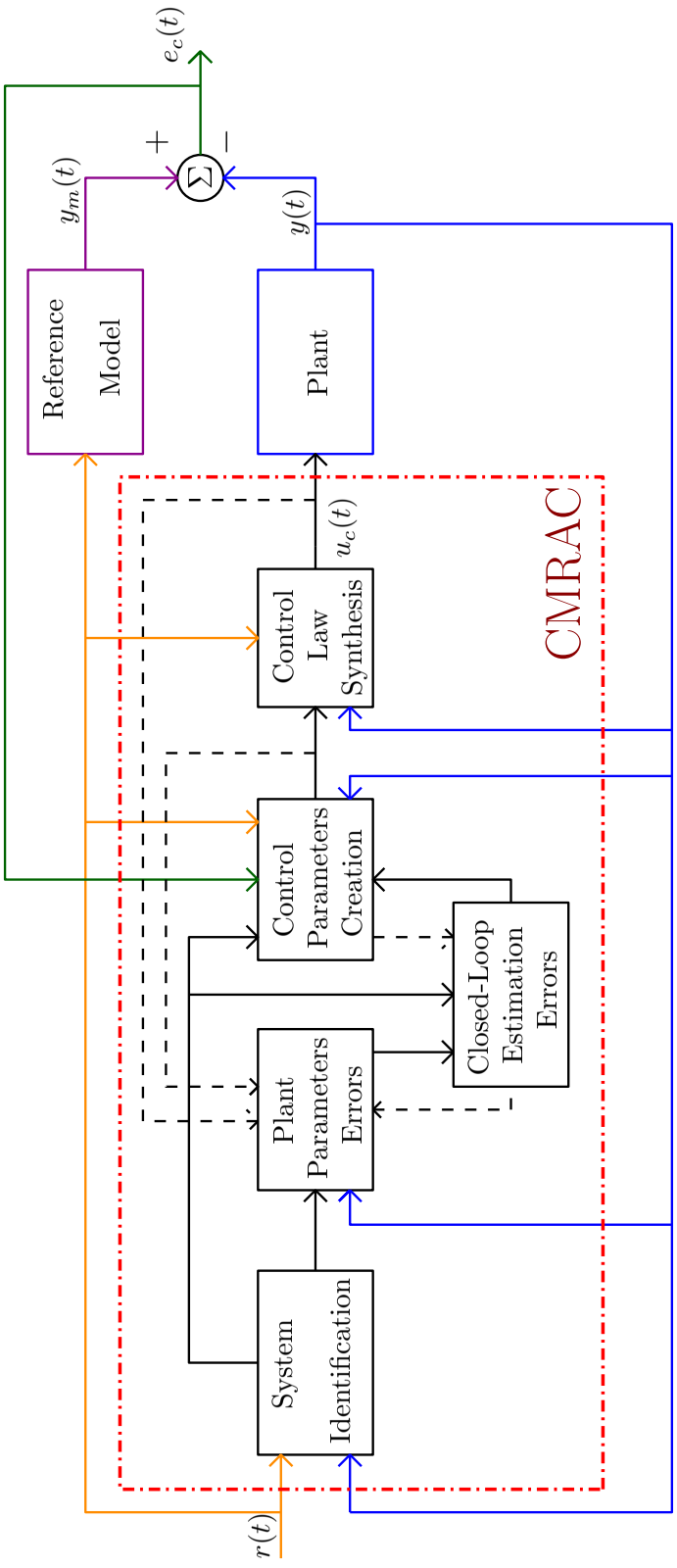

Figure 2.6: Structure of Combined Model Reference Adaptive Controller

2.1.4 Stability

Formation of both MRAC and CMRAC adaptive laws presented above is based on Lyapunov stability theory. The global stability of the system is assured by the existence of a Lyapunov function. Basic features of the Lyapunov stability theory used for the purposes of this diploma Thesis and the Lyapunov functions used for the stability proof of the CMRAC designed are presented below.

Lyapunov's Theory for Non-linear System's

Russian mathematician Lyapunov made fundamental contributions to the stability theory for nonlinear systems in the end of the nineteenth century. Lyapunov investigated the nonlinear differential equation

$$\frac{dx}{dt} = f(x) \tag{2.45}$$

$$f(0) = 0 \tag{2.46}$$

Since $f(0) = 0$, the equation has the solution $x(t) = 0$.

Lyapunov was interested in investigating whether the solution of equation (2.45) is stable with respect to perturbations. For this purpose he introduced the following stability theorem.

DEFINITION 1: Lyapunov stability

The solution $x(t) = 0$ to the differential equation (2.45) is called *stable* if for given $\varepsilon > 0$ there exists a number $\delta(\varepsilon) > 0$ such that the solutions with initial conditions $\| x(0) \| < \delta$ have the property

$$\| x(t) \| < \varepsilon \text{ for } 0 \leq t < \infty.$$

The solution is *unstable* if it is not stable. The solution is asymptotically stable if it is stable and δ can be found such that all solutions with $\| x(0) \| < \delta$ have the property that $\| x(t) \| \to 0$ as $t \to \infty$. It is noteworthy that Lyapunov stability refers to the stability of a particular solution and not to the differential equation.

Lyapunov developed a method for investigating stability that is based on the idea of finding a function with special properties. This method is described below.

DEFINITION 2: Positive definite functions

A continuously differentiable function V is called *positive definite* if:

1. $V(0) = 0$
2. $V(x) > 0$

Lyapunov's Stability Theorem

If there exists a function V that is positive definite such that its derivative along the solution of equation (2.45)

$$\frac{dV}{dt} = \frac{\partial V^\top}{\partial x}\frac{dx}{dt} = \frac{\partial V^\top}{\partial x} f(x) = -W(x) \tag{2.47}$$

is negative semi-definite, then the solution $x(t) = 0$ to (2.45) is stable. If $\frac{dV}{dt}$ is negative definite then the solution is also asymptotically stable. The function V is called *Lyapunov function* for the system (2.45). The Lyapunov functions used for the stability proof of CMRAC designed are

$$V_1 = \frac{1}{2}(e_c^2 + b_p\phi_\theta^2 + b_p\phi_k^2 + e_i^2 + n_\alpha^2 + n_b^2) \tag{2.48}$$

$$V_2 = \frac{1}{2}(|k_p|\phi_k^2 + |k_p|\phi_{\theta_1}^2 + |k_p|\phi_{\theta_0}^2 + |k_p|\phi_{\theta_2}^2 + n_{k_p}^2 + |k_p|n_\beta^2 + n_\alpha^2 + n_{\alpha_1}^2) \tag{2.49}$$

for systems of first and second order respectively. Their derivatives are

$$\frac{dV_1}{dt} = -a_m {e_c}^2 - {e_i}^2 - {e_\theta}^2 - {e_k}^2 \leq 0 \tag{2.50}$$

$$\frac{dV_2}{dt} = -\frac{{e_c}^2}{N_c} - \frac{{e_i}^2}{N_i} - {e_{\theta_1}}^2 - {e_{\theta_2}}^2 - {e_k}^2 - {e_{\theta_0}}^2 \leq 0 \tag{2.51}$$

According to the *Lyapunov's stability theorem*, since $\dot{V}_1, \dot{V}_2 \leq 0$, plant parameter estimates, control parameters and closed-loop estimation errors are uniformly bounded. Since these parameters are uniformly bounded, it follows that limit of the corresponding signals tends to zero, as time tends to infinite, which is the requirement for stable and effective performance of CMRAC.

2.2 Robustness of Adaptive Control

The analysis presented above has been carried out assuming that no other uncertainties or variations exist in the adaptive control system besides the parametric ones. However, since adaptive controllers are designed to control real physical systems, many types of non-parametric uncertainties are often present such as

- unmodeled dynamics, such as actuator dynamics or structural vibrations
- measurement noise
- external disturbances
- sampling delay

When the reference signal $r(t)$ and the plant's output signal $y_p(t)$ are persistently exciting, the adaptive control system has some robustness with respect to non-parametric uncertainties. When these signals are not persistently exciting, even small plant uncertainties may lead to serious problems for adaptive controllers. The major instability mechanism associated with non-parametric uncertainties is *parameter drift* and it is mainly caused by the noise with which measured signals are usually corrupted. The simplest explanation of the parameter drift problem is that non persistently exciting signals contain little information for the parameter adaptation mechanism to distinguish the parameter information from measurement noise. As a result, the adaptive control system is led to sudden instability and failure.

Dead-Zone

Dead-zone [13] is a technique for modifying the adaptation law so as to avoid the parameter drift problem. It is based on the fact that small control errors contain mostly noise and disturbance, therefore, the adaptation mechanism should be shut off for small control errors. Specifically, the adaptation gain (2.4) should be replaced by

$$\theta(t) = \begin{cases} \theta(t-1) - \gamma sgn(b_p) e_c(t) y_p(t) & \text{if} \quad |e_c| > \Delta \\ 0 & \text{if} \quad |e_c| < \Delta \end{cases} \tag{2.52}$$

where Δ is the size of dead-zone.

2.3 System Identification

System identification is a technique by which the parameters of a system's model can be estimated. This is usually performed by assuming a discrete time form for the system model and then using a recursive estimation algorithm (Figure 2.7) to calculate estimations of the parameters of the model from the measurements of input and output signals of the system.

Parameter estimation can be done either on-line or off-line. Off-line estimation may be preferable if the parameters are constant and there is sufficient time for estimation before control. However, when system plant parameters vary during its operation, on-line real time parameter estimation is necessary to keep track of their values. Since problems in the adaptive control context usually involve time varying parameters, on-line estimation methods are thus more relevant.

Three different system identification algorithms were used in this Thesis. These are [16]

- Least squares algorithm
- Instrumental variables algorithm
- Sequential learning algorithm

Mathematical implementation of the identification techniques mentioned above is presented below.

2.3.1 Least Squares Algorithm

Consider a discrete time transfer function model of a system with control input signal $u(t)$ and with output signal $y(t)$ subject to random noise. The model can be written in the form

$$Ay(t) = Bu(t-1) + Ce(t) \tag{2.53}$$

where

$$A = 1 + a_1 z^{-1} + \ldots + a_{n_a} z^{-n_a}$$
$$B = 1 + b_1 z^{-1} + \ldots + b_{n_b} z^{-n_b}$$
$$C = 1 + c_1 z^{-1} + \ldots + c_{n_c} z^{-n_c}$$

Introducing the unit backward shift operator z^{-1} defined by

$$z^{-i} x(t) = x(t-i) \tag{2.54}$$

equation (2.53) can be written in the more suitable for estimation purposes form

$$y(t) = \overline{x}^{\top}(t)\overline{\theta} + e(t) \tag{2.55}$$

where $\overline{\theta}$ is the vector of unknown parameters, defined by

$$\overline{\theta}^{\top} = [-a_1, \ldots, -a_{n_a}, b_0, \ldots, b_{n_b}, c_1, \ldots, c_{n_c}] \tag{2.56}$$

and $\overline{x}(t)$ is a regression vector partly consisting of measured input/output variables and defined by

$$\overline{x}^{\top}(t) = [y(t-1), \ldots, y(t-n_a), u(t-1), \ldots, u(t-n_b-1), e(t-1), \ldots, e(t-n_c)] \tag{2.57}$$

The values of $e(t-1), \ldots, e(t-n_c)$ are past values of the unobservable white noise disturbance and are usually unknown. For the purposes of this Thesis is assumed that C polynomial's coefficients are zero and the unknown noise no longer appears in equation (2.55). Hence, $\overline{x}(t)$ can be called *data vector*.

In order to determine vector $\overline{\theta}$ of true system parameters, a model of the system of the correct structure is further assumed

$$y(t) = \overline{x}^{\top}\hat{\theta} + \hat{\epsilon}(t) \tag{2.58}$$

where $\hat{\theta}$ is a vector of estimated model parameters and $\hat{\epsilon}(t)$ is the corresponding identification error at time t. $\hat{\theta}$ has to be selected so that identification error is minimized. The technique used for the calculation of $\hat{\theta}$ and the resulting minimization of identification error $\hat{\epsilon}(t)$ is *linear least squares*, which is described below.

Assuming that the system described by equation (2.55) has been running for the time required to form N consecutive data vectors, the system's model is rewritten in the form

$$y = X\hat{\theta} + \hat{\epsilon} \tag{2.59}$$

where

$$y^{\top} = [y(1), \ldots, y(N)]$$
$$\hat{\epsilon}^{\top} = [\hat{\epsilon}(1), \ldots, \hat{\epsilon}(N)]$$

and

$$X = \begin{bmatrix} \overline{x}^{\top}(1) \\ \overline{x}^{\top}(2) \\ \vdots \\ \overline{x}^{\top}(N) \end{bmatrix} \tag{2.60}$$

An estimation of parameters' vector $\hat{\theta}$ is selected so as the sum of squares of identification errors J is minimized

$$J = \sum_{t=1}^{N} \hat{\epsilon}^2(t) = \hat{\epsilon}^\top \hat{\epsilon} \tag{2.61}$$

The least squares estimation for the parameter vector $\overline{\theta}$ can be calculated after rewriting equation (2.61) in terms of the data vector and parameter vector and setting the first derivative of J with respect to $\hat{\theta}$ to zero

$$\hat{\theta} = [X^\top X]^{-1}[X^\top y] \tag{2.62}$$

This solution is a unique minimum as the second derivative of J with respect to $\hat{\theta}$ is positive definite.

Recursive Least Squares

In order for the identification algorithm to be useful in control schemes, the parameter estimation should be iterative so as the estimated parameters of the system model can be updated at each sample interval as new data become available.

The model created by past information $\hat{\theta}(t-1)$ is used to obtain an estimate $\hat{y}(t)$ of the current output. This is then compared with the real measured output $y(t)$ to generate the identification error $\epsilon(t)$. This in turn generates an update to the model which replaces $\hat{\theta}(t-1)$ with the new value $\hat{\theta}(t)$. In summary, the full recursive least squares (RLS) [16] algorithm for updating $\hat{\theta}(t)$ is presented below.

At time step t:

1. Formation of $\overline{x}(t)$ using the new data measured.

2. Formation of the identification error $\epsilon(t)$ using the equation

$$\epsilon(t) = y(t) - \overline{x}^\top(t)\hat{\theta}(t-1) \tag{2.63}$$

3. Formation of the covariance matrix $P(t) = [X^\top(t)X(t)]^{-1}$ using the equation

$$P(t) = P(t-1)[I_m - \frac{\overline{x}(t)\overline{x}^\top(t)P(t-1)}{1+\overline{x}^\top(t)P(t-1)\overline{x}(t)}] \tag{2.64}$$

   where $m = na + nb + 1$.

4. Updating of $\hat{\theta}(t)$ using the equation

$$\hat{\theta}(t) = \hat{\theta}(t-1) + P(t)\overline{x}(t)\epsilon(t) \tag{2.65}$$

5. After next time step elapses loop back to step 1.

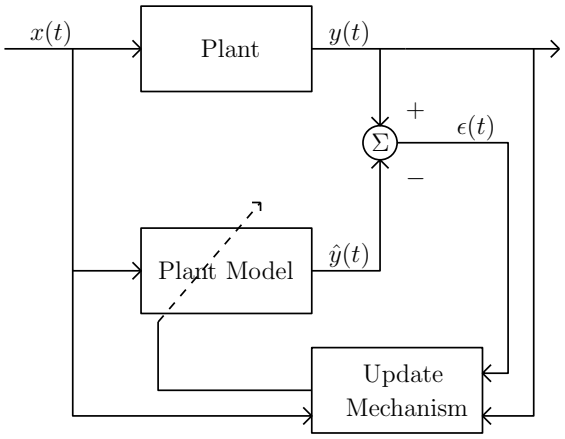

Figure 2.7: Schematic presentation of recursive estimation

2.3.2 Instrumental Variables Algorithm

Instrumental variables [15] is a system identification technique which produces unbiased estimates of the parameter vector $\theta(t)$ by using a vector of instrumental variables $v(t)$ of the same dimensions as data vector $x(t)$ such that the elements of $v(t)$ are uncorrelated with the noise corrupting the system. The instrumental variables $v(t)$ are often created by passing the input signal $u(t)$ through a known discrete time transfer function to obtain the signal $z(t)$ which replaces the output signal $y(t)$ in the vector $v(t)$. The technique used for the calculation of the estimations of a system's parameters is described below.

Consider the following discrete time transfer function of a system's model

$$y(t) = \frac{B}{A}u(t) + e(t) \tag{2.66}$$

where

$$B = b_1 z^{-1} + \ldots + b_{n_b} z^{-n_b}$$

$$A = 1 + a_1 z^{-1} + \ldots + a_{n_a} z^{-n_a}$$

Similarly to the least squares identification case, equation (2.66) can be written in a form more suitable for identification purposes

$$y = X\overline{\theta} + \overline{e} \tag{2.67}$$

where

$$y^{\top} = [y(t), \ldots, y(t+N)]$$

the output signal vector

$$\overline{e}^{\top} = [e(t), \ldots, e(t+N)]$$

the noise vector

$$X = \begin{bmatrix} \overline{x}(t) \\ \vdots \\ \overline{x}(t+N) \end{bmatrix}$$

the data matrix and

$$\overline{\theta}^{\top} = [-a_1, \ldots, -a_{n_a}, b_1, \ldots, b_{n_b}]$$

the unknown parameters vector.

The instrumental variable $z(t)$ would be generated as

$$z(t) = \frac{R}{Q}u(t)^1 \tag{2.68}$$

where

$$R = r_0 + r_1 z^{-1} + \ldots + r_{n_r} z^{-n_r}$$

$$Q = 1 + q_1 z^{-1} + \ldots + q_{n_q} z^{-n_q}$$

The instrumental vector is then constructed as

$$v(t) = [z(t-1), \ldots, z(t-n_a), u(t-1), \ldots, u(t-n_b)] \tag{2.69}$$

and

$$V = \begin{bmatrix} v(1) \\ v(2) \\ \vdots \\ v(N) \end{bmatrix} \tag{2.70}$$

Multiplying matrix (2.70) with equation (2.67), the estimations

$$\hat{\theta}_{iv} = [V^{\top}X]^{-1}V^{\top}y \tag{2.71}$$

can be produced, as the instrumental variables are uncorrelated with the noise $\overline{e}(t)$ and the factor $V^{\top}\overline{e}$ will be eliminated as $N \to \infty$.

Recursive Instrumental Variables

The instrumental variables algorithm [15] can be put in a recursive form in analogous manner to that used for the least squares algorithm.

The estimation of the parameter vector $\hat{\theta}_{iv}(t)$ at time t is given by the equation

$$\hat{\theta}_{iv}(t) = \hat{\theta}_{iv}(t-1) + P(t)v^{\top}(t)\epsilon(t) \tag{2.72}$$

[1]The discrete time transfer function used to generate the instrumental variables should be stable and in general $n_r \geq n_b$ or $n_q \geq n_a$.

where

$$\epsilon(t) = y(t) - \overline{x}(t)\hat{\theta}_{iv}(t-1) \tag{2.73}$$

and

$$P(t) = P(t-1)[I_m - \frac{v(t)\overline{x}^{\top}(t)P(t-1)}{1+\overline{x}^{\top}(t)P(t-1)v(t)}] \tag{2.74}$$

where $m = na + nb + 1$.

2.3.3 Sequential Learning Algorithm

Sequential learning algorithm [16] is a gradient method of system identification which replaces the covariance matrix $P(t)$ by an expression which is simpler to compute and requires less storage space comparing to the least squares technique. Equation (2.65) can be interpreted as an iterative minimization step as follows.

Consider the error criterion

$$\epsilon^2(t) = \frac{1}{2}[y(t) - \overline{x}^{\top}(t)\hat{\theta}(t-1)]^2 \tag{2.75}$$

The gradient with respect to $\hat{\theta}(t)$ is

$$\frac{d\epsilon^2(t)}{d\hat{\theta}(t-1)} = -[\overline{x}(t)\epsilon(t)] \tag{2.76}$$

Substituting (2.76) in (2.65) a gradient descent-like iteration arises

$$\hat{\theta}(t) = \hat{\theta}(t-1) - P(t)\frac{d\epsilon^2(t)}{d\hat{\theta}(t-1)} \tag{2.77}$$

where covariance matrix $P(t)$ can be viewed as a positive definite matrix which modifies the direction of the gradient adjustments. Hence, $P(t)$ can be replaced by an adjustment gain $\gamma_{sl}(t)$ selected in a simpler way.

In practice, when noise is present, $\gamma_{sl}(t)$ must be selected in a special manner so as the influence of the noise on the parameter estimates can be progressively reduced. Sequential learning algorithm uses an adjustment gain of the following form

$$\gamma_{sl}(t) = \frac{\alpha}{[\beta + \overline{x}^{\top}(t)\overline{x}(t)]} \tag{2.78}$$

where $\beta > 0$ and $0 < \alpha < 2$.

The recursive form of the sequential learning algorithm is analogous to that used for the least squares algorithm.

2.3.4 Forgetting Factors

The recursive estimation techniques presented above have the ability to estimate a constant parameter vector. However, in many practical cases the estimator will be required to track changes in a set of system model parameters. These changes may be even due to nonlinear phenomena after an operating condition change or due to variations which occur over time due to external factors. Furthermore, these changes may be associated even with known phenomena, which means that the time the parameters change will be known or with unknown phenomena, which means that there will be no prior knowledge of when and what changes will occur. In the last case, the recursive estimator will be required to adapt the parameter estimates with no prior knowledge about the origin of the variations being present.

In a control system the recursive estimator generates a system model which can be used for real time implementation of the corresponding controller. When a system source changes, it is important that the recursive estimator rapidly adapts the system's parameters estimates so as the corresponding controller adapts its parameters and maintains its design role.

Provided that there is sufficient excitation[2], then the equation (2.64) ensures that the elements of covariance matrix $P(t)$ decrease in size as the number of time steps increases. Thus as the estimates become more accurate they require less adjustment. Consequently, $P(t)$ can be interpreted as acting as an adjustment gain in equation (2.65). Manipulation of $P(t)$ matrix size is the basic mechanism for controlling the adaptive capabilities of the identification algorithm. The basic mechanism, therefore, for parameter tracking implementation is to control the size of $P(t)$ matrix.

For the purposes of this Thesis the technique used for tracking system's parameter changes is the *directional forgetting factor* technique [16]. A forgetting factor λ is a number between 0 and 1 which is used to progressively reduce the emphasis place on past information. Forgetting factor's technique concept can be understood by considering the way in which information is weighted in the least squares cost function. Specifically, normal least squares algorithm minimizes the cost function

$$J_t = \sum_{i=1}^{t} \hat{\epsilon}^2(i) \tag{2.79}$$

at each time step. In this cost function all values of $\hat{\epsilon}(i)$ from $i = 1$ to t carry an equal weighting.

The forgetting factor approach applies a differential weighting to the data by use

[2] see Appendix C

of the modified cost function

$$\overline{J}_t = \sum_{i=1}^{t} \lambda^{t-i} \hat{\epsilon}^2(i) \tag{2.80}$$

The forgetting mechanism, therefore, uses the influence of λ to progressively reduce the importance given to old data.

Using directional forgetting factor, equation (2.64) of the RLS algorithm is modified

$$P(t) = P(t-1)[I_m - \frac{\overline{x}(t)\overline{x}^\top(t)P(t-1)}{r^{-1}(t-1) + \overline{x}^\top(t)P(t-1)\overline{x}(t)}] \tag{2.81}$$

where

$$r(t) = \lambda^{'} - \frac{(1-\lambda^{'})}{\overline{x}^\top(t+1)P(t)\overline{x}(t+1)} \tag{2.82}$$

where $\lambda^{'}$ is similar to a fixed forgetting factor.

Chapter 3

Design of Identifiers and Controllers

The design of identifiers and controllers is presented in this chapter. Stability and convergence properties of adaptive controllers and system identifiers designed were evaluated before the implementation of the load control system for CAT marine diesel engine at LME. Evaluation took place using both computer simulations and experiments, using heat exchanger experimental device (Figure 1.5). Simulink models, created for structuring of system identifiers and adaptive controllers, are presented in this chapter. Diagrams depicting the control setup at the IC engine test bench together with the corresponding Simulink models are also presented here. Finally a mathematical model of water brake used for testing of the controllers before being used at the implementation of the load control system of CAT marine diesel engine at LME, is provided in this chapter. Results from the evaluation trials are presented in chapter 4.

3.1 System Identification Schemes

3.1.1 Computer Simulations

Simulink model of Figure 3.1 was created for the evaluation of least squares system identification algorithm performance by making computer simulations while model of Figure 3.2 was created for the formulation of recursive least squares algorithm. Models used for the performance evaluation and implementation of the other two identification algorithms are similar and their presentation is omitted.

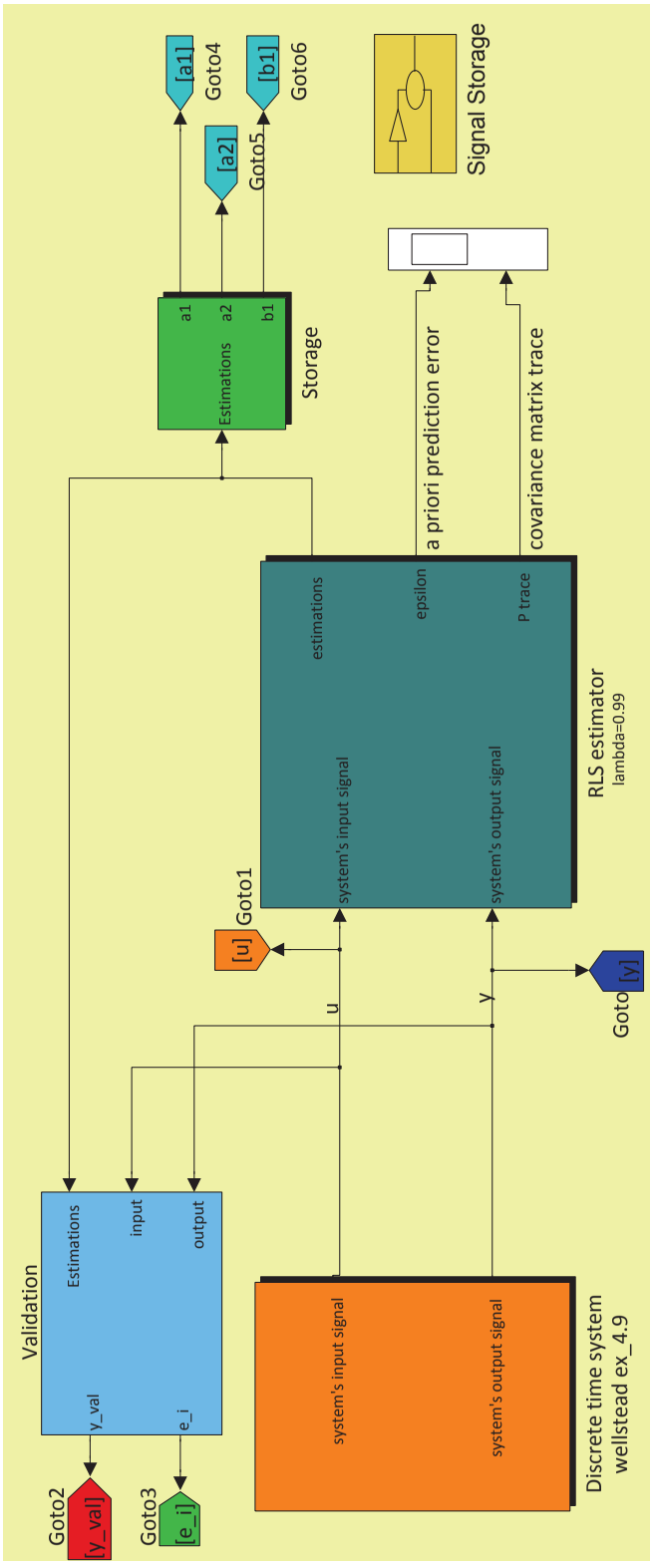

Figure 3.1: Simulink model used for the evaluation of recursive least squares identification algorithm using computer simulations

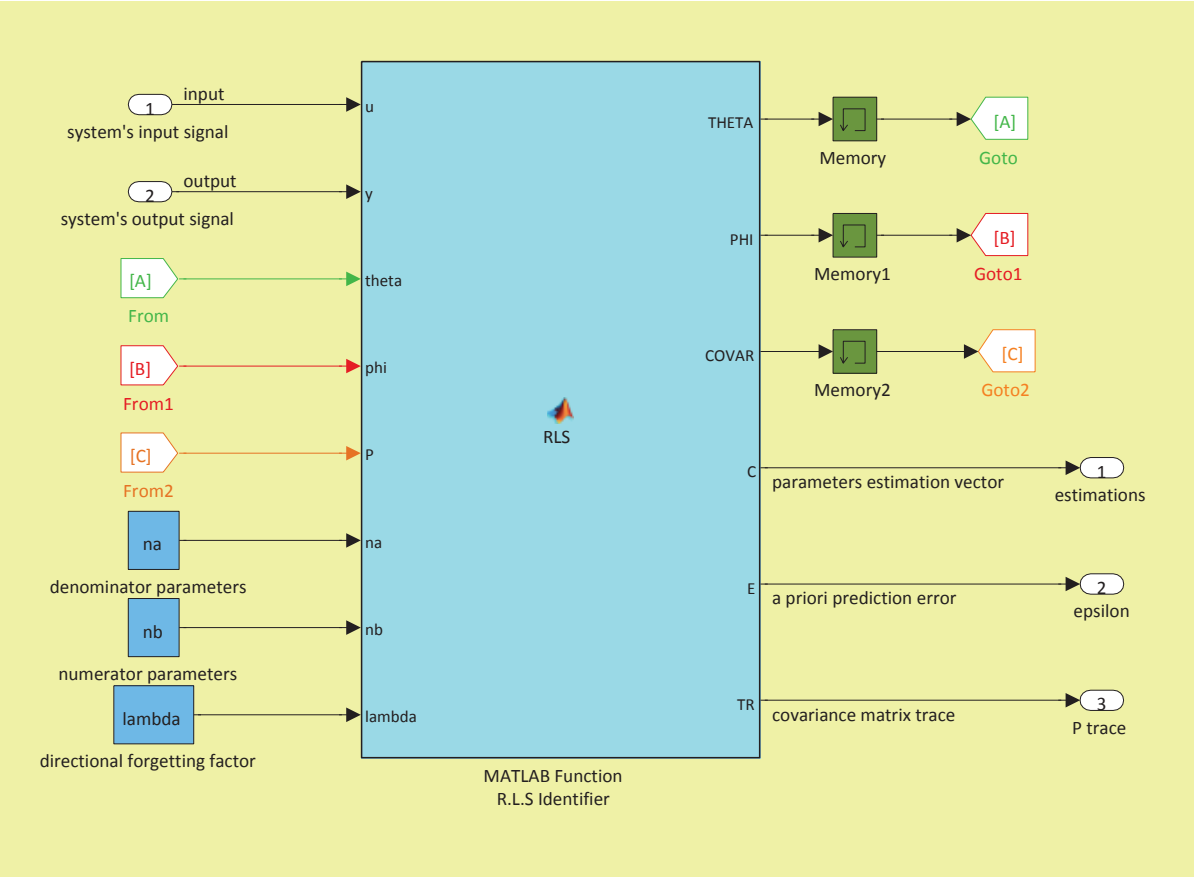

Figure 3.2: Simulink model used for the implementation of recursive least squares identification algorithm

3.1.2 Heat Exchanger Experimental Device

Various aspects of system identification algorithms, like algorithm's robustness in the presence of measurement noise and external disturbances were evaluated using the heat exchanger experimental device (Figure 1.5). Simulink model of Figure 3.3 was created for the application of least squares system identification algorithm on heat exchanger plant. It was used for data acquisition and on-line identification experimental trials. On-line system identification of heat exchanger plant using instrumental variables and sequential learning algorithms was performed using Simulink models similar to that in Figure 3.3.

3.1.3 Data from Water Brake Operation

Signals of analog output valve command and torque, measured during water brake operation, were fed to sequential learning identification algorithm using Simulink model in Figure 3.4 so as to evaluate performance of the identifier when signals measured from a real process were given as inputs to the algorithm. Moreover, a second order mathematical model of water brake plant could be produced. Model in Figure 3.4 was created for an initial check of identifiers performance before applied on CAT diesel engine's plant.

3.1.4 System Identification Toolbox

System identification toolbox of MATLAB was also used during the evaluation process of various identification algorithms. It was used for quick comparisons between different methods, for mathematical models creation (both of discrete and continuous time) and for stability analysis of the latter.

The mathematical model of water brake, created using identification toolbox, used for computer simulated evaluation trials of MRAC and CMRAC (presented in chapter 5) is presented below.

```
% Discrete-time IDPOLY model: A(q)y(t) = B(q)u(t) + e(t)
% A(q) = 1 - 1.699 (+-0.0006829) q^-1 + 0.6996 (+-0.0006827) q^-2
%
% B(q) = 1.597 (+-0.06409) q^-1 - 1.292 (+-0.06411) q^-2
%
% Estimated using ARX on data set water_brake_measurements
% Loss function 0.000895613 and FPE 0.000895619
```

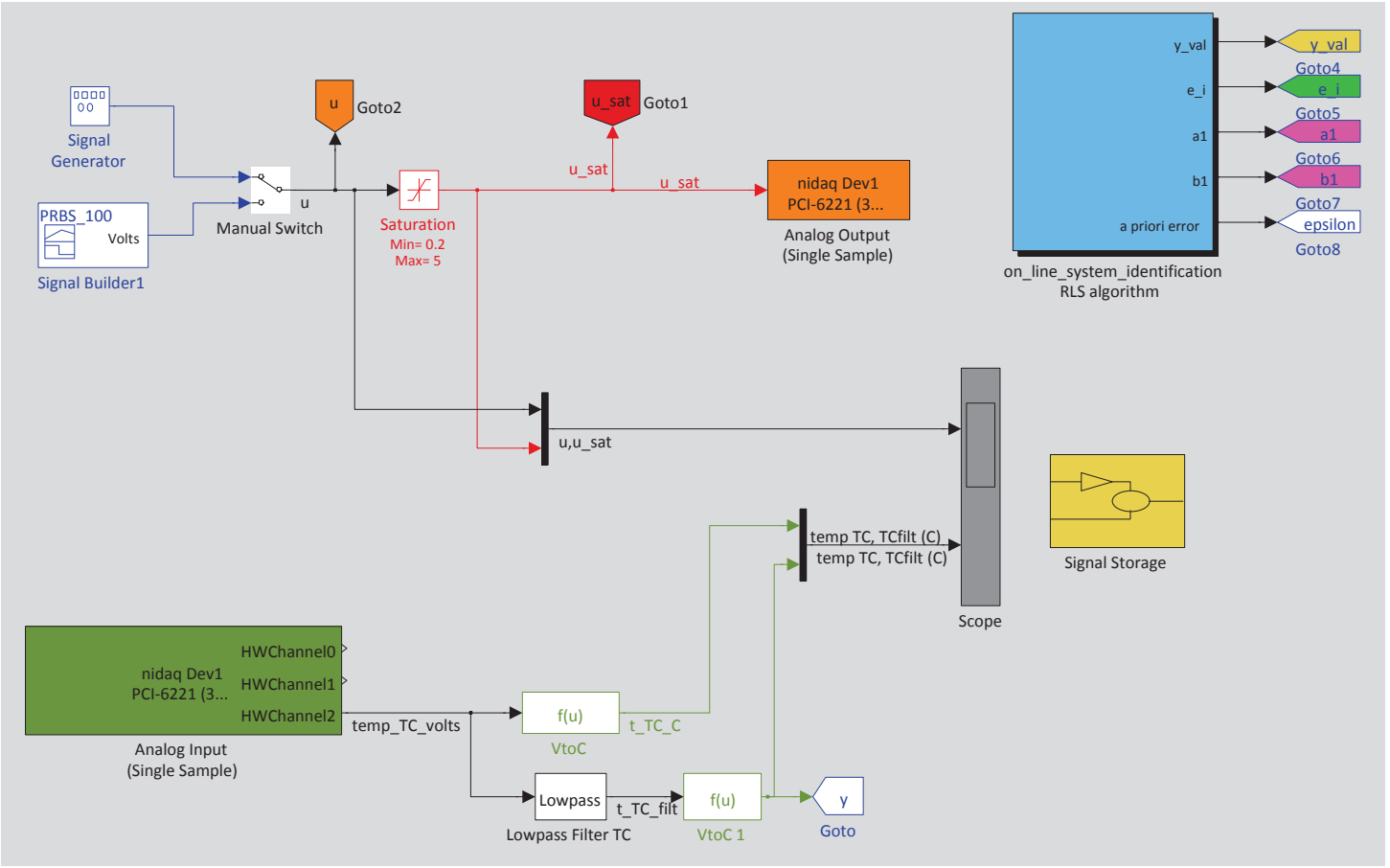

Figure 3.3: Simulink model used for the implementation of heat exchanger on-line recursive least squares system identification

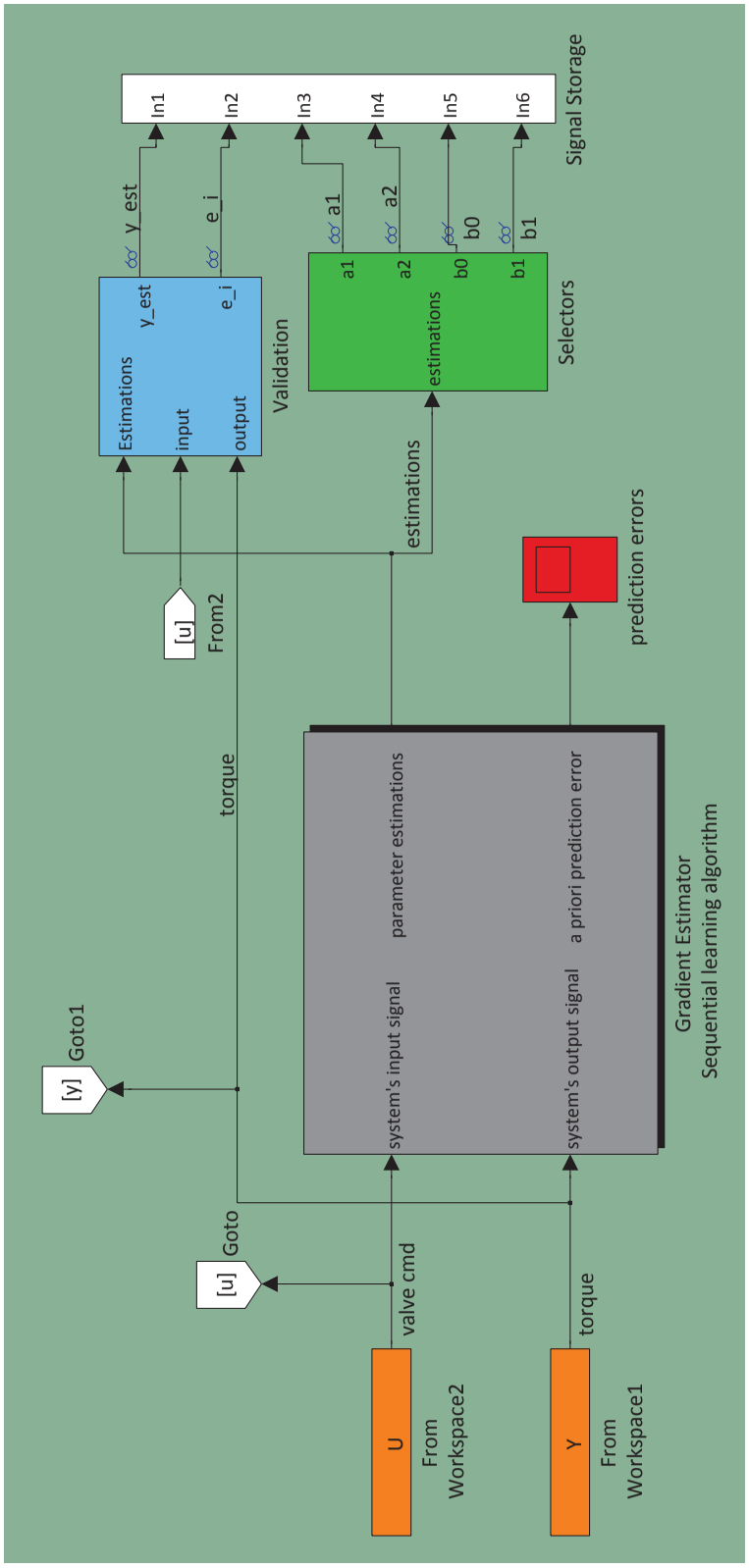

Figure 3.4: Simulink model used for the evaluation of sequential learning identification algorithm using measured signals from water brake experimental trials

3.2 Adaptive Control Schemes

3.2.1 Computer Simulations

Performance and stability properties of the three versions of Combined Model Reference Adaptive Control (CMRAC) designed for the purposes of this Thesis was initially evaluated by making computer simulation trials. Computer simulations of model reference adaptive control (MRAC) were also made for performance comparisons. Simulink models created for the implementation of these evaluation trials are presented below.

Model in Figure 3.6 was used for the evaluation of a closed loop control system consisting of MRAC and a first order system plant of heat exchanger. Model in Figure 3.5 was created for the formulation of MRAC algorithm for first order discrete time systems. Model in Figure 3.8 was created for the evaluation of a closed loop control system consisting of a MRAC and the second order plant of water brake, created using the Identification Toolbox of MATLAB (presented in the previous section). Model in Figure 3.9 implements MRAC for second order discrete time systems via Simulink.

Finally, evaluation of a closed loop control system consisting of CMRAC and the first order system plant of heat exchanger was performed using Simulink model in Figure 3.7. Simulink models used for performance tests of the rest versions of CMRAC designed are similar to Figure 3.7, therefore, their presentation is omitted. Model in Figure 3.10 was used for the evaluation of a closed loop control system consisting of a CMRAC with SL identifier and the second order plant of water brake which was also used in model shown in Figure 3.8 formulation.

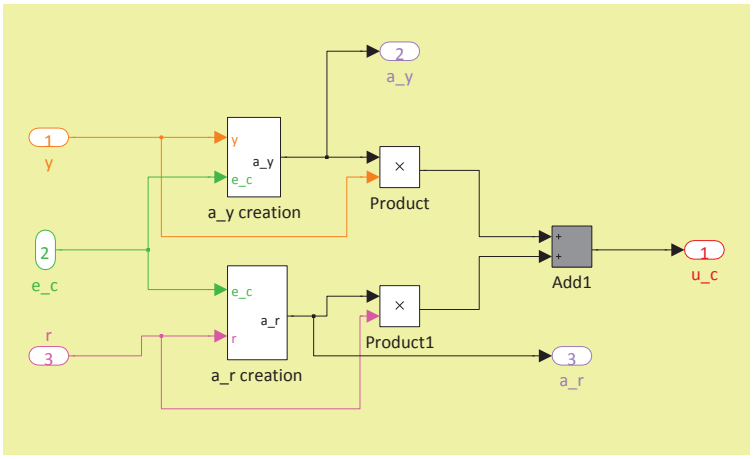

Figure 3.5: Simulink model used for the implementation of MRAC for systems of first order

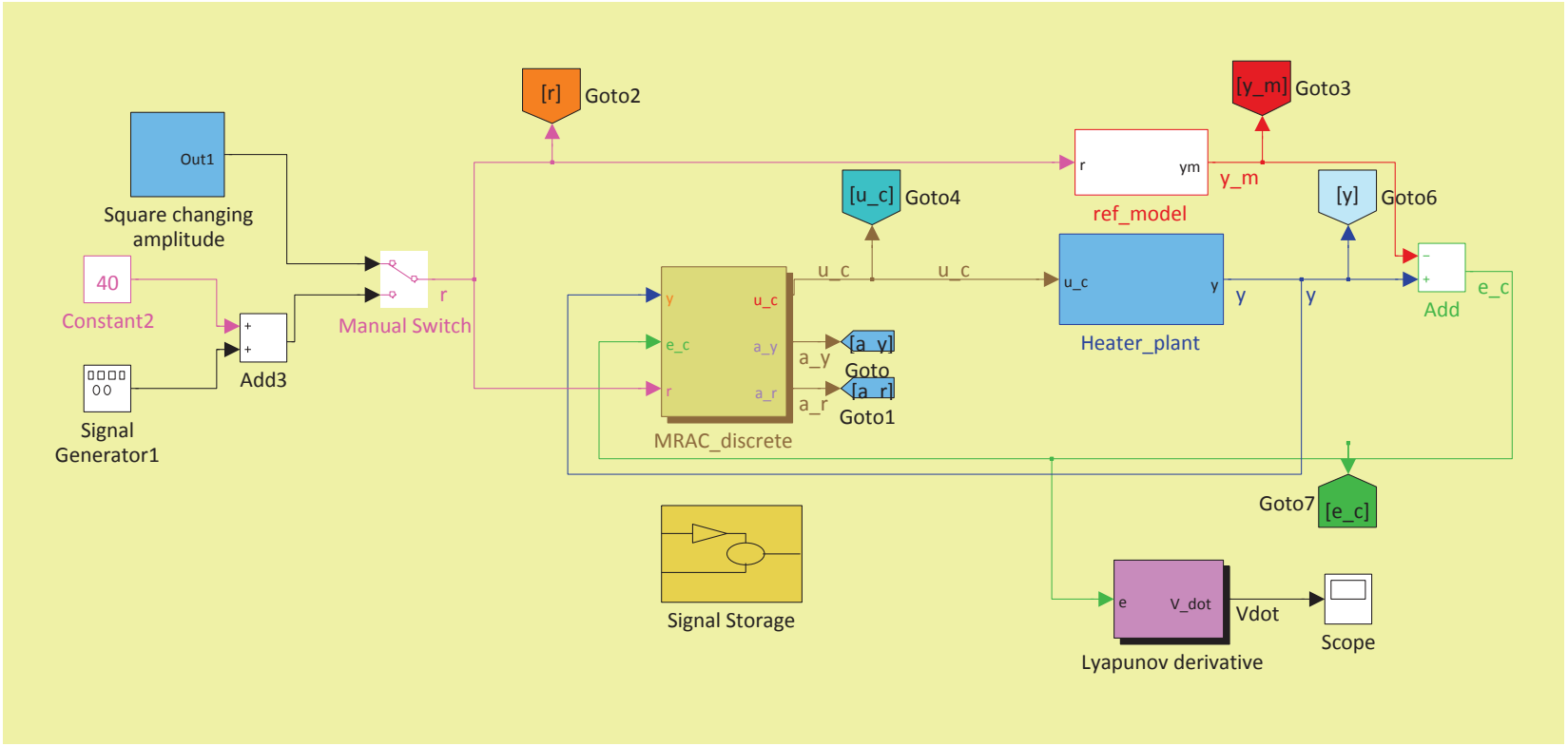

Figure 3.6: Simulink model used for the evaluation of a closed loop control system using MRAC on first order system plant of heat exchanger

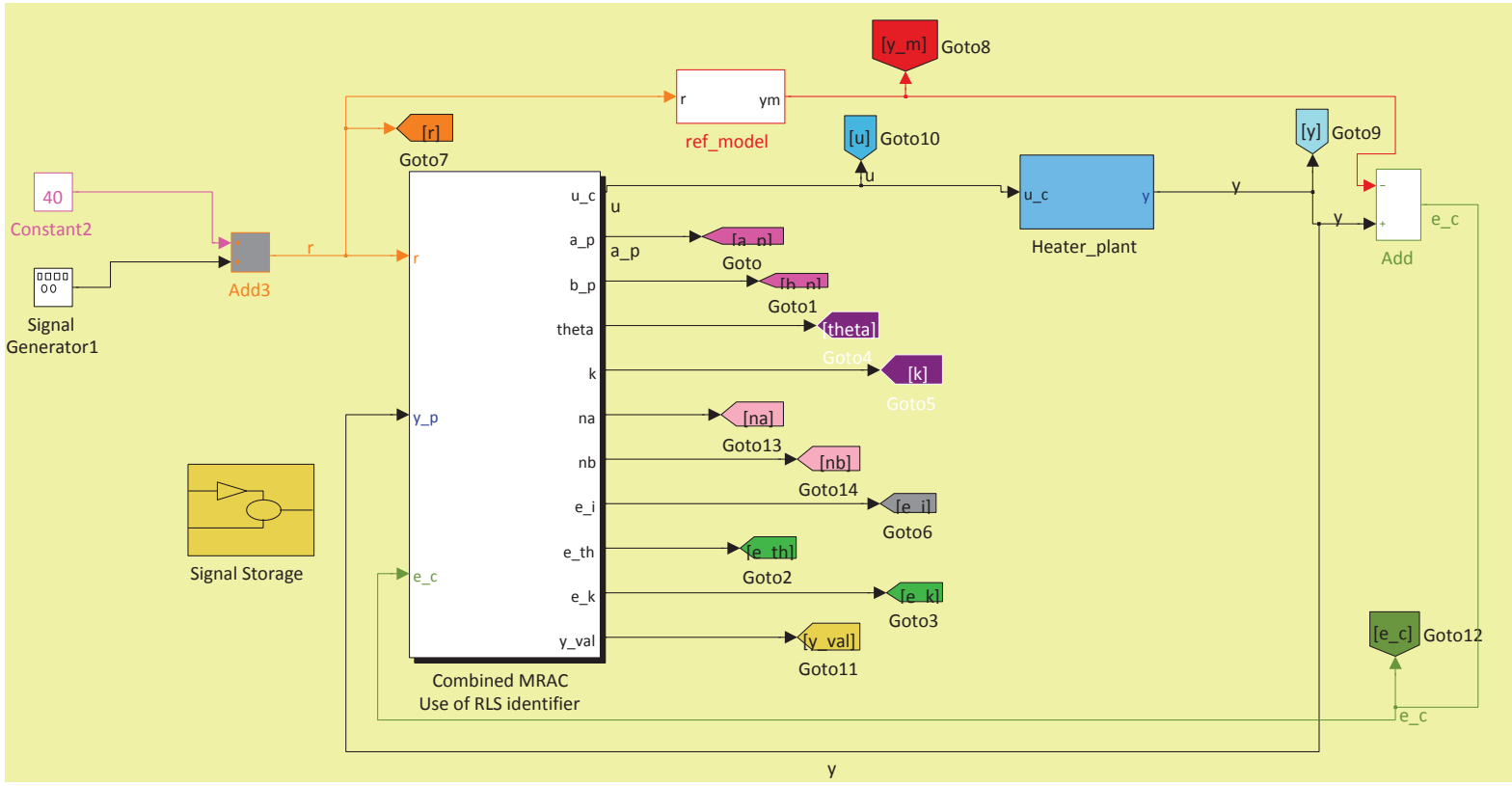

Figure 3.7: Simulink model used for the evaluation of a closed loop control system using CMRAC with RLS identifier on first order system plant of heat exchanger

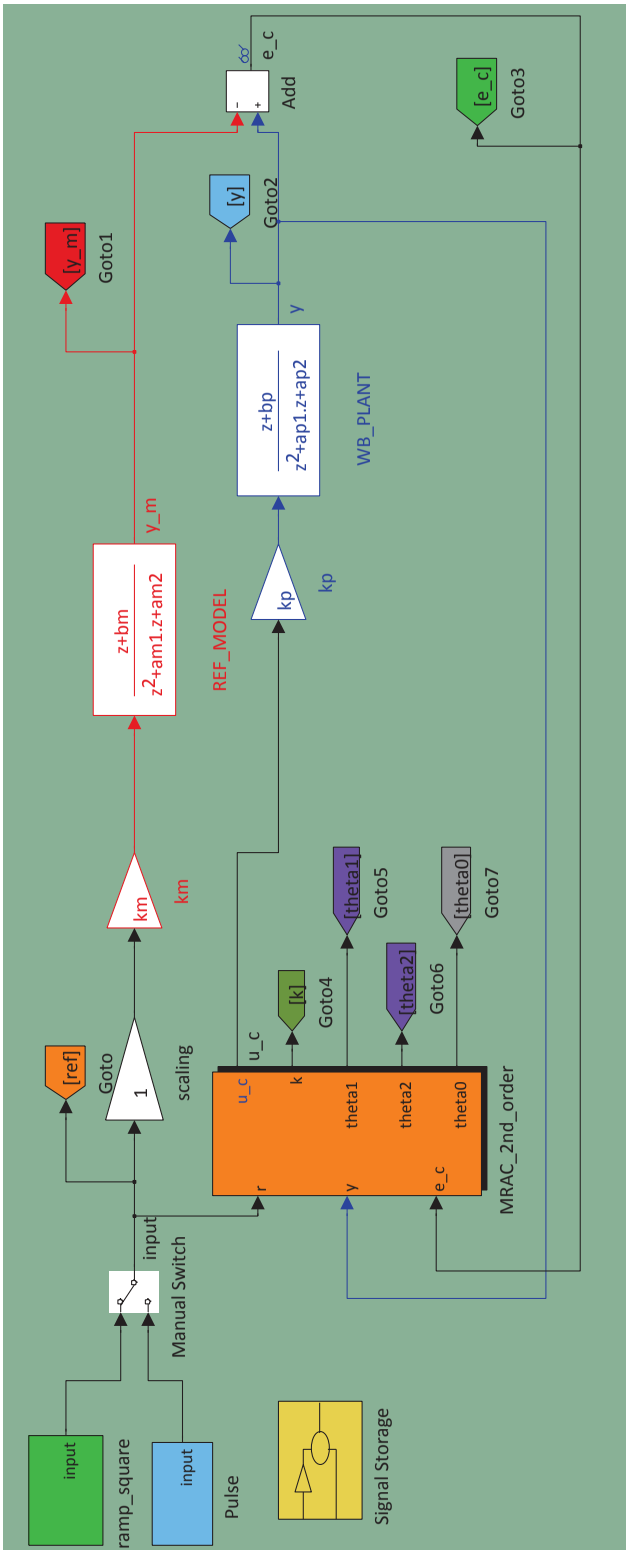

Figure 3.8: Simulink model used for the evaluation of a closed loop control system using MRAC on second order system plant of water brake

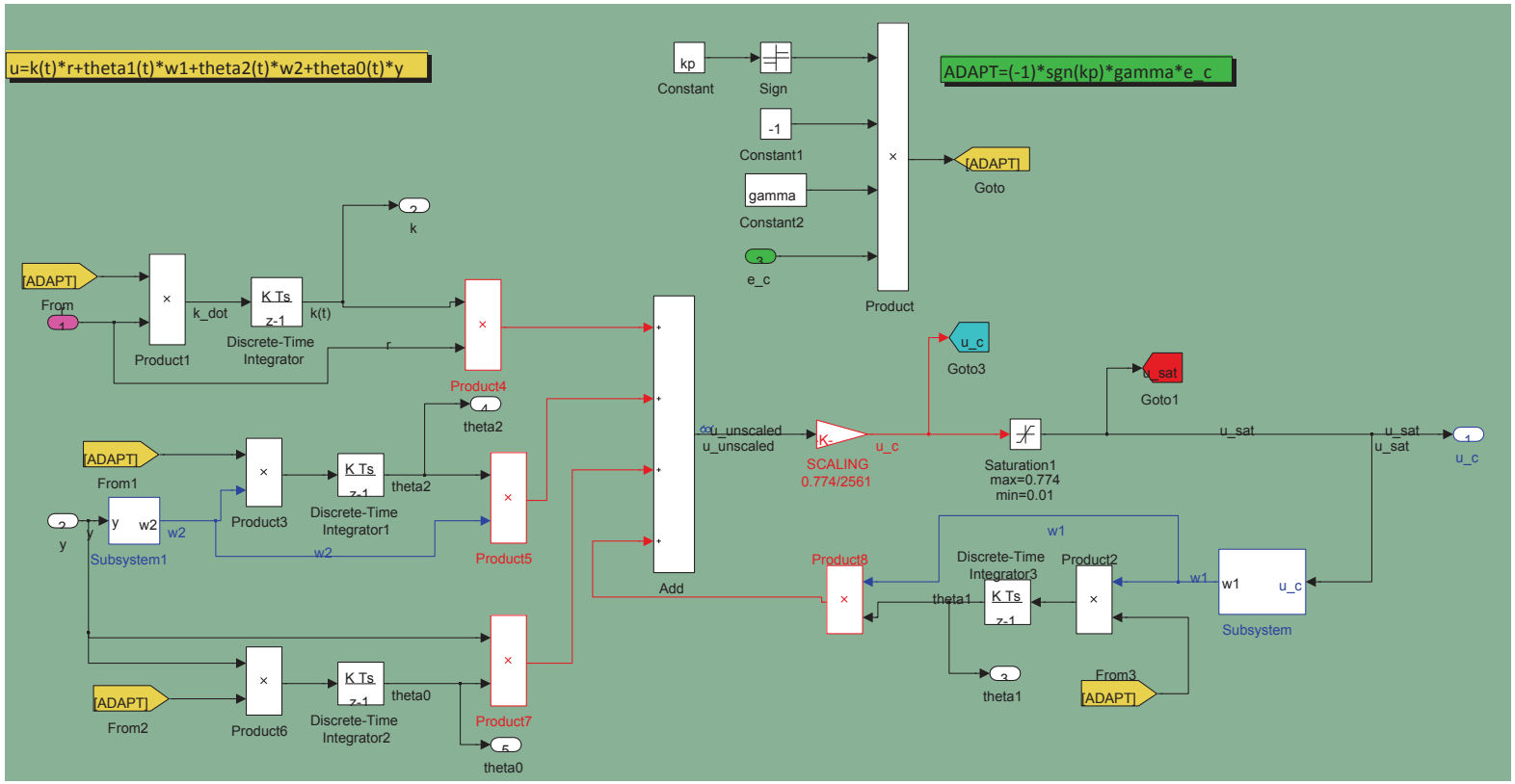

Figure 3.9: Simulink model used for the implementation of MRAC for systems of second order

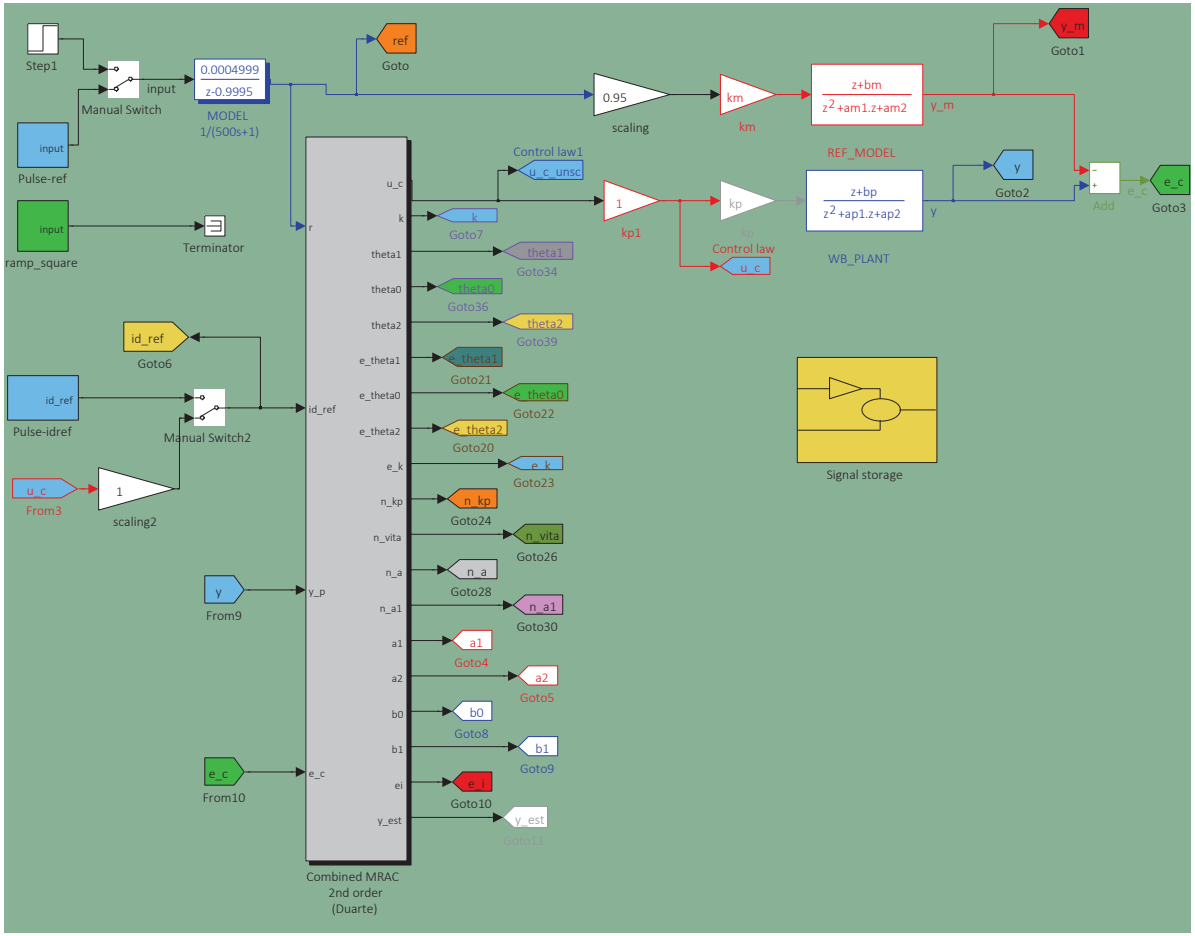

Figure 3.10: Simulink model used for the evaluation of a closed loop control system using CMRAC with S.L identifier on second order system plant of water brake

3.2.2 Heat Exchanger Experimental Device

Performance and various aspects of the three different versions of CMRAC algorithms designed, presented in chapter 4, were also tested using heat exchanger experimental device (Figure1.5). Simulink model in Figure 3.13 was created for experimental evaluation of CMRAC with RLS identifier while model shown in Figure 3.12 was created for experimental evaluation of direct MRAC. Remaining versions of CMRAC were evaluated using Simulink models similar to that shown in Figure 3.13.

Figure 3.11 is a simplified diagram of the closed loop control system setup of heat exchanger device. Controller is fed with temperature measurements, by a temperature sensor (thermocouple), and with the desired air temperature as temperature reference. Then, it produced a voltage signal (control law) using power electronics which was applied across the heating resistance. The latter heats the air stream in order to obtain the desired air temperature.

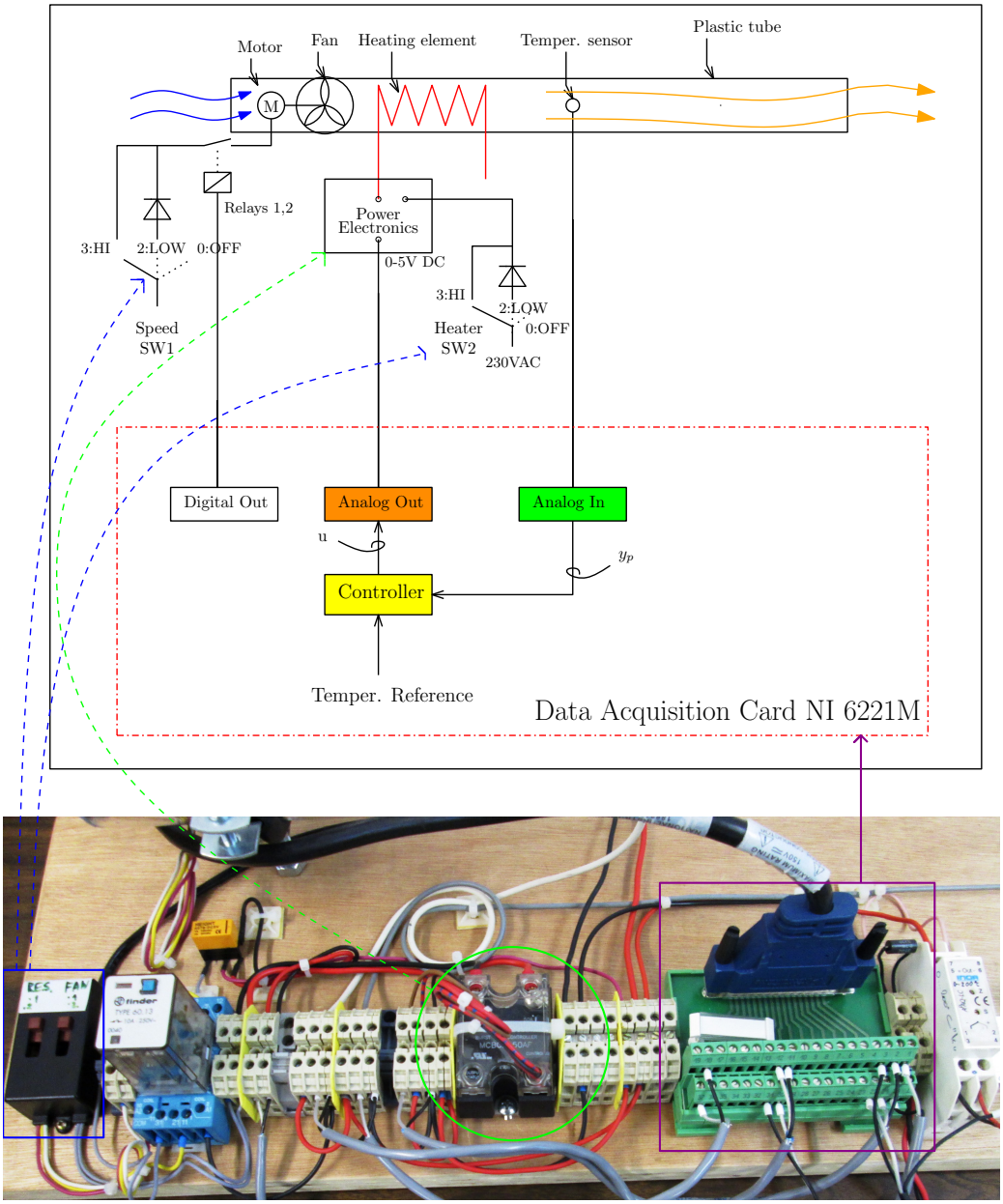

Figure 3.11: Control setup of heat exchanger experimental device at LME

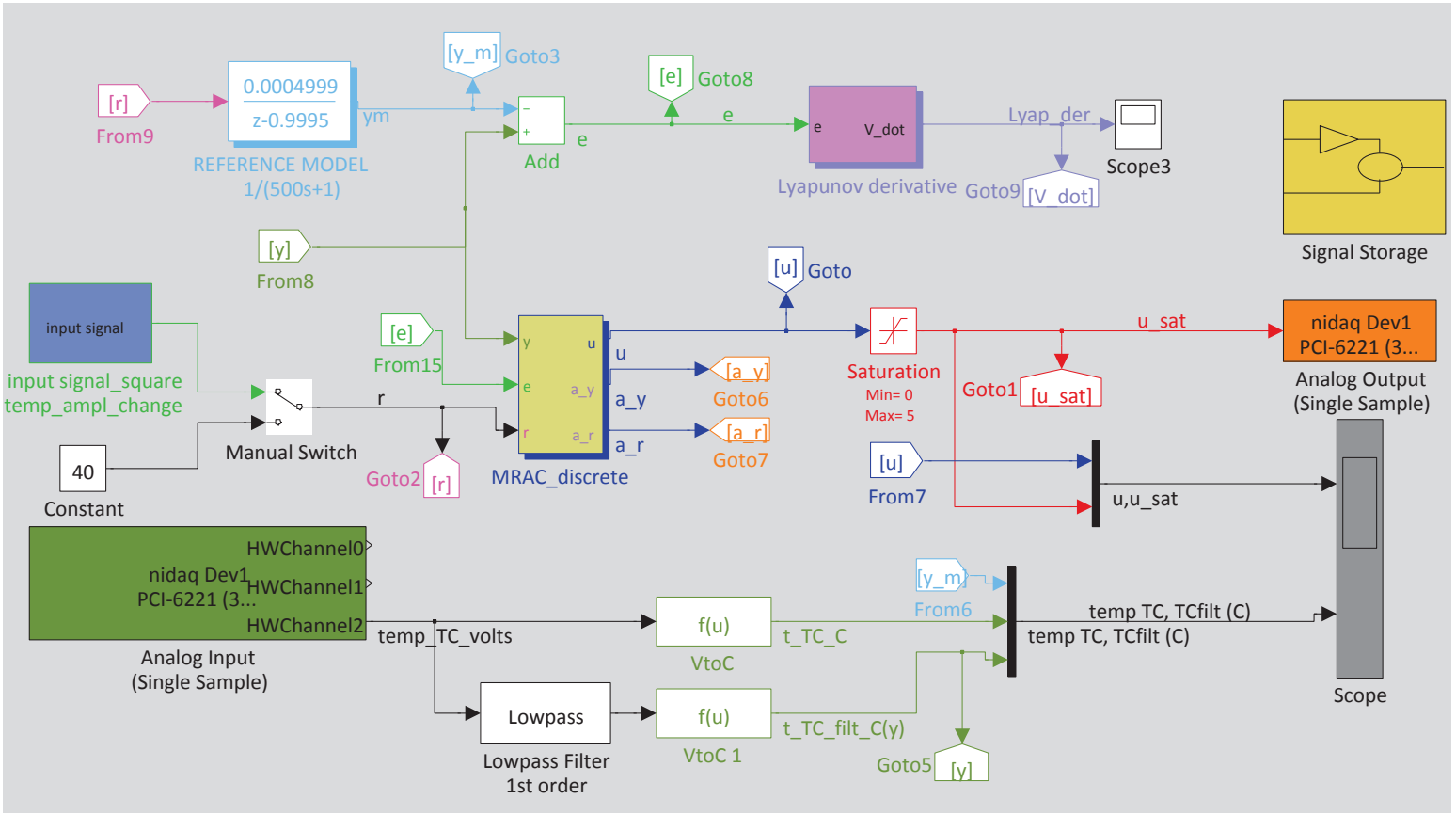

Figure 3.12: Simulink model used for the evaluation of a closed loop control system using direct MRAC on heat exchanger experimental device

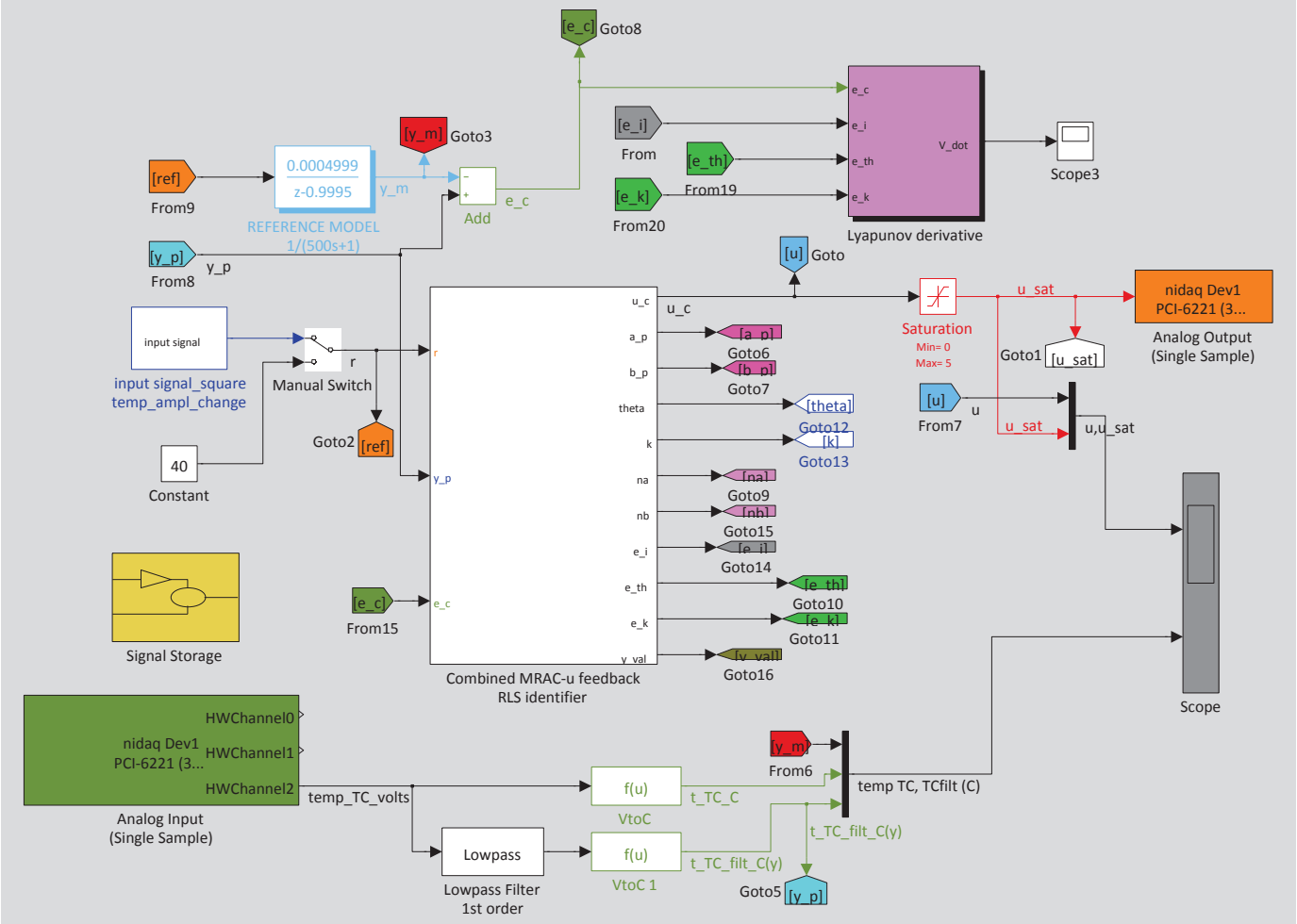

Figure 3.13: Simulink model used for the evaluation of a closed loop control system using CMRAC with RLS identifier on heat exchanger experimental device

3.2.3 Water Brake at CAT Test Bench

Final experimental evaluation trials of the adaptive controllers designed were performed at powertrain facilities of LME using CAT diesel engine test bench (Figure 3.18). Simulink model in Figure 3.15 was used for the implementation of experimental tests of CAT diesel engine load control system made with CMRAC and SL identifier. The same Simulink model was used for experimental tests of load control system made with MRAC. Regarding the control platform, the real time rapid prototyping tools of dSPACE were used, under MATLAB/Simulink (Figure 3.17). All analog sensors and actuators are connected to the dSPAC DS1103 controller board (Figure 3.16).

Figure 3.14 is a simplified diagram of CAT diesel engine's test bench control setup. Applied torque by the water brake is measured by a load cell installed on the arm of the dynamometer. Control command is supplied to the outlet analog water valve, through a electronic/pneumatic transducer, which converts the electric signal to proportional air quantity as supply to the valve. Water outlet valve control leads to water brake fill level control and consequently to applied on engine's shaft torque control. The desired torque level is fed to water brake controller as torque reference signal.

Figure 3.19 shows a water brake's free end view while Figure 3.20 shows the water output analog valve of water brake and its arm with the loadcell. Figure 3.21 shows CATERPILLAR marine diesel engine at LME. Finally, Figure 3.22 shows a water brake's coupled end view.

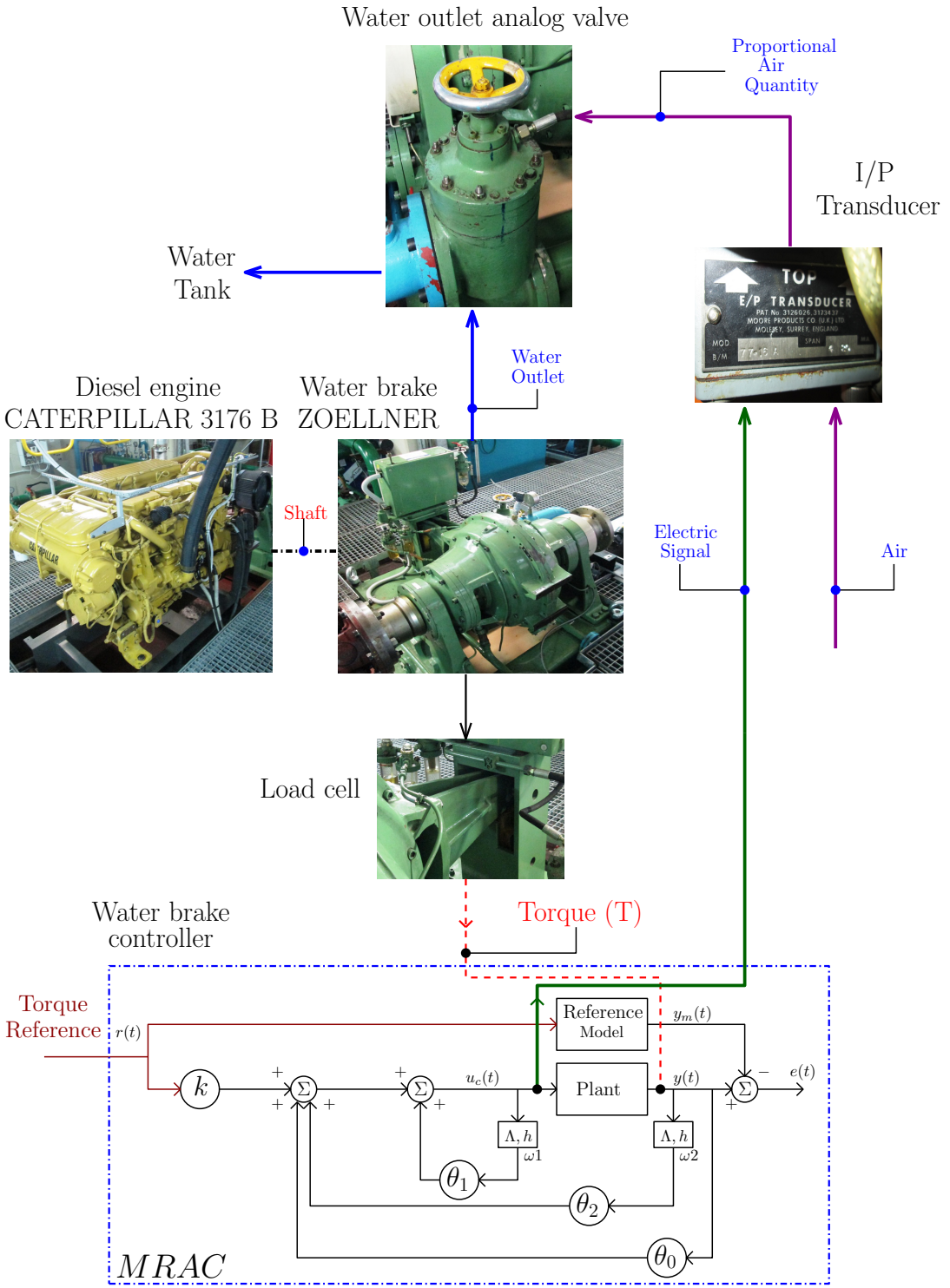

Figure 3.14: Control setup of CAT test bench in LME

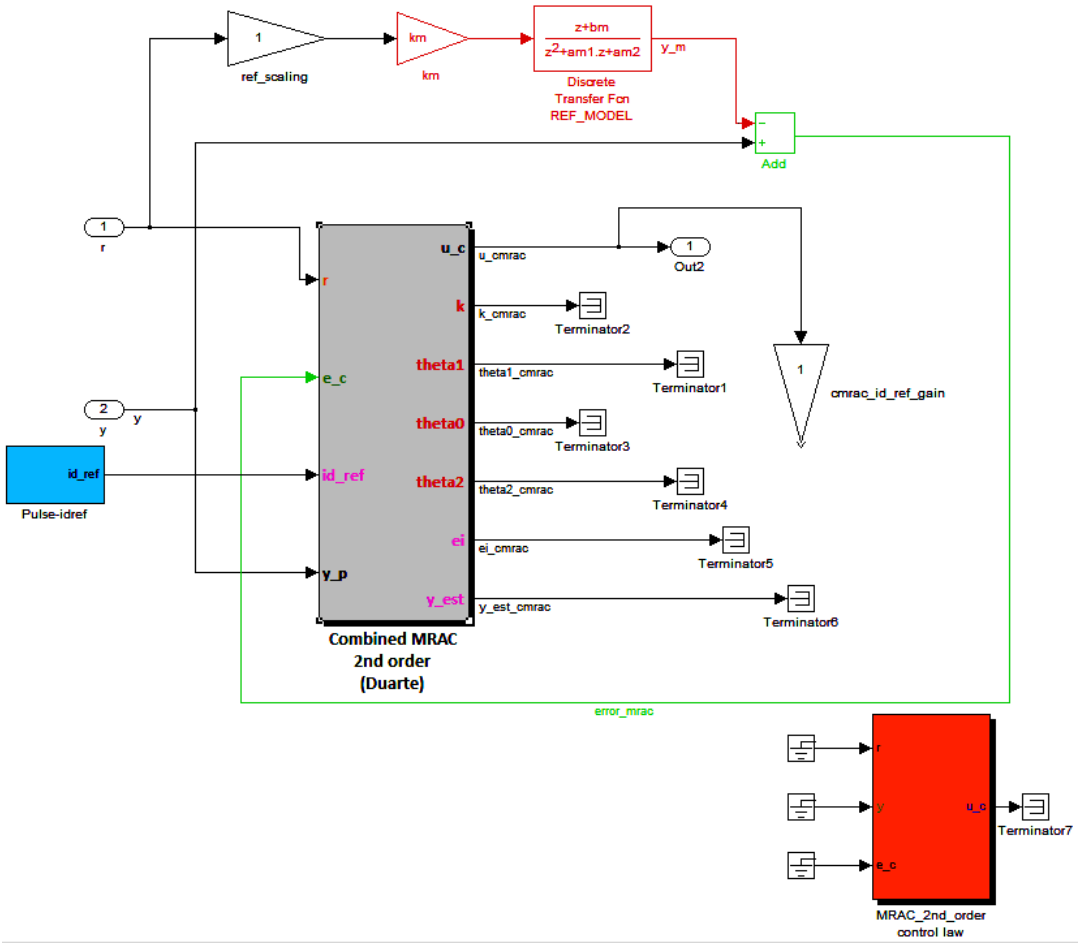

Figure 3.15: Simulink model used for load control of CAT diesel engine at LME using CMRAC with SL identifier

Figure 3.16: dSPACE DS1103 electronic control board

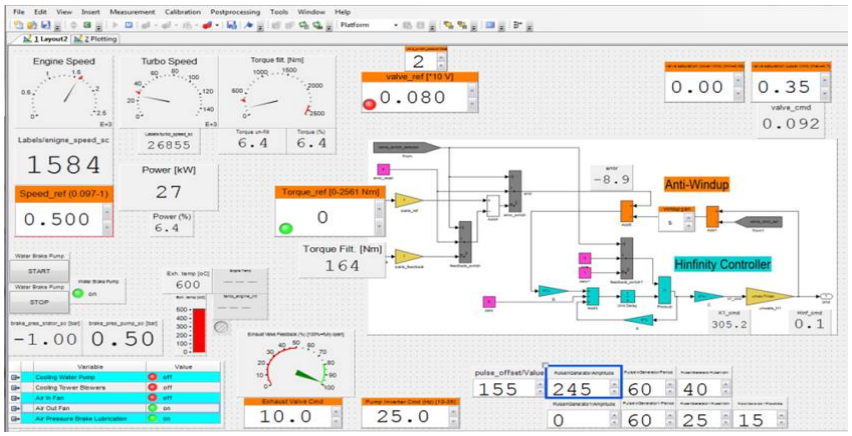

Figure 3.17: dSPACE rapid prototyping tools under MATLAB/Simulink

Figure 3.18: CAT marine diesel engine test bench at LME

Figure 3.19: Water Brake at LME - view from free end

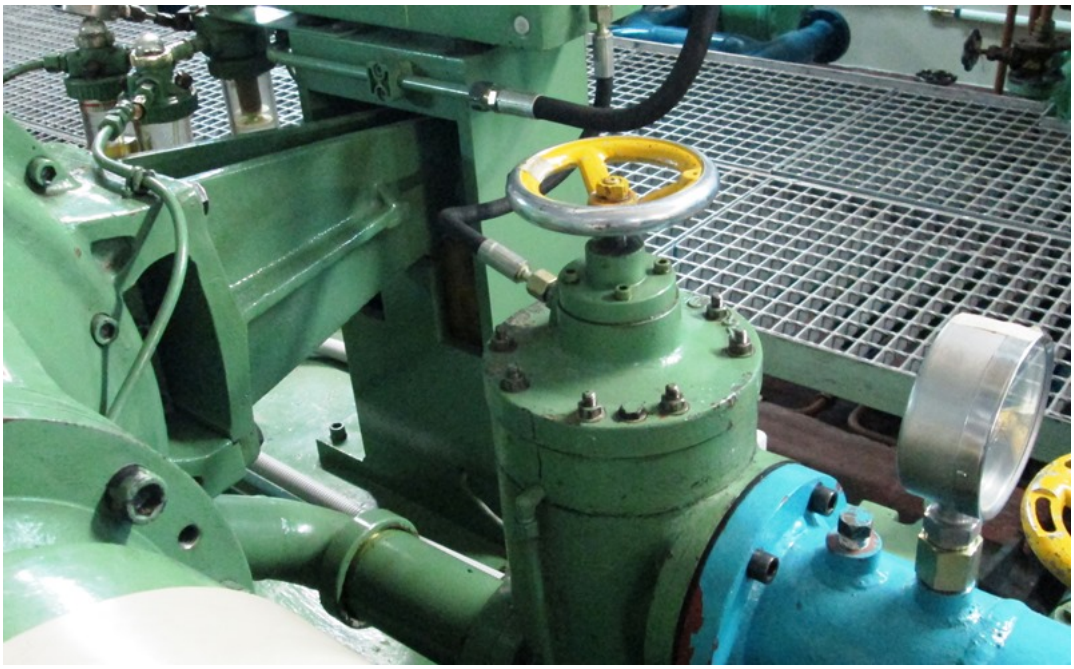

Figure 3.20: Water output analog valve and arm with loadcell

Figure 3.21: CAT marine diesel engine at LME

Figure 3.22: Water Brake at LME - view from coupled end

Chapter 4

Experimental Evaluation of Identifiers and Controllers

This chapter shows results from the experimental evaluation of system identifiers and controllers designed, which were presented in detail in the previous chapter. Testing was performed through computer simulations and on a laboratory device of LME. Final results from water brake test are the subject of the next chapter.

4.1 Evaluation of System Identification Algorithms

Results of system identification algorithms evaluation process, designed for the purposes of this Thesis, are presented in this section. Performance trials were implemented using both computer simulations and heat exchanger experimental device. Identification error and estimated plant parameters are the basic variables monitored for the evaluation of each identification algorithm performance.

Tables 4.1 and 4.2 are summarizing the trials made for each type of system identification algorithm using computer simulations and heat exchanger experimental device respectively.

Table 4.3 evaluates different aspects of each identification algorithm performance. *Adaptability* refers to the capacity of the algorithm to cope with different input signals of various frequencies and produce acceptable results. *Start-up tuning* refers to the amount of effort initially needed to make the algorithm work properly. *Optimal tuning* refers to the amount of effort needed to optimize the algorithm's function. *Needs in computer memory* refers to the storage space needed for the parameters and variables of each algorithm except from the space needed for the storage of estimated parameters. *Implementation simplicity* refers to the amount of effort needed to format the identi-

fication algorithm using MATLAB/Simulink. Finally, *stability* refers to the ability of the algorithm to produce stable estimations not only in optimal tuning but also close to optimal tuning.
All evaluation trials were performed using MATLAB/Simulink.

Table 4.1: System Identification Evaluation Trials-Computer Simulations

Plant \ **Trial**		Constant Plant Parameters	Changing Plant Parameters	Low Frequency Input Signal	High Frequency Input Signal
Literature Plant	RLS	✓	✓	×	×
	RIV	✓	✓	×	×
	SL	✓	✓	×	×
Heat Exchanger Plant	RLS	×	×	✓	✓
	RIV	×	×	✓	✓
	SL	×	×	✓	✓

Table 4.2: System Identification Evaluation Trials-Experimental Trials

System Plant \ **Evaluation Trial**		$\lambda = 0.99$	$\lambda = 0.95$	$\gamma_{sl} = 1$	$\gamma_{sl} = 0.7$
Heat Exchanger Device	RLS	✓	✓	×	×
	RIV	✓	✓	×	×
	SL	×	×	✓	✓

Table 4.3: System Identification Algorithms Evaluation

Identification Algorithm / **Criterion**	RLS	RIV	SL
Response to plant parameters changes	Good	Good only in optimal tuning	Good
Response to forgetting factor changes	Good	Bad	Good
Response to high rate amplitude changes	Satisfactory	Unstable	Good
Adaptability	Good	Bad	Good
Start-up tuning	Regular	Difficult	Easy
Optimal tuning	Regular	Always Difficult	Regular
Needs in computer memory	Big	Very Big	Normal
Implementation simplicity	Regular	Difficult	Regular
Stability	Good	Good only in optimal tuning	Good

4.1.1 Computer Simulations

System identification algorithms evaluation through computer simulations were performed using two system plant mathematical models. The first plant was taken from a literature example [16], so that results comparisons and check of the system identification algorithms proper design and function could be done by making similar simulations. It was a second order system plant represented by a discrete time transfer function. The second plant was a first order mathematical model of heat exchanger experimental device formed using data measured from a heat exchanger's reaction curve[1] to a step input. This model gives accurate results for temperature changes between 30 and 45 ^oC degrees since the open-loop measurement used for its calculation was a corresponding change of temperature. The model was used to perform simulations in order to gain some experience in tuning the three types of identification algorithms and make tuning of experimental evaluation of the system identification algorithms easier.

Simulations on the literature plant were performed with both constant and changing plant parameters so as to simulate the conditions of a real process as better as possible. Plant parameters change was achieved by a duplication of discrete transfer function's gain. Simulations on heat exchanger plant were performed with input signals of two different frequencies as latter's value affects identification algorithm effectiveness.

System excitation was applied using four different input signals

- Square signal
- Sinusoidal signal
- Square signal of changing frequency (PRBS signal)
- Sinusoidal signal of changing frequency (Chirp signal)

These types of input signals are *persistently exciting*[2] and are the most frequently used signals for system identification purposes.

Most representative results of all the trials performed, using mathematical models presented above, and tables with the values of each algorithm tuning parameters are presented below. Comments on identification algorithms performance are also listed for each trial. The type of input signal, the plant parameters estimations, the identification error and the validation of estimated plant output signal are depicted in the following figures for each plant used and for each kind of evaluation trial performed.

More results from evaluation trials of system identification algorithms using computer simulations can be found in Appendix A.

[1] This kind of system identification is known as *process reaction curve method*

[2] More details about *persistent excitation* can be found in Appendix C

Computer Simulations using Plant from Literature - Comments

- Constant plant parameters
  - RLS algorithm, Figures 4.1, 4.2, A.1, A.2 and Tables 4.4, A.1.
    - Low values of identification error.
    - Smooth variation of estimated parameters.
  - RIV algorithm, Figures A.5, A.7 and Tables A.3, A.4 respectively.
    - Low values of identification error.
    - Smooth variation of estimated parameters.
    - Sharp oscillation at the beginning of identification process using sinusoidal input signal. Fast elimination of it.
  - SL algorithm, Figures A.9, A.10 and Table A.5.
    - Low values of identification error.
    - Smooth variation of estimated parameters.
- Changing plant parameters
  - RLS algorithm, Figures A.3, A.4 and Table A.2.
    - Successful estimation of output signal's change of amplitude.
    - Fast elimination of identification error's peak at the time of output signal's amplitude duplication.
  - RIV algorithm, Figures A.6, A.8 and Tables A.3, A.4 respectively.
    - Unsuccessful estimation of output signal's amplitude change using square input signal. Unstable performance.
    - Slow minimization rate of identification error using sinusoidal input signal.
    - Sharp variation of estimated parameters at the time of plant parameters change.
  - SL algorithm, Figures 4.3, 4.4, A.11, A.12 and Tables 4.5, A.6 respectively.
    - Successful estimation of output signal's change of amplitude.
    - Small peak of identification error at the time of plant parameters change. Fast elimination of it.

Table 4.4: RLS tuning parameters

	n	λ	$\hat{\theta}_0$	$\overline{x}_0$	P_0
RLS	3	0.99	I_{31}	I_{31}	$1000 * I_3$

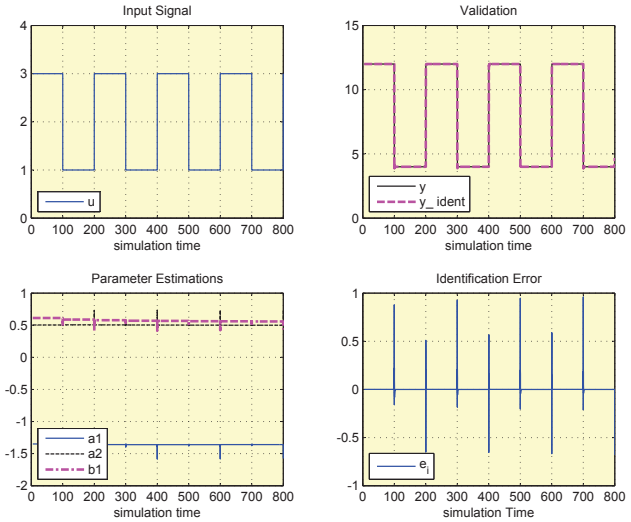

Figure 4.1: Results of RLS identification applied on literature plant stimulated with square input signal

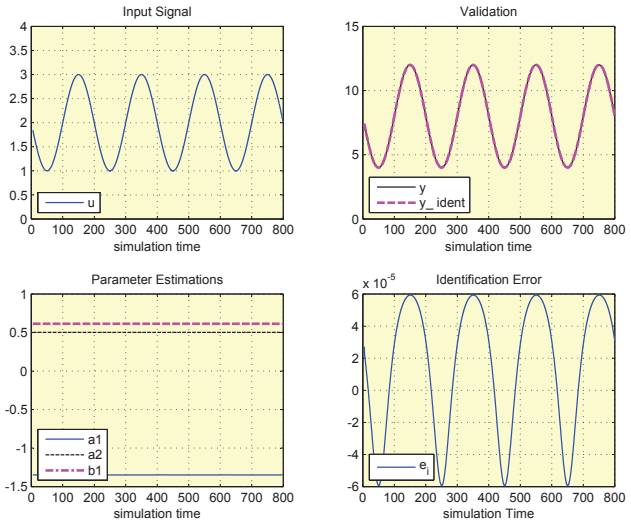

Figure 4.2: Results of RLS identification applied on literature plant stimulated with sinusoidal input signal

Table 4.5: SL tuning parameters

	n	γ_{sl}	$\hat{\theta}_0$	$\overline{x}_0$
SL	3	1	I_{31}	I_{31}

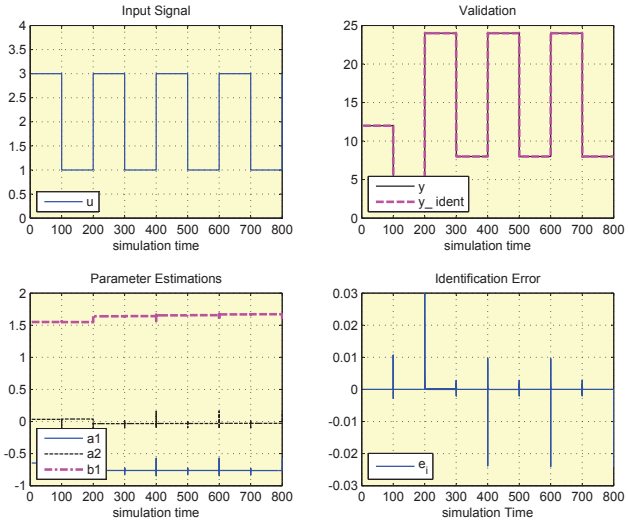

Figure 4.3: Results of SL identification applied on literature plant with changing parameters stimulated with square input signal

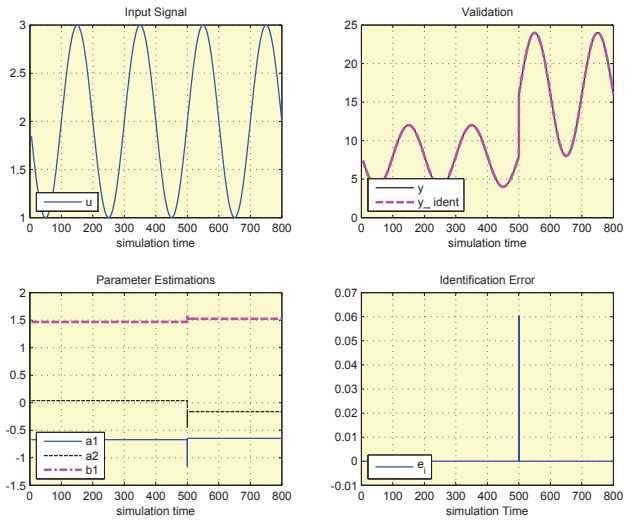

Figure 4.4: Results of SL identification applied on literature plant with changing parameters stimulated with sinusoidal input signal

Computer Simulations using Heat Exchanger Plant - Comments

- Input signal of low frequency
  - RLS algorithm, Figures 4.5, 4.6 and Table 4.6.
    - Slow rate of identification error minimization.
    - Smooth variation of estimated parameters.
  - RIV algorithm, Figures A.13, A.14 and Table A.7.
    - Slow rate of identification error minimization. Need for bigger simulation time in order for the identification error to be minimum.
    - Smooth variation of estimated parameters.
    - Sharp oscillation of estimated output signal and estimated parameters at the beginning of identification process using sinusoidal input signal. Fast elimination of it.
  - SL algorithm, Figures A.17, A.18 and Table A.9.
    - Fast rate of identification error minimization. Low values of identification error.
    - Smooth variation of estimated plant parameters.
- Input signal of high frequency
  - RLS algorithm, Figures 4.7, 4.8 and Table 4.7.
    - Faster rate of identification error minimization. Better performance of system identification algorithm.
  - RIV algorithm, Figures A.15, A.16 and Table A.8.
    - Slight improvement of identification algorithm performance.
    - Same characteristics of estimated parameters and output signal's estimation fluctuations using sinusoidal input signal.
  - SL algorithm, Figures A.19, A.20 and Table A.10.
    - Faster rate of identification error minimization. Better performance of system identification algorithm.
    - Low values of identification error.

Table 4.6: RLS tuning parameters

	n	λ	$\hat{\theta}_0$	$\overline{x}_0$	P_0
RLS	2	0.99	I_{21}	I_{21}	$1000 * I_2$

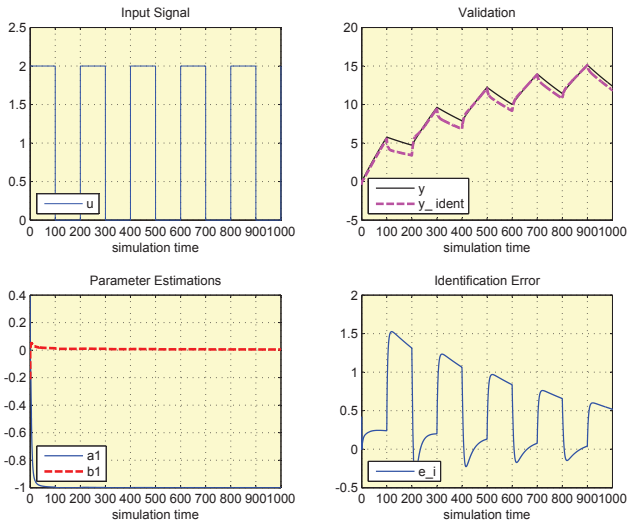

Figure 4.5: Results of RLS identification applied on heat exchanger plant stimulated with square input signal of low frequency

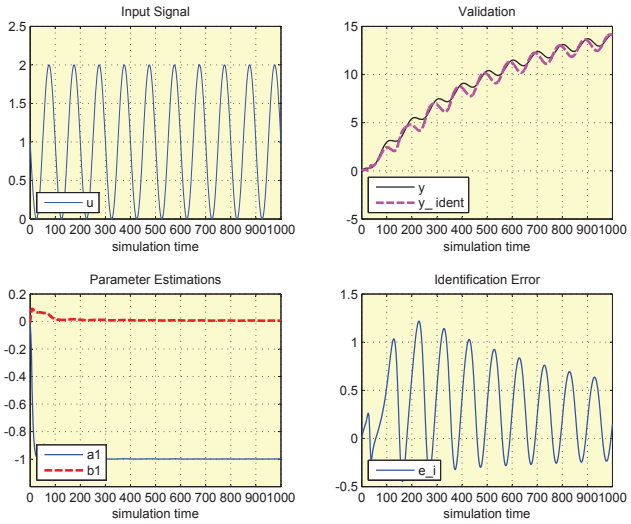

Figure 4.6: Results of least squares system identification applied on heat exchanger plant stimulated with sinusoidal input signal of low frequency

Table 4.7: RLS tuning parameters-Input of high frequency

RLS	n	λ	$\hat{\theta}_0$	$\overline{x}_0$	P_0
	2	0.99	I_{21}	I_{21}	$1000 * I_2$

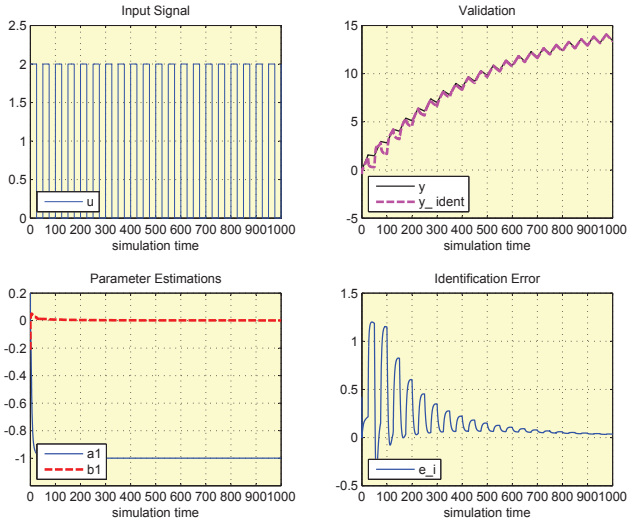

Figure 4.7: Results of RLS identification applied on heat exchanger plant stimulated with square input signal of high frequency

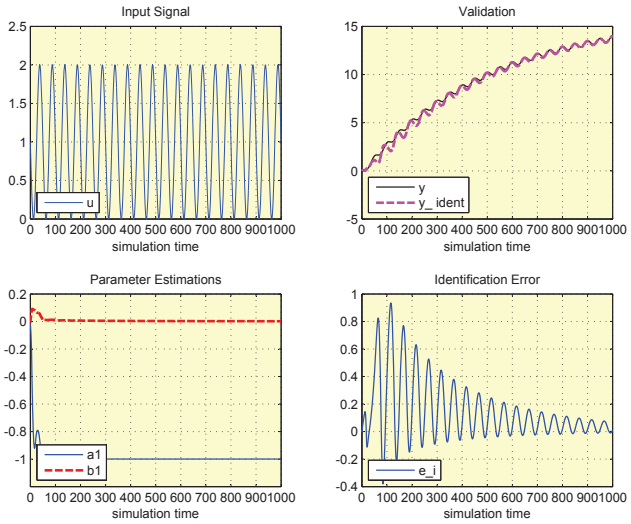

Figure 4.8: Results of RLS identification applied on heat exchanger plant stimulated with sinusoidal input signal of high frequency

4.1.2 Experiments using Heat Exchanger Experimental Device

Evaluation of system identification algorithms was completed using heat exchanger experimental device. Identifiers performance was tested in on-line real-time identification processes. Moreover, the algorithms designed were tested in a laboratory environment and on a real process characterized with many features that most real processes have like measurement noise, external disturbances and varying environmental conditions (performance of identification algorithms during winter and summer period was not the same).

Most representative results of the trials performed and tables with the values of each algorithm tuning parameters are presented in this section. The depicted Results, for each system identification algorithm, were produced using different values of directional forgetting factor λ and of scalar gain γ_{sl} so that their effect in the performance of identification algorithm can be clearly shown. Values of λ used were λ = 0.99 and λ = 0.95 and values of γ_{sl} used were γ_{sl} = 0.7 and γ_{sl} = 1 as they are most commonly used in practice [16].

Comments on identification algorithms performance are also listed for each experimental trial. More results from evaluation trials of system identification algorithms using heat exchanger device can be found in Appendix A.

Experimental Trials using Heat Exchanger - Comments

- R.L.S algorithm, Figures 4.9, 4.10, A.21, A.22 and Tables 4.8, A.11.
  - Stable performance of the identification algorithm. Almost unaffected by directional forgetting factor changes.
- R.I.V algorithm, Figures 4.11, 4.12, A.23, A.24 and Tables 4.9, A.12.
  - Unstable performance when λ = 0.99 and square input signal used.
  - Small and slowly eliminating oscillation of estimated output signal when λ = 0.99 and sinusoidal input signal used.
  - Stable performance when λ = 0.95 used for both types of input signal. Smaller and faster eliminating oscillation of estimated output signal.
- S.L algorithm, Figures 4.13, 4.14, A.25, A.26 and Tables 4.10, A.13.
  - Stable performance using both values of scalar gain γ_{sl}.
  - Low values of identification error. Smooth variation of estimated plant parameters.

Table 4.8: RLS tuning parameters

	n	λ	$\hat{\theta}_0$	$\overline{x}_0$	P_0
RLS	2	0.99	I_{21}	I_{21}	$1000 * I_2$

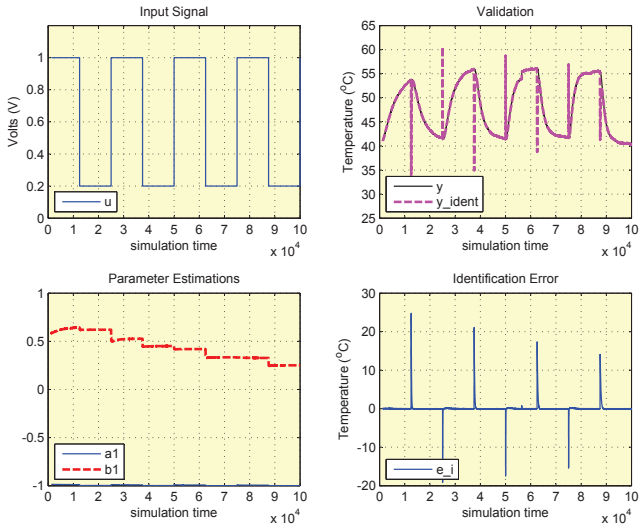

Figure 4.9: Results from RLS identification applied on heat exchanger experimental device stimulated with square input signal

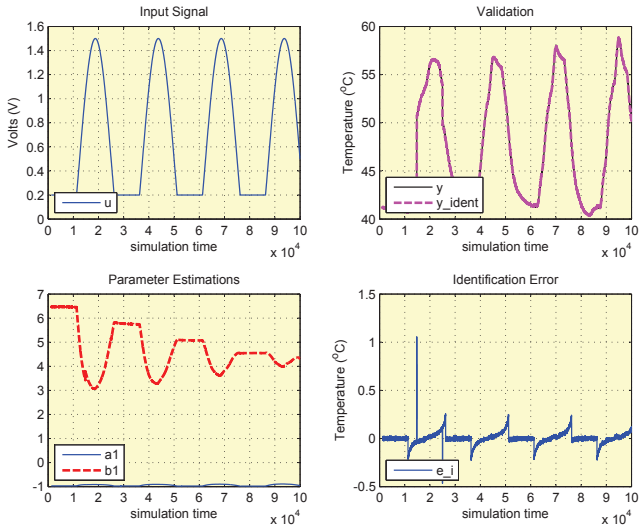

Figure 4.10: Results from RLS identification applied on heat exchanger experimental device stimulated with sinusoidal input signal

Table 4.9: RIV tuning parameters

RIV	n	λ	$\hat{\theta}_0$	$\overline{x}_0$	v_0	P_0
	2	0.99	$[-0.1 - 0.1]^\top$	$[-0.1 - 0.1]^\top$	$[-0.1 - 0.1]^\top$	$1000 * I_2$

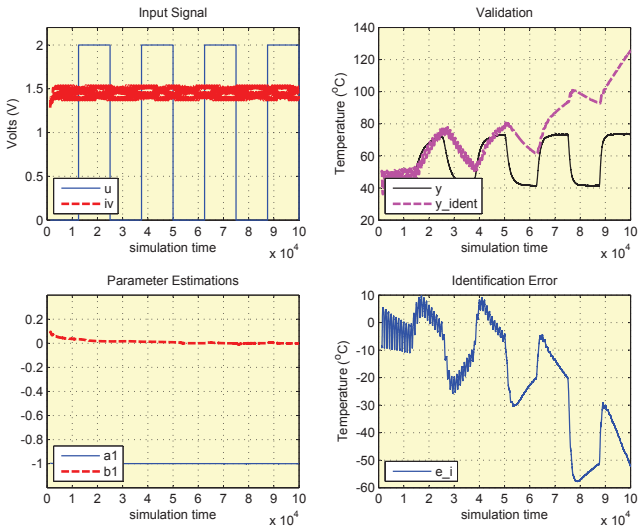

Figure 4.11: Results from RIV identification applied on heat exchanger experimental device stimulated with square input signal

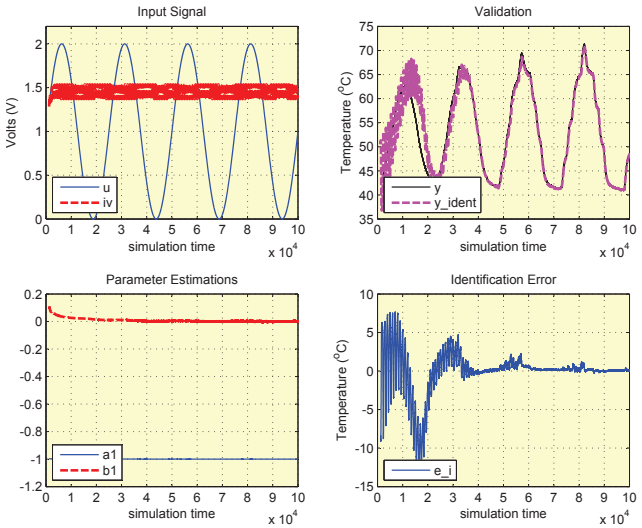

Figure 4.12: Results from RIV identification applied on heat exchanger experimental device stimulated with sinusoidal input signal

Table 4.10: SL tuning parameters

SL	n	γ_{sl}	$\hat{\theta}_0$	$\overline{x}_0$
	2	1	I_{21}	I_{21}

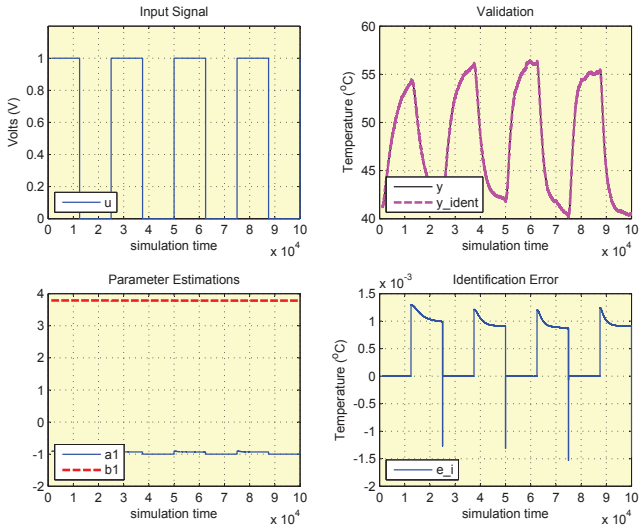

Figure 4.13: Results from SL identification applied on heat exchanger experimental device stimulated with square input signal

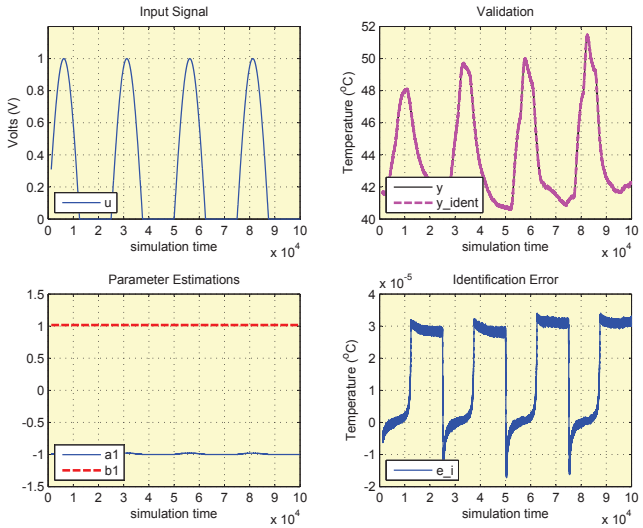

Figure 4.14: Results from SL identification applied on heat exchanger experimental device stimulated with sinusoidal input signal

4.1.3 Conclusions

Generally, all system identification algorithms used had satisfactory performance with the identification error converging to zero. The rate of identification error's minimization was sufficiently high and variation of estimated plant parameters was quite smooth which is necessary for small oscillations[3] of estimated plant output signal. Negative values and high values[4] of input signal amplitude caused unstable performance of all identification algorithms.

Amplitude Change

An increase of one hundred percent (100%) in plant output signal amplitude seemed not to affect the performance of identification algorithms except from the performance of RIV algorithm. Increase of 100% in output signal amplitude and high rate of input signal change of amplitude caused unstable performance of RIV algorithm by generating sharp variations of estimated plant parameters and increasing identification error. This algorithm performed better when the increase in output signal amplitude was smaller and the rate of input signal change of amplitude was lower (sinusoidal input signal) or restricted (use of a rate limiter). Increase of plant output signal much greater than 100% caused instabilities to all the identification algorithms.

Input Signal Frequency

An increase of one hundred percent (100%) in input signal frequency seemed to improve the performance of all system identification algorithms used by increasing the rate of identification error minimization (Figures 4.5, 4.6 and 4.7, 4.8). However, frequency increase had to be carefully tuned as very high values of input signal frequency caused identification algorithms malfunctions. RIV algorithm took more time in order to minimize the identification error and stabilize its estimation of output signal. In addition, its performance was less improved comparatively to the performance of the other two identification algorithms.

Forgetting Factor

RLS algorithm was almost unaffected by the change of directional forgetting value between the limits selected. In contrast, RIV algorithm's stability was strongly affected. Furthermore, oscillations of estimated output signal were eliminated using a directional

[3]The absence of estimated output signal oscillations is very important for the stable performance of a Combined Model Reference Adaptive Controller.

[4]High values of input signal amplitude usually excite system dynamics of high order.

forgetting factor of lower value. SL algorithm performance was almost unaffected by the change of scalar gain γ_{sl} value, too. Identification error was the lowest possible when γ_{sl} was equal to 1.

4.2 Evaluation of Control Algorithms

Results of controllers evaluation process are presented in this section. The three versions of Combined Model Reference Adaptive Controllers (CMRAC) designed were evaluated using both computer simulations and heat exchanger laboratory device. Control error, control law, controller parameters and closed-loop estimation errors are some of the signals monitored for the evaluation of each controller performance. Transient and steady-state response of closed-loop control systems were also examined. Computer simulations and experiments were also performed using direct Model Reference Adaptive Control (MRAC) in order to compare its results with those taken from simulations and experiments using CMRAC.

Table 4.11 summarizes the evaluation trials performed through computer simulations presented in this section.

Table 4.11: Control Evaluation Trials-Computer Simulations

System Plant \ **Evaluation Trial**		Reference of constant amplitude	Reference of changing amplitude	Use of dead zone
Literature Plant	CMRAC-RLS	✓	×	✓
	CMRAC-RIV	✓	×	✓
	CMRAC-SL	✓	×	✓
	MRAC	✓	×	✓
Heat Exchanger Plant	CMRAC-RLS	✓	✓	✓
	CMRAC-RIV	✓	✓	✓
	CMRAC-SL	✓	✓	✓
	MRAC	✓	✓	✓

Table 4.12 summarizes the experimental evaluation trials performed and presented in this section. Table 4.13 shows mean values of control error of all the experimental control evaluation trials presented in this chapter which is a simple criterion for control algorithms effectiveness comparison.

Table 4.14 evaluates different aspects of each control algorithm performance. *Adaptability* refers to the capacity of the algorithm to cope with reference signals of higher amplitude. *Start-up tuning* refers to the amount of effort initially needed to make the algorithm work properly. *Optimal tuning* refers to the amount of effort needed

Table 4.12: Control Evaluation Trials-Heat Exchanger Experimental Device

System Plant \ Evaluation Trial		Reference of constant amplitude	Reference of changing amplitude	Use of dead zone
Heat Exchanger Device	CMRAC-RLS	✓	✓	✓
	CMRAC-RIV	✓	✓	✓
	CMRAC-SL	✓	✓	✓
	MRAC	✓	✓	✓

Table 4.13: Mean values of control error from experimental evaluation trials

Reference \ Trial		Reference of constant amplitude	Reference of constant amplitude dead-zone	Reference of changing amplitude	Reference of changing amplitude dead-zone
Square	MRAC	−0.3537	−0.4324	−0.4153	−0.3825
	CMRAC-RLS	−0.4342	−0.0211	−0.4312	−0.5036
	CMRAC-RIV	−0.5542	−0.7136	−0.6817	−0.5309
	CMRAC-SL	−0.4764	−0.6290	−0.4890	−0.4958
Sinusoidal	MRAC	−0.2931	−0.3118	×	×
	CMRAC-RLS	−0.4172	−0.3596	×	×
	CMRAC-RIV	−0.4130	−0.7228	×	×
	CMRAC-SL	−0.3490	−0.3188	×	×

to optimize algorithm's function. *Needs in computer memory* refers to the storage space needed for the parameters and variables of each algorithm. *Implementation simplicity* refers to the amount of effort needed to format the control algorithm using MATLAB/Simulink. Finally, *stability* refers to the ability of the algorithm to produce stable results and maintain its convergence properties not only in optimal tuning but also close to optimal tuning.

Table 4.14: Control Algorithms Evaluation

Criterion \ Controller	MRAC	CMRAC-RLS	CMRAC-RIV	CMRAC-SL
Response to reference model amplitude changes	Good only in optimal tuning	Good	Good only in optimal tuning	Good
Response to presence of measurement noise	Stable	Stable	Stable	Stable
Performance using dead-zone	Satisfactory	Good	Bad	Good
Adaptability	Satisfactory	Regular	Bad	Regular
Start-up tuning	Easy	Regular	Difficult	Easy
Optimal tuning	Regular	Regular	Always Difficult	Regular
Needs in computer memory	Small	Normal	Big	Normal
Implementation simplicity	Easy	Regular	Difficult	Regular
Stability	Good only in optimal tuning	Good	Good only in optimal tuning	Good

4.2.1 Computer Simulations

Evaluation of the three different versions of CMRAC designed (CMRAC-RLS, CMRAC-RIV, CMRAC-SL) and of direct MRAC using computer simulations were performed using two system plant mathematical models. The first plant was taken from an example in the literature [3] so that results comparisons and check of control algorithms proper design and function could be done by making similar simulation trials. This was a first order system plant represented by a discrete time transfer function. The second plant was a first order discrete time system plant of heat exchanger device used for simulating heating and cooling processes of air temperature. It was calculated in the same way as the one presented in the previous section. This plant was used to perform simulations using all of the controllers in order to gain some experience in tuning control algorithms when changes in reference signal were imposed and when robustness technique of dead-zone was applied.

Evaluation trials using literature plant were performed with reference input signals of constant amplitude. Three different types of reference input signals were used

- Step reference signal
- Square reference signal
- Sinusoidal reference signal

Simulations with the plant of heat exchanger were performed using not only reference input of constant amplitude but also of changing amplitude. Reference changes of amplitude, in the simulations performed with heat exchanger plant, were representing air temperature changes and all of them were within the temperature range where the plant mathematical model was producing accurate results.

Most representative results of all the control evaluation trials performed along with tables with the values of control algorithms tuning parameters are presented below. Except from the figures depicting the values of control law, control parameter estimations and control error, figures depicting the trajectories of controller parameters, plant parameter errors and of closed-loop estimation errors are included which are representative of control systems stability and convergence properties. Comments on control algorithms performance for each evaluation trial are shown below.

More results from evaluation trials of control algorithms using computer simulations can be found in Appendix B.

Computer Simulations using Plant from Literature - Comments

CMRAC

In general, the performance of CMRAC was satisfactory whatever the type of reference signal being used was. Control error and closed-loop estimation errors were fluctuating close to zero value. Control parameters estimates fluctuation was very smooth and system's transient response was oscillatory only at the beginning of each evaluation trial having small or no overshoot. Trajectories of controller parameters and closed-loop estimation errors were converging to a small region of the plane which is a proof of control algorithm's stable performance. Corresponding Figures are 4.15 to 4.18, B.5, B.6, B.9, B.10 and Tables 4.15, 4.16, B.3 and B.5.

CMRAC-RIV did not perform well when any type of the reference signals used was applied. Control error and closed-loop estimation errors were not converging to zero and as a result system's response could not "follow" the response of reference model. Trajectories of control parameters and closed-loop estimation errors were also not converging to a stable value and to zero, respectively. Corresponding Figures are B.7 and B.8 and Table B.4.

MRAC

MRAC performance was seriously affected by the choice of reference signal. MRAC performed very well when step reference input was used. Control parameters reached a stable value and control error converged fast to zero. Transient response was characterized by small overshoot and small settling time. However, when square or sinusoidal reference signal was used performance of MRAC was not satisfactory. Convergence of control error and control parameters was unsuccessful. Corresponding Figures are B.1 to B.4 and Tables B.1 and B.2.

Table 4.15: CMRAC-RLS identifier tuning parameters

CMRAC_ RLS	γ	n	λ	$\hat{\theta}_0$	$\overline{x}_0$	P_0
	2	2	1	I_{21}	I_{21}	$1000 * I_2$

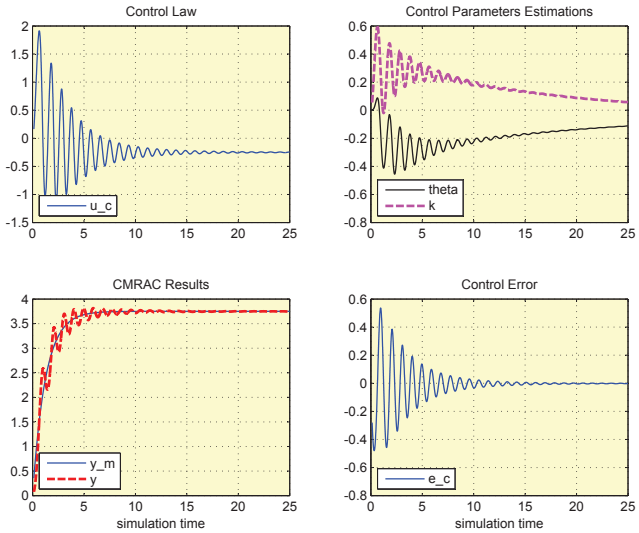

Figure 4.15: CMRAC-RLS of literature plant stimulated with step input signal

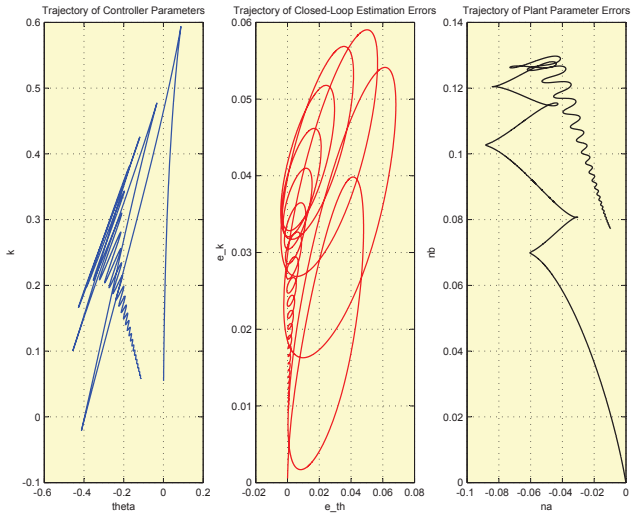

Figure 4.16: Trajectories of closed-loop estimation errors, plant parameter errors and controller parameters presented in Figure 4.15

Table 4.16: CMRAC-SL identifier tuning parameters

CMRAC_ SL	γ	n	γ_{sl}	$\hat{\theta}_0$	$\overline{x}_0$
	2	2	1	I_{21}	I_{21}

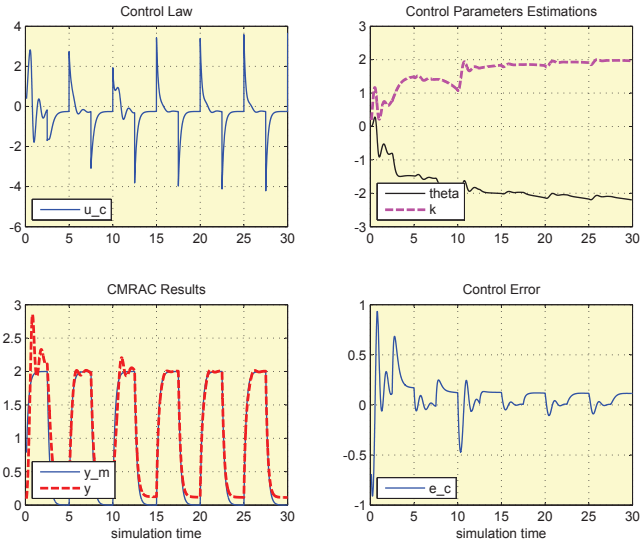

Figure 4.17: CMRAC-SL of literature plant stimulated with square input signal

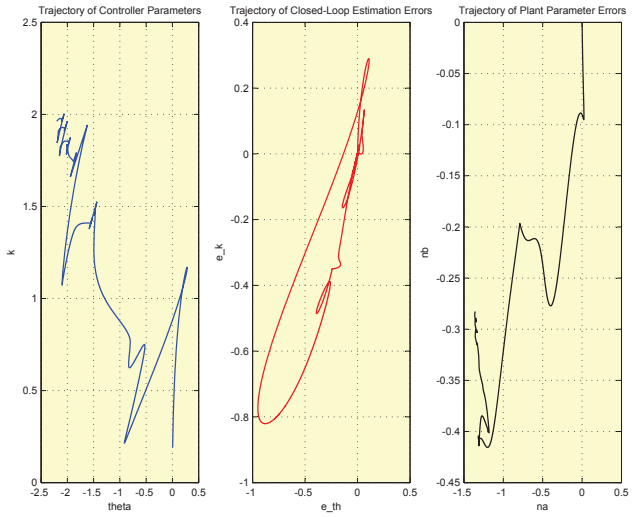

Figure 4.18: Trajectories of closed-loop estimation errors, plant parameter errors and controller parameters presented in Figure 4.17

Computer Simulations using Heat Exchanger Plant - Comments

Reference Signal of Constant Amplitude

Both MRAC and CMRAC performed well when a reference signal of constant amplitude was used. Control error and closed-loop estimation errors were converging to zero with the trajectories of the latter and of control parameters converging to a small area of the plane. Overshoot occurred at the beginning of the evaluation trials and when amplitude of reference model response changed, was very fast eliminated. Corresponding Figures are B.12, B.13, B.16, B.17 and Tables B.6, B.8.

Performance of CMRAC-RIV was unsuccessful when square reference signal was used. Control error and closed-loop estimation errors were not converging to zero value. System's response remained oscillatory through the whole duration of the evaluation trial. Performance of CMRAC-RIV was satisfactory when sinusoidal reference signal was used. Corresponding Figures are B.14, B.15 and Table B.7.

Reference Signal of Changing Amplitude

Both MRAC and CMRAC performed successfully when the change of amplitude in reference model response occurred leading to a system's response close to the corresponding one of reference model. However, the system's response tended to be more oscillatory when reaching higher values after reference model change of amplitude occurred. These oscillations were of bigger amplitude when CMRAC-RIV was used. The trajectories of controller parameters and closed-loop estimation errors verified the fact that each of them converged to the desired value required for a good performance. Corresponding Figures are 4.19, 4.20, B.18, B.19, B.22, B.23 and Tables 4.17, B.9, B.11.

CMRAC-RIV performance was again less satisfactory as it did not perform well when reference model change of amplitude occurred. System's response was even more unstable when it obtained bigger values of temperature. Corresponding Figures are B.20, B.21 and Table B.10.

Use of Dead-one

Use of dead-zone robustness technique eliminated the oscillations of system response either the change of reference model amplitude occurred or not. It was applied so as to minimize control error faster and to improve system's transient response. Corresponding Figures are 4.21, 4.22, B.26, B.27 and Tables 4.18, B.13.

CMRAC-RIV performance remained unstable even when technique of dead-zone was used. Corresponding Figures are B.24, B.25 and Table B.12.

Table 4.17: CMRAC-RLS tuning parameters

CMRAC-RLS	γ	n	λ	$\hat{\theta}_0$	$\overline{x}_0$	P_0
	10^{-4}	2	0.99	I_{21}	I_{21}	$1000 * I_2$

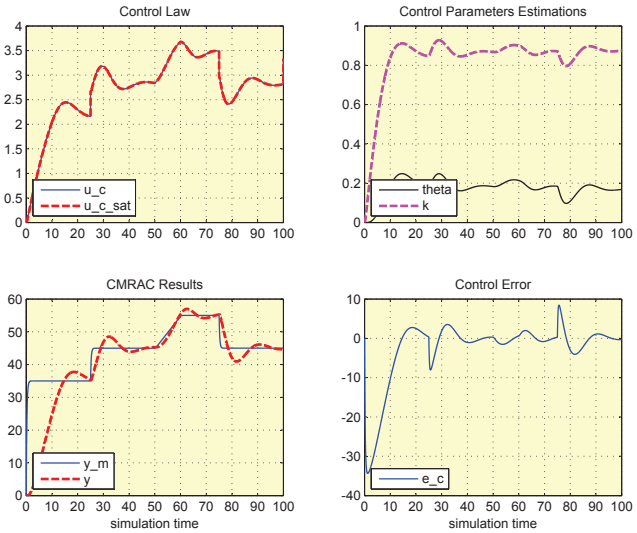

Figure 4.19: CMRAC-RLS of heat exchanger plant stimulated with square input signal of changing amplitude

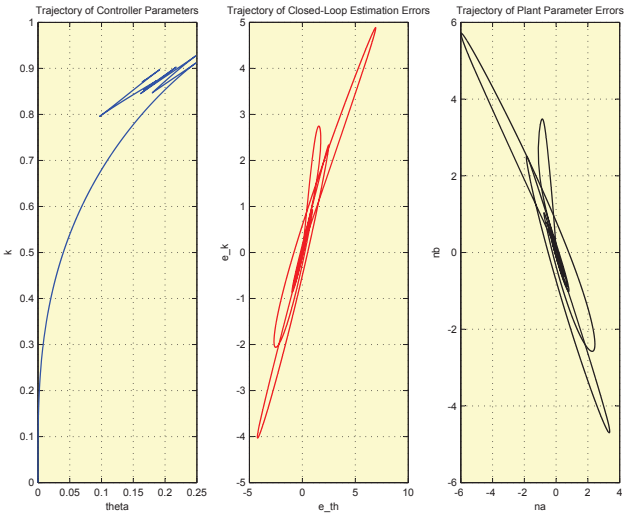

Figure 4.20: Trajectories of closed-loop estimation errors, plant parameter errors and controller parameters presented in Figure 4.19

Table 4.18: CMRAC-DZ-RLS tuning parameters

	γ	Δ	n	λ	$\hat{\theta}_0$	$\overline{x}_0$	P_0
CMRAC-RLS	10^{-4}	1	2	0.99	I_{21}	I_{21}	$1000 * I_2$

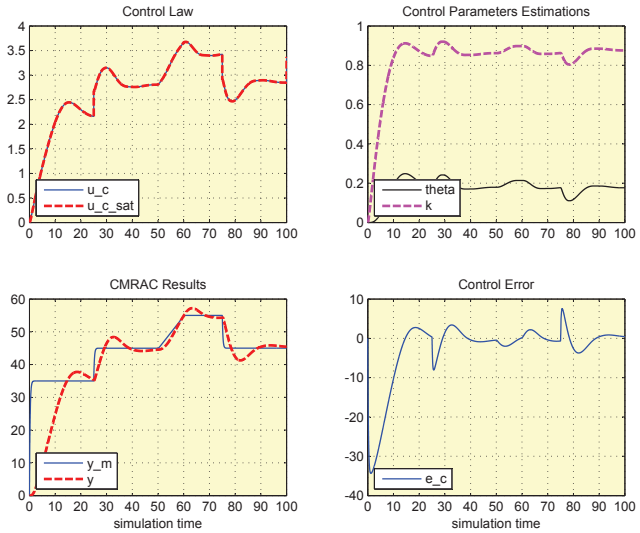

Figure 4.21: CMRAC-RLS of heat exchanger plant stimulated with square input signal of changing amplitude. Use of dead-zone

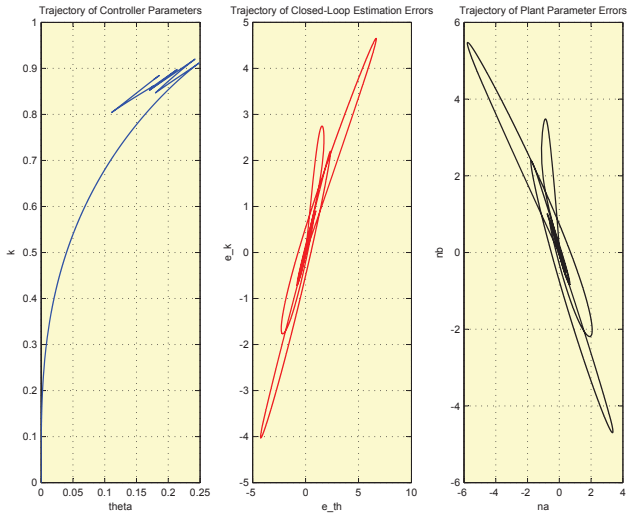

Figure 4.22: Trajectories of closed-loop estimation errors, plant parameter errors and controller parameters presented in Figure 4.21

4.2.2 Experiments using Heat Exchanger Experimental Device

Results of experimental evaluation of CMRAC performed using heat exchanger experimental device, are presented in this section. Evaluation of MRAC was also performed so as its results can be compared with the respective ones of CMRAC. Evaluation trials were performed using

- Reference signal of constant amplitude
- Reference signal of constant amplitude and dead-zone robustness technique
- Reference signal of changing amplitude
- Reference signal of changing amplitude and dead-zone robustness technique

Control law values, produced by the controllers under experimental evaluation, are equal to voltage values applied across the heating resistance of heat exchanger device. These values are automatically limited[5] between $0\,V$ and $5\,V$ as negative voltage values have no importance and values over $5V$ cause heating resistance overheating.

The duration of each experimental evaluation trial was as big as needed so that one cycle of heating and cooling process of air temperature could be implemented. Second cycle of heating and cooling could not be implemented as more computer memory was needed. In addition, in all the experimental trials the thermocouple and heating resistance were placed close enough so as to minimize measurement delay.

Tuning of control algorithms was done by trial and error. Sample time of all the experiments was 0.25 sec. Most representative results of the experimental control evaluation trials performed and tables with the values of control algorithms tuning parameters are presented below. Except from the figures depicting the values of control law, control parameter estimations and control error, figures depicting the trajectories of controller parameters, plant parameter errors and of closed-loop estimation errors which are representative of control systems stability and convergence properties are also presented. Comments on control algorithms performance for each experimental trial are shown below.

More results from evaluation trials of control algorithms using heat exchanger experimental device can be found in Appendix B.

[5]Using the *saturation* block in Simulink models 3.12 and 3.13

Experimental Trials using Heat Exchanger Device - Comments

Reference Input of Constant Amplitude

Most of the experimental evaluation trials were characterized by a slow transient response having big overshoot and by a faster but oscillatory steady-state response. Values of control error were satisfactorily small and fluctuating close to zero. Trajectories of controllers parameters and closed-loop estimation errors showed that the controllers designed have good convergence properties.

Experimental performance of the controllers designed were less satisfactory when sinusoidal reference signal was used. However, system response still fluctuated around the desired one.

Corresponding Figures are B.28 to B.35 and Tables B.14 to B.17.

Reference Input of Constant Amplitude-Use of Dead-Zone

Use of dead-zone robustness technique led to an experimental closed-loop response free of oscillations both in transient and in steady-state response. Overshoot was also eliminated while controllers parameters and closed-loop estimation errors converged to desired values.

CMRAC-RIV performance was not satisfactory as system response remained oscillatory and control error generated did not converge to zero.

Corresponding Figures are 4.23 to 4.30 and Tables 4.19 to 4.22.

Reference Input of Changing Amplitude

A change in reference model amplitude had an effect in the form of experimental closed-loop response by making it more oscillatory when the change occurred. However, these oscillations were characterized by small amplitude and system's response signal fluctuations were very close to the response of reference model. Moreover, trajectories of control parameters and closed-loop estimation errors showed that the controllers were maintaining their good convergence properties.

Corresponding Figures are B.36 to B.43 and Tables B.18 to B.21.

Reference Input of Changing Amplitude-Use of Dead-Zone

Application of dead-zone eliminated oscillations of system's response only when cooling of air temperature occurred, after the change of reference model amplitude. Oscillatory response, after system response reached higher values of air temperature, was unavoidable. All of the controllers, though, maintained their convergence and stability properties and performed properly.

Corresponding Figures are B.44 to B.51 and Tables B.22 to B.25.

Delay of Transient Response

Delay of the experimental closed loop transient response before reaching the desired values of air temperature, during the initial time steps of the experimental evaluation trials, was due to the initial negative values of the control law. The initial values of reference model response were below the ambient temperature of the air. As a result, the controller tended to decrease air's temperature, in order to decrease the values of control error. However, this could not be implemented, as negative values of control law-voltage were not accepted by the heating resistance and the latter didn't have the ability to cool the air below the ambient temperature. Values of control law quickly became positive, as the reference model response quickly reached values above the ambient temperature of the air. The time needed by the controller to create the first positive values of control law constituted the initial delay of the experimental closed loop transient response.

Table 4.19: MRAC tuning parameters

	γ	Δ
MRAC	10^{-8}	1

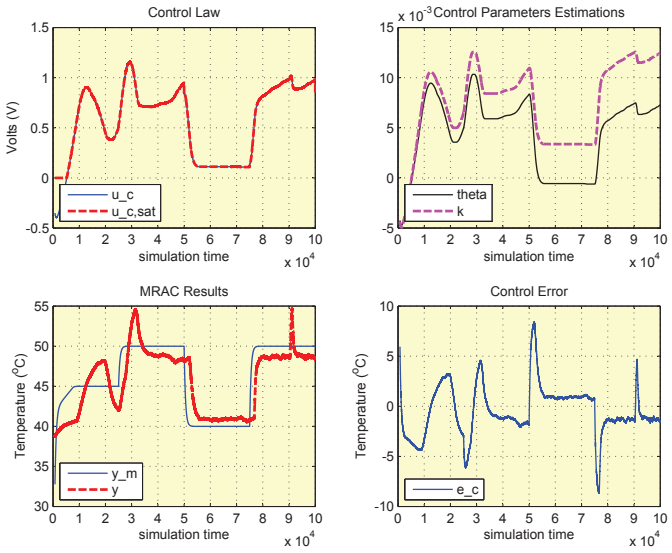

Figure 4.23: MRAC of heat exchanger device stimulated with square input signal. Use of dead-zone

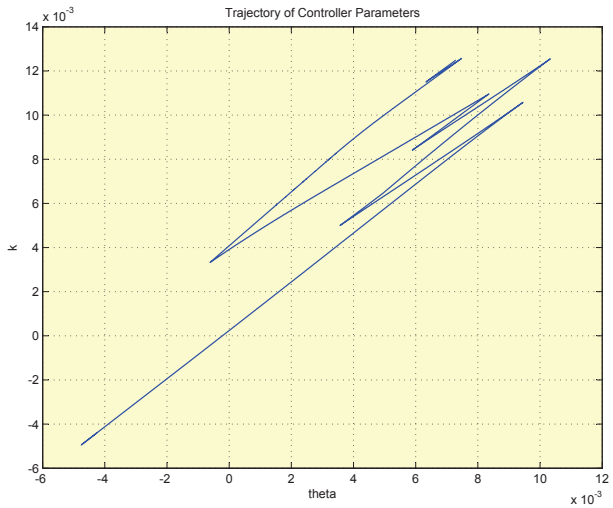

Figure 4.24: Trajectory of controller parameters presented in Figure 4.23

Table 4.20: CMRAC-RLS tuning parameters

	γ	Δ	n	λ	$\hat{\theta}_0$	$\overline{x}_0$	P_0
CMRAC-RLS	$7 * 10^{-9}$	1	2	0.99	Z_{21}	Z_{21}	$1000 * I_2$

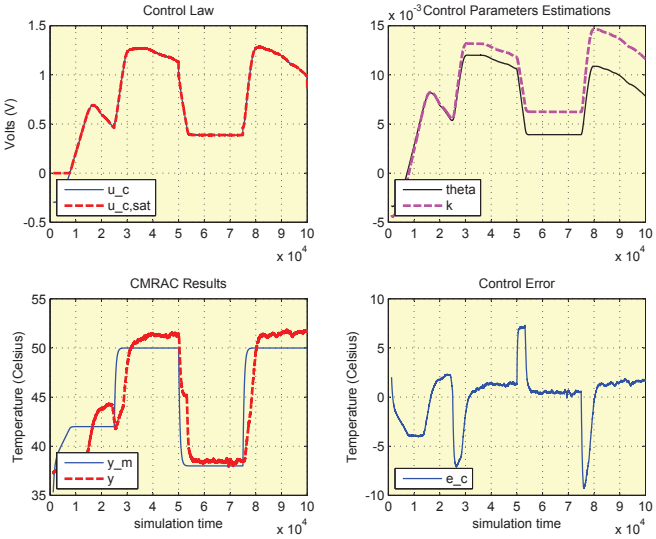

Figure 4.25: CMRAC-RLS of heat exchanger device stimulated with square input signal. Use of dead-zone

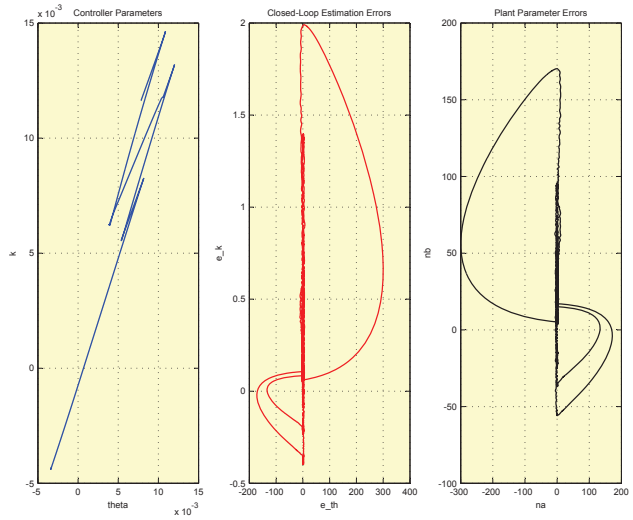

Figure 4.26: Trajectories of closed-loop estimation errors, plant parameter errors and controller parameters presented in Figure 4.25

Table 4.21: CMRAC-RIV tuning parameters

	γ	Δ	n	λ	$\hat{\theta}_0$	$\overline{x}_0$	v_0	P_0
CMRAC-RIV	$6 * 10^{-9}$	1	2	0.95	$[-0.1 \quad -0.1]^\top$	$[-0.1 \quad -0.1]^\top$	$[-0.1 \quad -0.1]^\top$	$1000 * I_2$

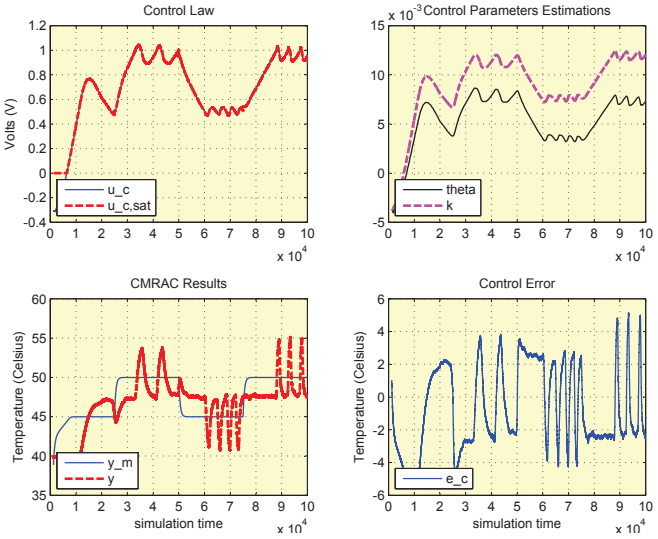

Figure 4.27: CMRAC-RIV of heat exchanger device stimulated with square input signal. Use of dead-zone

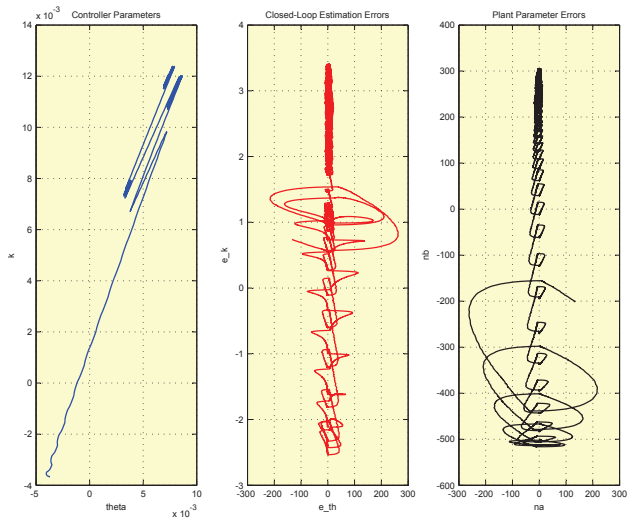

Figure 4.28: Trajectories of closed-loop estimation errors, plant parameter errors and controller parameters presented in Figure 4.27

Table 4.22: CMRAC-SL tuning parameters

	γ	Δ	n	γ_{sl}	$\hat{\theta}_0$	$\overline{x}_0$
CMRAC-SL	$7 * 10^{-9}$	1	2	1	Z_{21}	Z_{21}

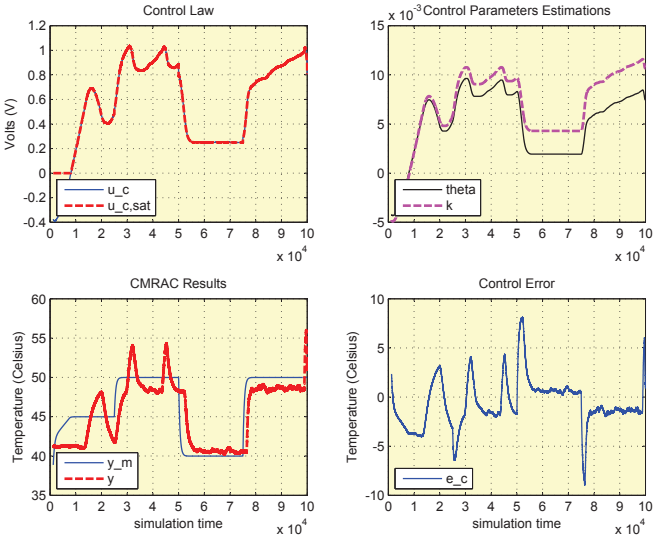

Figure 4.29: CMRAC-SL of heat exchanger device stimulated with square input signal.Use of dead-zone

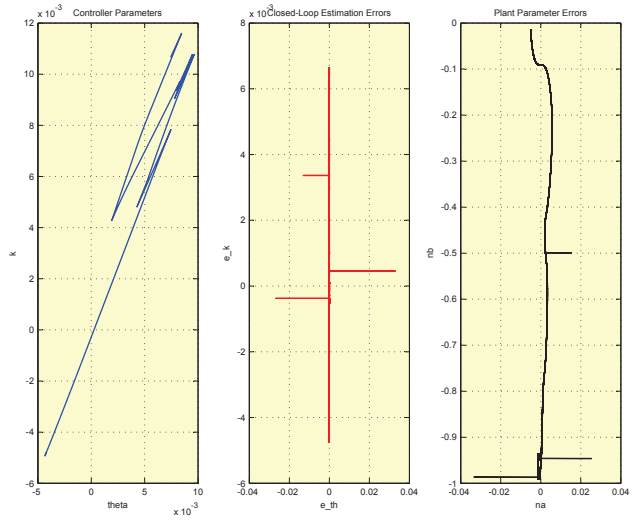

Figure 4.30: Trajectories of closed-loop estimation errors, plant parameter errors and controller parameters presented in Figure 4.29

4.2.3 Conclusions

In general, the evaluation trials performed showed that CMRAC had satisfactory performance. Control error fluctuations were close to zero value and closed-loop estimation errors were converging to zero, something which showed that the deviation of the estimated coefficients of the closed-loop transfer function, calculated by the control algorithm, from those of the reference model was very small. Furthermore, trajectories of controllers parameters and of closed-loop estimation errors proved that the controllers designed have good convergence properties.

CMRAC using instrumental variables identifier (CMRAC-RIV) did not perform as well as the remaining versions of CMRAC. Control error values and trajectories of controller parameters and closed-loop estimation errors showed that CMRAC-RIV had weaker convergence properties.

Use of Reference Signal of Changing Amplitude

Both computer simulations and experimental evaluation trials performed using reference signal of changing amplitude, showed that the oscillatory system's response after the change of reference's amplitude occurred was unavoidable. Use of dead-zone robustness technique was necessary in order to eliminate oscillations at parts of system's response which represent heating and cooling processes of air temperature, when square or sinusoidal reference signal was used. CMRAC-RIV performed worse when reference input of constant amplitude and dead-zone were used, as it produced the biggest control error values (see Table 4.13). However, as trajectories of controllers parameters and closed-loop estimation errors showed, the latter maintained its convergence properties.

Effect of Identification Algorithm Used

Evaluation of system identification algorithms used, presented in the previous section, showed that the instrumental variables algorithm did not perform well in most occasions. Taking into account the conclusions made for CMRAC-RIV, it is clear that the performance of the system identification part of CMRAC algorithm strongly affected performance of CMRAC. Identification error and plant parameters estimations values, which are produced by the identification algorithm and used by CMRAC algorithm for control law synthesis, must be a result of identification algorithm good performance in order for the CMRAC to work properly.

All of the identification algorithms maintained their performance characteristics (referred in previous section) during control evaluation trials as they were operating independently of the control algorithms. As a result, CMRAC-RLS and CMRAC-SL

performed better than CMRAC-RIV during control evaluation trials implementation. Conclusions for the performance of identification algorithms in control evaluation trials can be drawn from plant parameter errors trajectories.

Actuator Nonlinearity

During the implementation of the experimental evaluation trials of the designed controllers, a nonlinearity in power electronics actuator was observed. The amount of electricity fed through to the heating resistance by the actuator seemed to be bigger when the voltage applied to the latter was equal to $0.5V$, $1V$, $1.5V$ and so on. Whenever the voltage applied to the actuator (calculated by the control law) was taking any other value, the amount of electrical power fed was decreased or increased disproportionately to the control law.

As a result, experimental closed-loop response, in most of the results presented in this chapter, was characterized by peaks which were absent in the control-law signal. These oscillations were occurring during steady-state response (when square reference signal used) or when system response had to follow a sinusoidal air temperature reference. Oscillations created due to this nonlinearity could not be eliminated with the use of dead-zone robustness technique.

Chapter 5

Experimental Results from Water Brake

Results from the final experimental evaluation tests of the controllers designed, using the water brake at the powertrain facility in LME, are presented in this chapter. These results are representative of the performance trials implemented at CAT 3176B marine diesel engine test bench, in LME, during the final stage of this diploma Thesis. Basic aim of these trials was to test the stability and convergence properties of the controllers designed for the engine load control system. In all trials, CAT diesel engine was operated in low load transient regime.

MRAC and CMRAC designed were used for the implementation of two different load control systems of CAT marine diesel engine, applied on the water brake coupled to the latter. Firstly, both system identification and control algorithms, were tested through computer simulations using real measured signals, taken from water brake operation, and a second order mathematical model of water brake, respectively. During the final stage of the diploma Thesis implementation, one version of the CMRAC and MRAC was installed in the control platform of CAT 3176B (Simulink model in Figure 3.15) marine diesel engine test bench for the conduction of a series of experimental evaluation tests. Representative results of all the evaluation trials performed and conclusions regarding the performance of the controllers are presented in the following sections.

5.1 CMRAC Trials

5.1.1 Computer Simulation Results

Representative computer simulation results from the evaluation trials of the CMRAC version selected for the final experimental trials implementation are presented below.

These trials were performed in order to test controller's performance and limitations, using a mathematical model of water brake plant (see section 3.1.4), before final experimental tests be made. Computer simulation results of sequential learning and least squares identification algorithms evaluation trials, used for two different CMRAC versions synthesis, are also presented. These trials were performed so as to test algorithms' performance and stability properties when real measured signals of valve command and water brake torque were used as inputs to the algorithm.

System Identification Trials

Figures 5.1 and 5.2 show results from computer simulation trials of SL and RLS algorithm respectively while Tables 5.1 and 5.2 show details of their tuning parameters. It can be seen that both SL and RLS identification algorithms were able to estimate the dynamics of torque signal (y signal) with high precision. Values of identification error prove that both algorithms performance was satisfactory and stable. A proportional gain was used for the amplification of the input signal used (valve command) so that the necessary, for a good algorithm performance, level of amplitude can be generated. Modifications of the input signal characteristics were necessary in order for the identification algorithm to maintain its stability and convergence properties.

Computer simulation trials using RIV identification algorithm were also performed. Algorithm's tuning was very difficult and its performance was totally unstable. Therefore, presentation of results is omitted.

Table 5.1: SL tuning parameters

	n	γ_{sl}	$\hat{\theta}_0$	$\overline{x}_0$
SL	4	1	Z_{41}	Z_{41}

Table 5.2: RLS tuning parameters

	n	λ	$\hat{\theta}_0$	$\overline{x}_0$	P_0
RLS	4	1	I_{41}	I_{41}	$100 * I_4$

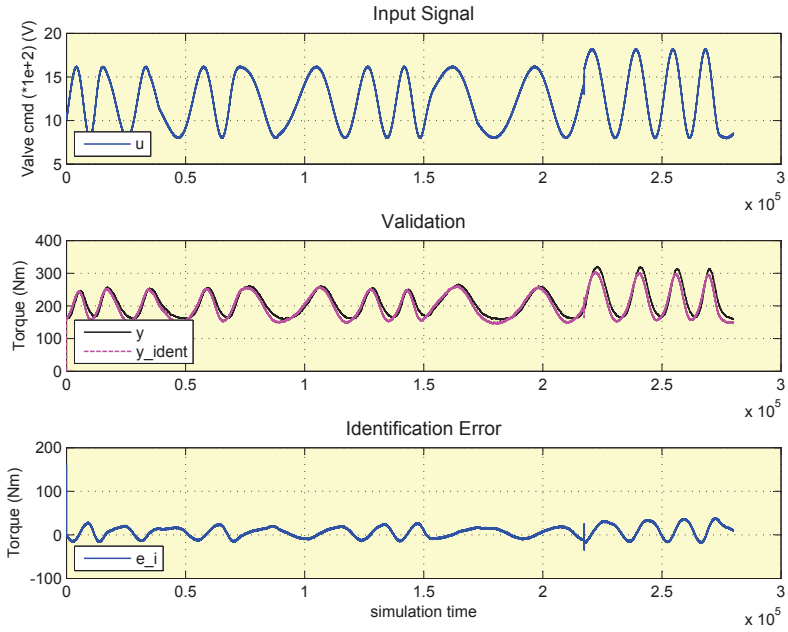

Figure 5.1: Computer simulation results of SL identification algorithm applied on torque measurements taken from water brake operation

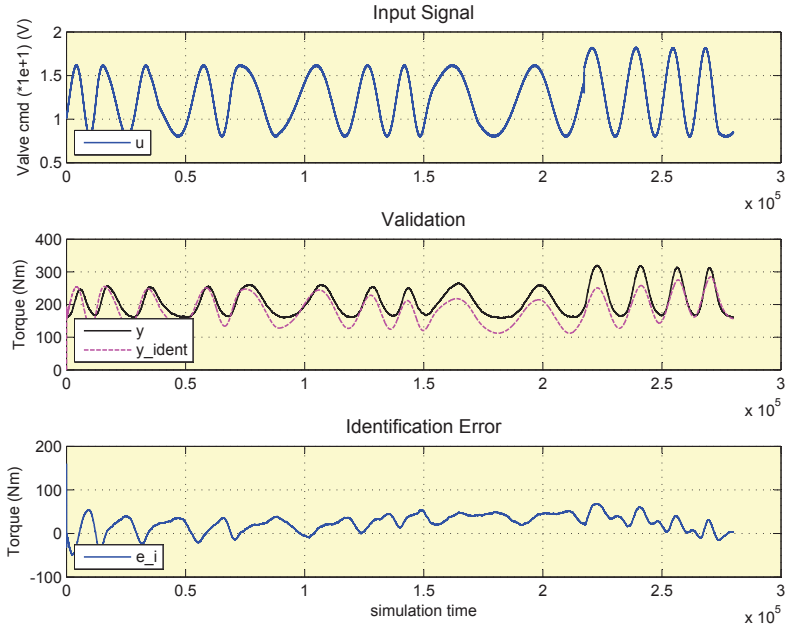

Figure 5.2: Computer simulation results of RLS identification algorithm applied on torque measurements taken from water brake operation

Control Trials

Figure 5.4 shows computer simulations results of CMRAC-SL applied on a second order discrete time system plant of water brake and Table 5.3 shows values of its tuning parameters. These trials were performed as an initial test of the second order extension of CMRAC before being tested experimentally on the real plant of water brake at LME facilities. An external square signal (Figure 5.3) was used as input of the identification algorithm as the latter was not able to operate properly using the control law (valve command) as input. The reference signal and the reference model used were the same to those used in the experimental trials performed. A first order discrete time filter was used in order to make transient response of reference signal, when a change in its amplitude occurs, smoother and avoid over-excitation of the closed loop control system.

Results show that CMRAC-SL performed very well by producing a control law close to the expected, comparing to real valve command measurements, values and a control error converging to zero very fast. The controller had very good convergence properties and stability to big changes of reference amplitude. It is also clear that the use of dead-zone technique is unnecessary since there are no oscillations in the system response signal.

Computer simulation trials of CMRAC-RLS were also implemented. Controller performance was unsatisfactory and unstable producing big control error. Therefore, presentation of the results is omitted.

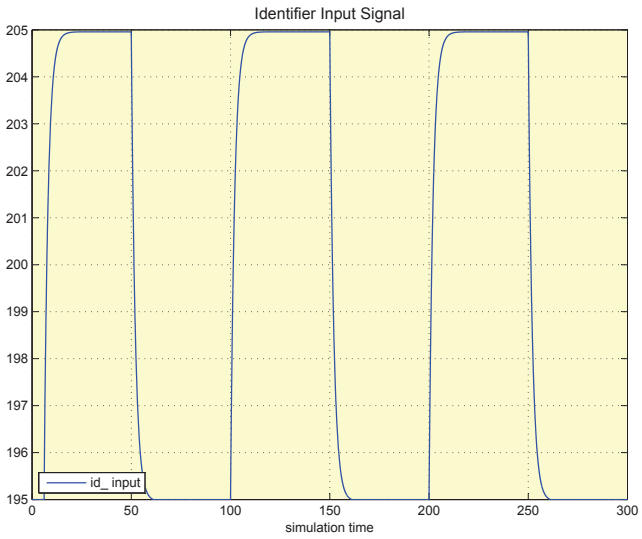

Figure 5.3: SL algorithm external input signal

Table 5.3: CMRAC-SL tuning parameters

	γ	n	γ_{sl}	$\hat{\theta}_0$	$\overline{x}_0$
CMRAC-SL	$1 * 10^{-6}$	4	1	I_{41}	I_{41}

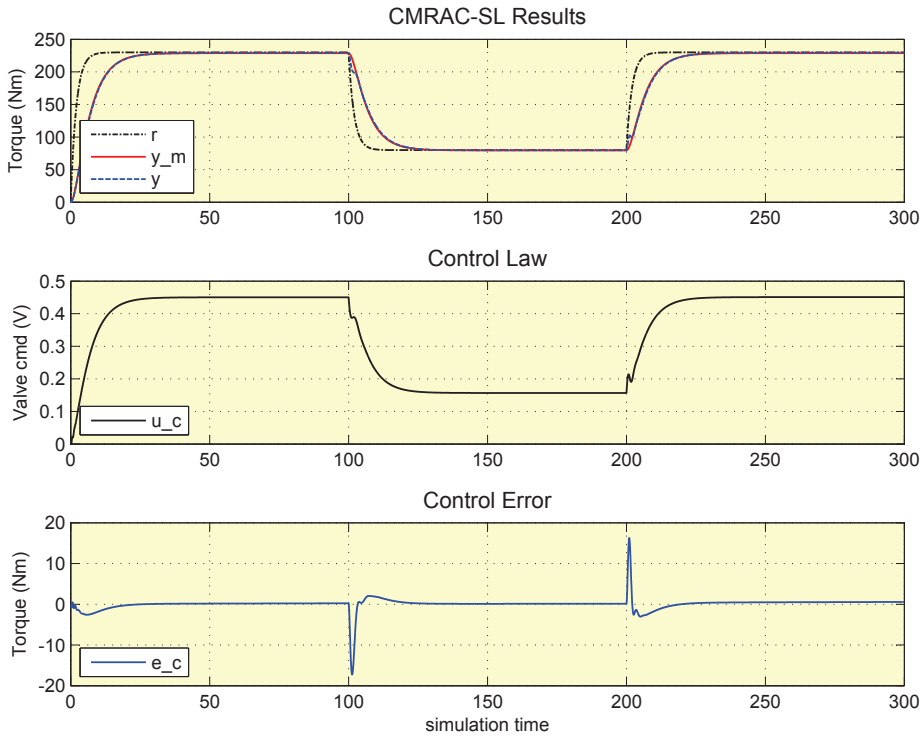

Figure 5.4: Computer simulation results of CMRAC with SL identifier applied on a second order water brake plant

5.1.2 Experimental Results

Table 5.4: CMRAC-SL tuning parameters

	γ	n	γ_{sl}	$\hat{\theta}_0$	$\overline{x}_0$
CMRAC-SL	$1 * 10^{-9}$	4	1	I_{41}	I_{41}

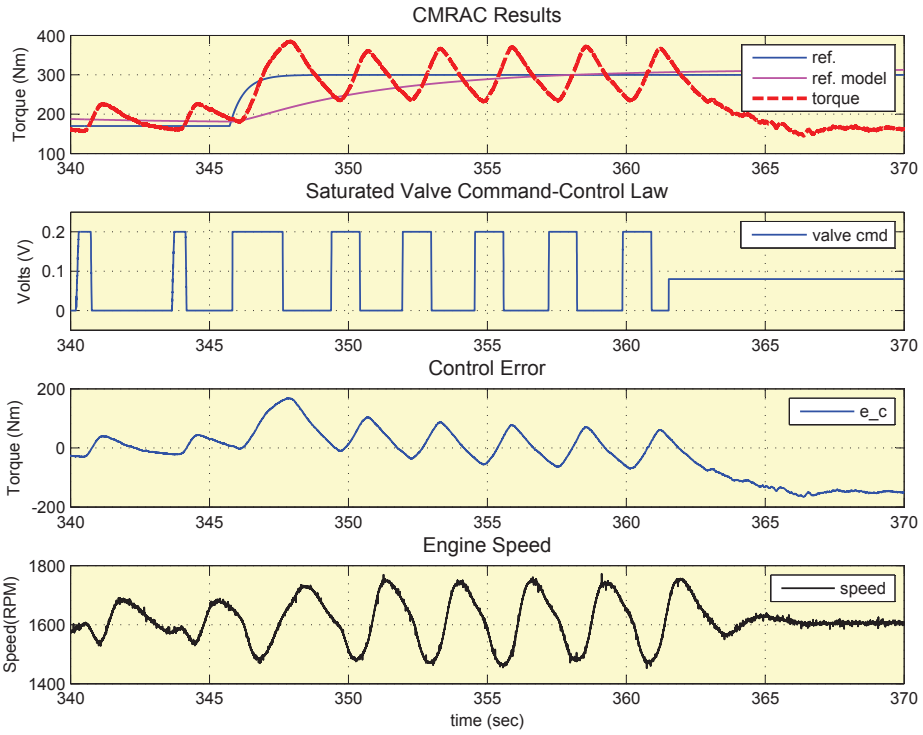

Figure 5.5: Experimental results of CMRAC with SL identifier applied on water brake plant at CAT diesel engine test bench

The fact that CMRAC-RLS did not perform well in computer simulation evaluation trials led to selection of CMRAC-SL as the controller to be used for the experimental tests implementation. Figure 5.5 shows the experimental results of CMRAC-SL applied on water brake plant at CAT diesel engine's test bench and Table 5.4 shows CMRAC-SL tuning parameters values. Signals of measured torque and engine's speed show that system's response to control law input was unstable leading to a control error which did not converge to zero. Oscillatory system response is due to the high amplitude fluctuations of the control law signal produced (see Figure 5.6) which were much greater than the required valve command values for stable and smooth operation of the water brake. Even though the adaptation gain γ was set very small it had no effect on the decreasing

control law rate of change. Figure 5.7 shows that the SL identifier of the CMRAC used did not perform well, too, by overestimating the parameters of water brake plant and producing large identification error. Big identification error led in control parameters overestimation and finally in bad and unsatisfactory performance of the control system. The fact that mean value of the control error produced by the controller was close to zero, was the only positive characteristic of CMRAC performance.

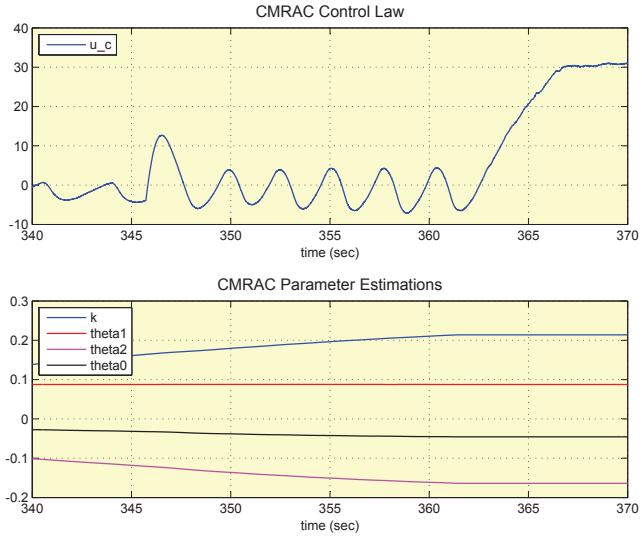

Figure 5.6: CMRAC parameter estimations from experimental trial on water brake plant

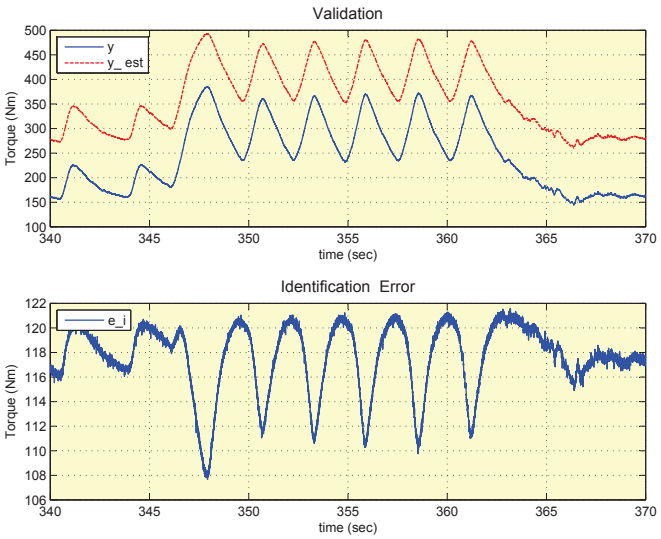

Figure 5.7: SL identification results from experimental trial on water brake plant

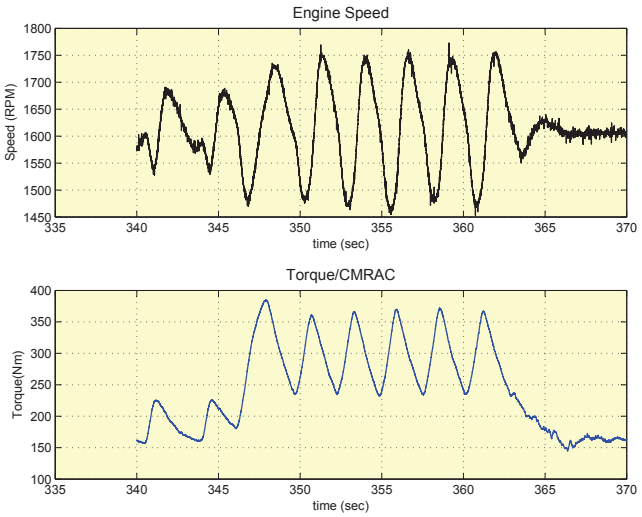

Figure 5.8: Engine speed and Torque changes from CMRAC-SL experimental test on water brake plant

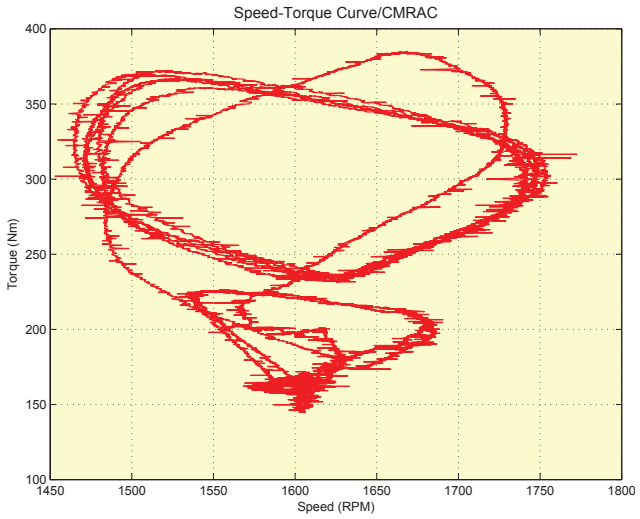

Figure 5.9: Engine speed-Torque curve during CMRAC-SL experimental test conduction

Figure 5.8 shows CAT diesel engine speed and torque changes measured during CMRAC-SL experimental test on water brake plant. Figure 5.9 shows the corresponding diesel engine's torque to speed curve. This is not converging to a small area of the plane during engine's operation which proves that engine's torque and speed were not kept constant during the experimental trial. On the contrary, torque signal's fluctuations covered a big area of the plane which indicates the unstable performance of CMRAC.

5.2 MRAC Trials

5.2.1 Computer Simulations Results

Representative results of the computer simulation evaluation trials of MRAC, for second order systems control, are presented below. As in the case of CMRAC, these trials were performed as a prior test of controller's stability and convergence properties before the final experimental tests implementation.

Control Trials

Figure 5.11 shows the results from computer simulation of MRAC applied on a second order discrete time system plant of water brake while Table 5.5 shows MRAC tuning parameter value. Figure 5.10 shows MRAC parameters fluctuations during computer simulation. These trials were performed as an initial test of the second order extension of MRAC before being tested experimentally on the real plant of water brake at LME facilities.

Results prove that MRAC designed has very good convergence and stability properties to big changes of reference amplitude. Control error convergences to zero and control law values are very close to the real expected valve command values. Fluctuations of control law are very smooth, leading to a system response with no oscillations. Use of dead-zone is unnecessary.

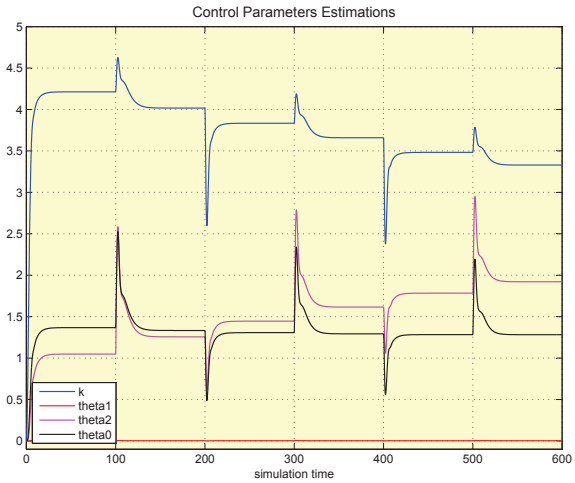

Figure 5.10: MRAC parameter estimations from computer simulation trial on second order water brake plant

Table 5.5: MRAC tuning parameters

MRAC	γ
	10^{-4}

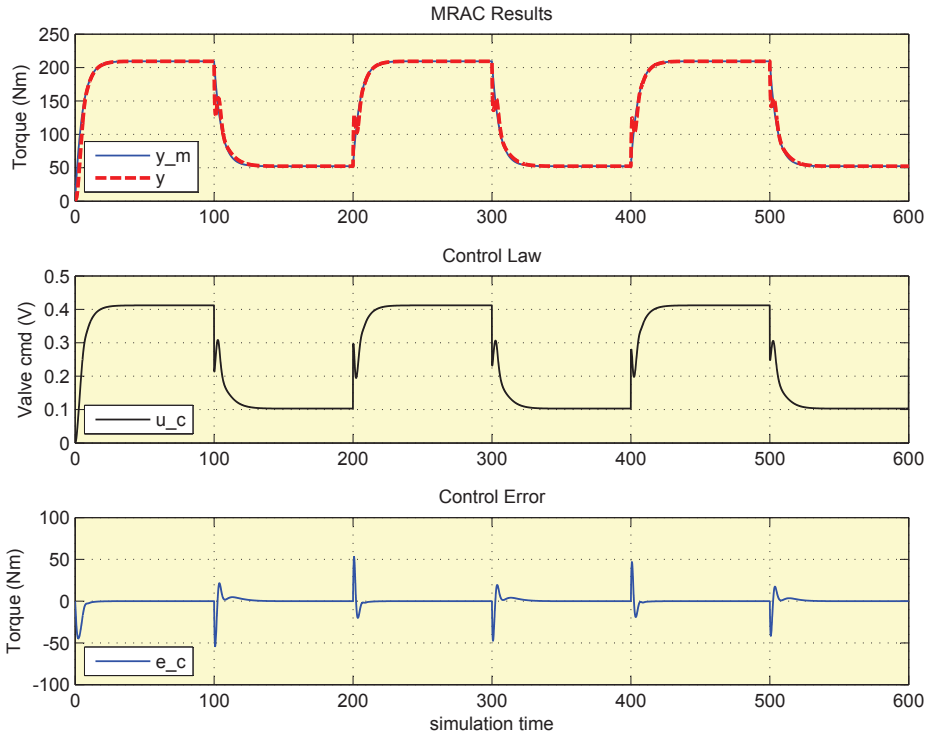

Figure 5.11: Computer simulation results of MRAC applied on a second order water brake plant

5.2.2 Experimental Results

Table 5.6: MRAC tuning parameters values-Water Brake-Test Bench Trial

MRAC	γ
	10^{-6}

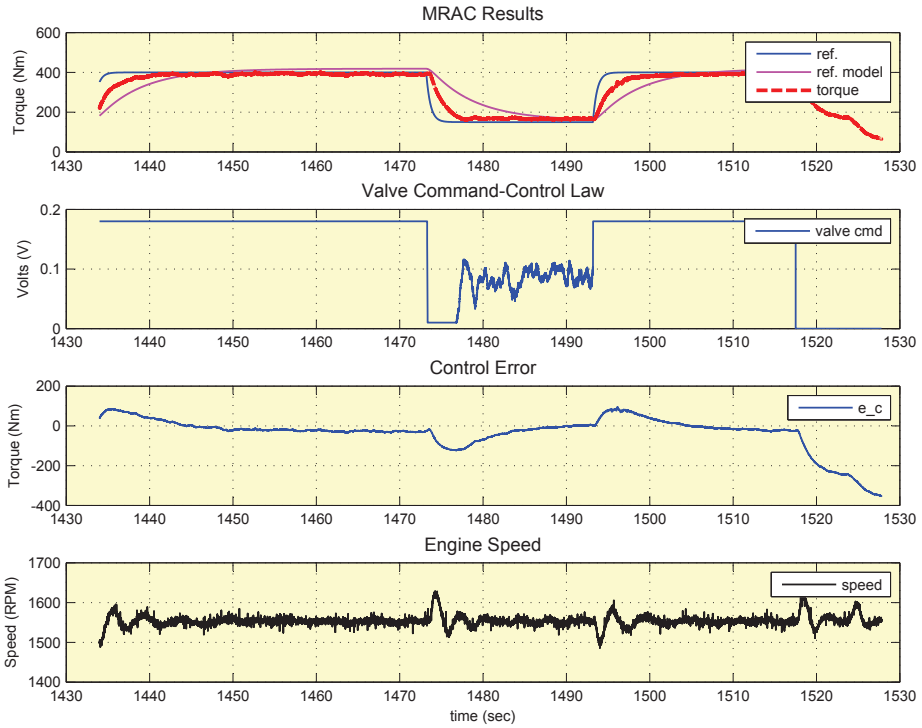

Figure 5.12: Experimental results of MRAC applied on water brake plant at CAT diesel engine test bench at LME

Figure 5.12 shows the experimental results of MRAC of second order applied on water brake plant at CAT diesel engine test bench in LME and Table 5.6 shows MRAC tuning parameter value. During the initial stages of this trial the control law produced by the controller was providing large values, as in the case of CMRAC experimental trial (see Figure 5.6). The rate of change of the control law signal was also very high. As a result, the response produced was oscillatory with large amplitude leading to a control error signal which was not converging to zero. In order to make system's response more stable and smoother, a proportional gain was used, in order to decrease control law values and make it fluctuate among the desired values. In addition, the technique of dead-zone was used in order to improve robustness of the controller in the presence of measurement noise and unmodelled system dynamics. As a result, oscillations of the

torque signal were eliminated and the closed loop control system performed better.

Observing the response signal of water brake plant (i.e torque) having small settling time, no overshoot and being close to the desired response of reference model, performance of Model Reference Adaptive Load Control system is considered satisfactory. Moreover, torque response signal is tracking the changes of torque reference amplitude smoothly and fast.

Figure 5.13 shows the engine speed variations during the load transients. It can be seen that speed is kept around its reference value of about 1550 rpm with small overshoots during load changes, as expected. Constant speed is maintained by the separate engine speed-fuel controller. Figure 5.13 also shows CAT marine diesel engine torque signal measured during MRAC experimental test on water brake plant.

Figure 5.14 shows the diesel engine's torque to speed curve from the experimental trial of MRAC. It is clear that during high load steady state system response (Figure 5.13), torque signal is converging to a small area of the plane (area 1) which proves that engine's torque and speed were kept constant during the corresponding time period of the experimental trial. Engine's torque and speed are also kept constant during low load steady state system response and this can be seen in area 2. Remaining fluctuations in diesel engine's torque-speed curve correspond to a path during the transient system response which in turn corresponds to separate speed signal peaks of amplitude.

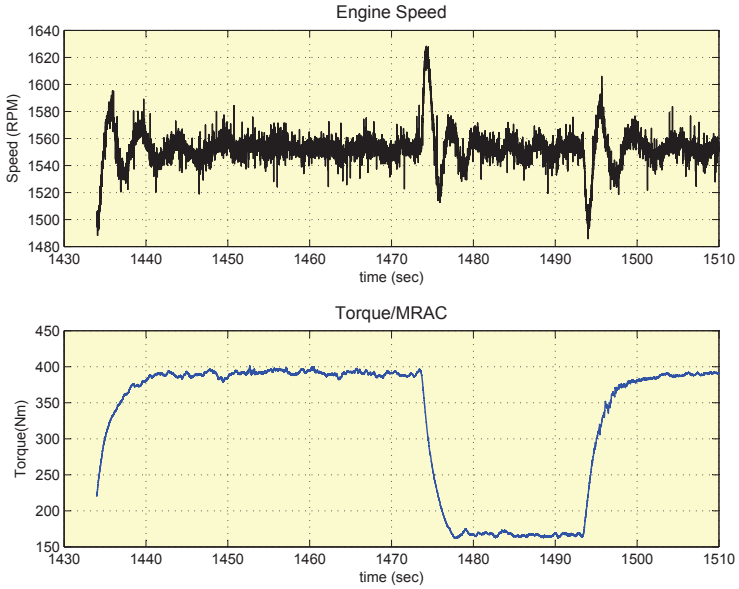

Figure 5.13: Engine speed and Torque changes from MRAC experimental test on water brake plant

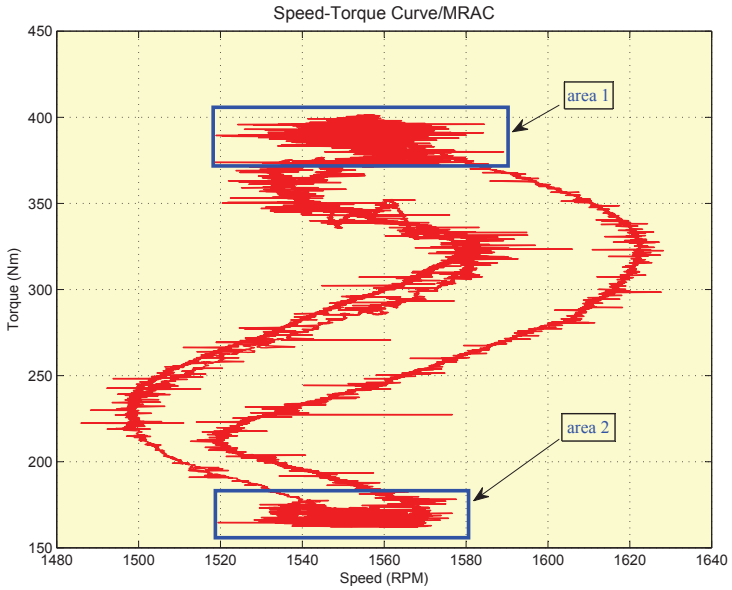

Figure 5.14: Engine speed-Torque curve during MRAC experimental test conduction

5.3 Conclusions

Following the completion of the experimental trials of MRAC and CMRAC, conclusions regarding controllers' performance could be made. Presence of measurement noise, external disturbances and unmodeled dynamics of higher order, characteristics of most real processes, made the adaptive controllers perform with an unstable behaviour. System response was oscillatory with large amplitude, a fully unstable condition which can lead to failure of control system (controller parameters turn to infinite). In the case of CMRAC, the overestimation of system plant parameters led to large identification error which in turn led to overestimated controller parameters. Control law was characterized by fluctuations of high rate of change and values larger than the desired ones for a good and stable performance.

It seems that modifications of adaptive laws in order to be more robust, when nonlinearities, noisy measurements and external disturbances are present, are necessary for a satisfactory and stable performance. Dead-zone technique was the one used for robustness optimization of MRAC due to its simplicity and its effectiveness which was tested using heat exchanger experimental device. Moreover, use of proportional gains also seems to be necessary in order for the control law to be smaller and close to the desired values. In the case of CMRAC used, the performance of the system identification part seems to be of great importance as bad identifier performance led to unavoidable bad controller performance. Therefore, better tuning of the identifier and modifications on the mechanism which estimates plant parameters are necessary, too.

To conclude, combination of robustness optimization techniques and modifications in the mechanism which generates the control law, is an option able to improve Model Reference Adaptive Control performance.

Chapter 6

Conclusions and Future Work

6.1 Conclusions

Experimental results of CMRAC evaluation trials, presented in this Thesis, prove that CMRAC algorithm is more effective in dealing with a simple process, like temperature control of an air stream (heat exchanger), rather than with a more complex, like the load control of a marine diesel engine. Performance of CMRAC, when applied on a process accurately mathematical modelled by a first order system, was stable and robust having good convergence properties. On the other hand, when it was set to control a complex process, characterized by non-linearities and dynamics of higher order, control algorithm lost its stability properties leading to unacceptable performance. Therefore, the Combined Model Reference Adaptive Controller, as presented by the mathematical equations in chapter 2, was not able to control a real process in the presence of unmodelled dynamics, measurement noise and external disturbances, features that most real processes have. Conclusions referred above, also apply to MRAC controllers designed as presented by the mathematical equations in chapter 2.

Use of techniques for creating robust adaptive control laws seems to be necessary and much important for satisfactory performance characteristics of both MRAC and CMRAC designed. Use of dead-zone technique, in the adaptive law synthesis algorithm part, seems to improve the robustness and performance characteristics of the control system. This can be proved by comparing experimental results like those shown in Figures B.30 and 4.25 and those shown in Figures 5.12 and 5.5.

Performance of CMRAC is strongly affected by the performance and the effectiveness of the identification part of its integrated algorithm, as values of identification error and of plant parameters estimations are used for the creation of the control law at any time instants. Figure 5.5 shows that large identification error causes overestimation of control parameters, leading to an oscillatory system's response with big

overshoot. Therefore, proper tuning of the identification algorithm is something which needs special treatment by the Control Engineer. Moreover, selection of the identification algorithm to be used for a CMRAC system implementation, also needs to be done very carefully after examining the dynamical characteristics and the working conditions of the system plant to be controlled. An appropriately selected and well tuned identification algorithm combined with a well tuned and robust control algorithm are required for the creation of a stable and effective control system with the required convergence properties.

Results from system identification algorithms evaluation trials show that the estimation of the parameters of both first and second order system plants mathematical models was successfully implemented. Use of forgetting factor technique made the identification algorithms able of tracking even plant parameters changes of 100%. The assumption of absence of noise in the response signal, of the system to be identified, resulted in a simple, though accurate, identification algorithm formation. Furthermore, the identification algorithms designed can produce accurate results even if white noise is present, as experimental results from evaluation trials using heat exchanger device proved. On the other hand, experimental results from trials at water brake plant proved that the inability of identification algorithms to estimate coloured noise and higher order characteristics, of the measured torque signal, caused its unsatisfactory performance. Moreover, features of identification algorithms' input signal are crucial for the stable and robust performance of the identifier.

6.2 Future Work

Controller Modifications for Robustness

Except from technique of dead-zone, applied on controllers designed for their robustness optimization, there are other techniques, [7]. Purpose of all of these techniques is to modify the adaptive law of the control algorithm, designed for an ideal plant, so that they can retain their stability properties in the presence of plant parameter uncertainties. The idea behind these techniques is to modify the adaptive laws so that the time derivative of the Lyapunov function, used to analyze the stability properties of the controller, become negative. Some of these techniques are *leakage* technique and the *parameter projection* technique which keeps parameter estimates within an a priori defined bounded space.

It should be pointed that a very important step, in the control systems design process, before the application of robustness techniques is the analysis of mechanisms which cause instability phenomena in adaptive systems [7], such as the *parameter drift*

problem mentioned in chapter 2.

Measurement Noise Identification

In system identification algorithms analysis, as presented in chapter 2, it was assumed that noise polynomial (C) coefficients, in equation (2.53), are zero. In other words, the unobservable noise, with which the measured system's output signal is usually corrupted in a real process, was neglected for the purposes of this Thesis. Noise polynomial coefficients estimation [16] will possibly lead to a more precise estimation of a complex plant parameters (like that of water brake) as measured signals fed to the identification algorithm are definitely corrupted with noise or other external disturbances.

Furthermore, use of an identification algorithm able to estimate parameters of a non-linear system plant, like the *maximum likelihood estimator* or other stochastic identifiers [8],[16], could also be more appropriate for on-line real-time identification of a system like that of water brake.

Time Varying Forgetting Factor

All of the system identification algorithms and control algorithm evaluation trials were implemented using a constant forgetting factor. However, a constant forgetting factor may lead to unbounded magnitude in certain directions of covariance matrix P in the absence of persistently exciting signals. Unboundedness of the covariance matrix is undesirable since it can lead in violent oscillations of the estimated parameters and as a result to unstable performance of the identification algorithm. To keep the benefits of a constant forgetting factor and to avoid the possibility of covariance matrix unboundedness, it is desirable to use a forgetting factor tuning technique so that data forgetting is activated when input signals are persistently exciting and suspended when they are not.

Forgetting factor tuning techniques are presented in [13]. More forgetting factor tuning techniques are presented in [16]. One of them is able to deal with unpredicted changes in system parameters by monitoring and using the identification error $\epsilon(t)$ for the adaptation of the forgetting factor.

Unmodeled Dynamics

In a real process, many types of non-parametric uncertainties can be present. Since adaptive controllers are designed to control physical systems, such non-parametric uncertainties are unavoidable. Therefore, creation of a mathematical model which accurately describes the actual plant to be controlled as well as simply enough from the

control design point of view, over an operating range, is necessary. For the robustness properties of control algorithms to be improved, a characterization in mathematical form of the types of plant uncertainties, that are usually present in practice, is very important. Computer simulations using plant models with uncertainties could be very important for the complete performance evaluation of the controllers designed. Evaluation trials including unmodeled dynamics are presented in [13] whereas mathematical modelling of various plant uncertainties is presented in [7].

Appendix A

Evaluation of System Identification Algorithms

Supplementary results of identification algorithms evaluation trials are presented in this chapter. The first section refers to results produced through computer simulations. The second one refers to results from experimental evaluation trials using heat exchanger experimental device (1.5). Use of PRBS and chirp signals, as identification algorithms stimulatory signals, is presented.

A.1 Computer Simulations Results

Figures A.1 to A.12 show results from computer simulation trials using the same literature plant with this used for simulation trials presented in section 4.1.1. Figures A.13 to A.20 show results from computer simulation tests using the heat exchanger's first order discrete time mathematical model which was also used for the computer simulation evaluation trials of identification algorithms presented in section 4.1.1 .

The type of input signal, the plant parameters estimations, the identification error and the validation of estimated plant output signal are depicted in the following figures for each plant used. Tables with each algorithm's tuning parameters are also depicted.

Table A.1: R.L.S tuning parameters

	n	λ	$\hat{\theta}_0$	$\overline{x}_0$	P_0
R.L.S	3	0.99	I_{31}	I_{31}	$1000 * I_3$

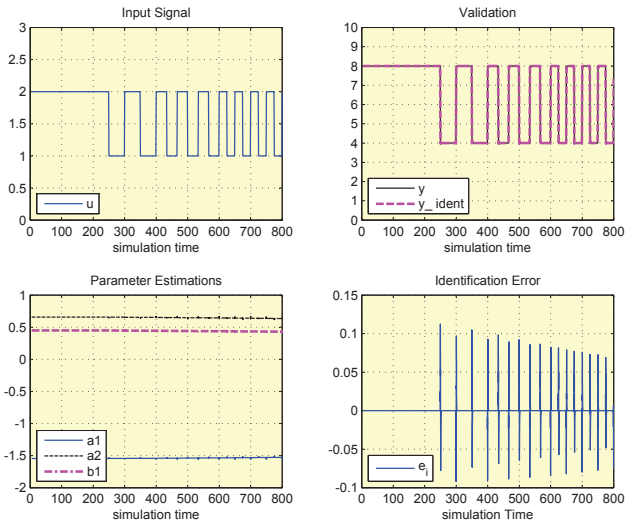

Figure A.1: Results of RLS identification applied on literature plant stimulated with P.R.B.S input signal

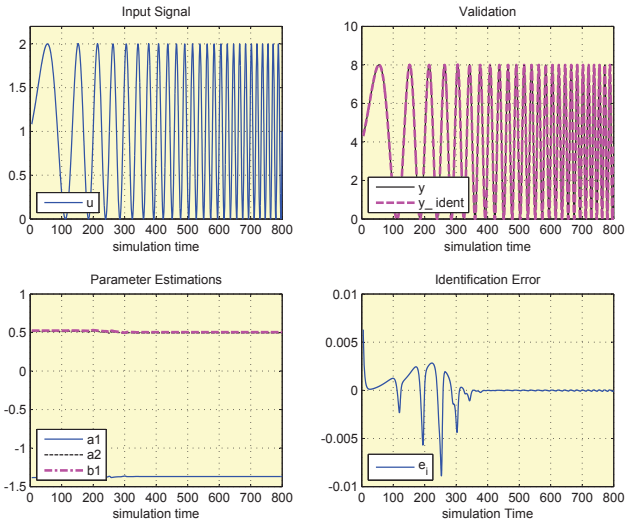

Figure A.2: Results of RLS identification applied on literature plant stimulated with chirp input signal

Table A.2: RLS tuning parameters

	n	λ	$\hat{\theta}_0$	$\overline{x}_0$	P_0
RLS	3	0.99	I_{31}	I_{31}	$1000 * I_3$

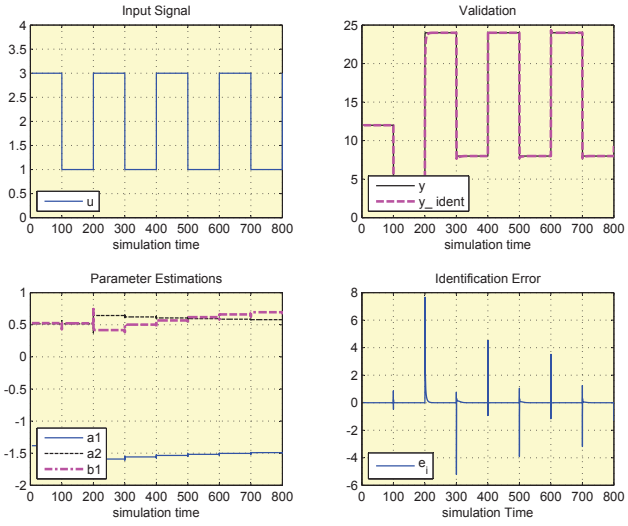

Figure A.3: Results of RLS identification applied on literature plant with changing parameters stimulated with square input signal

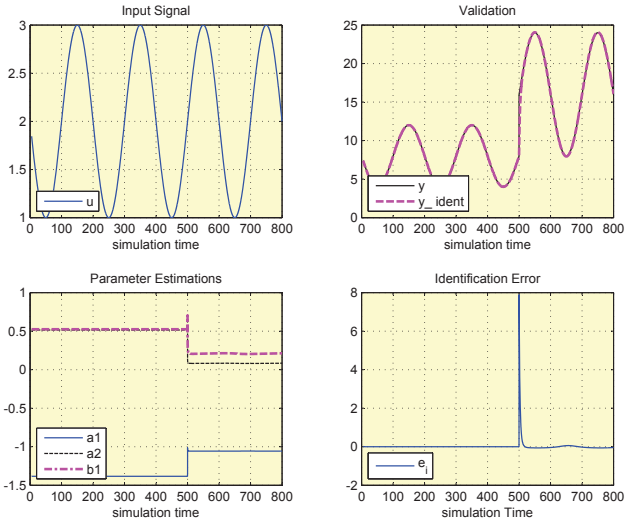

Figure A.4: Results of RLS identification applied on literature plant with changing parameters stimulated with sinusoidal input signal

Table A.3: RIV tuning parameters

	n	λ	$\hat{\theta}_0$	$\overline{x}_0$	v_0	P_0
RIV	3	0.99	I_{31}	I_{31}	I_{31}	$1000 * I_3$

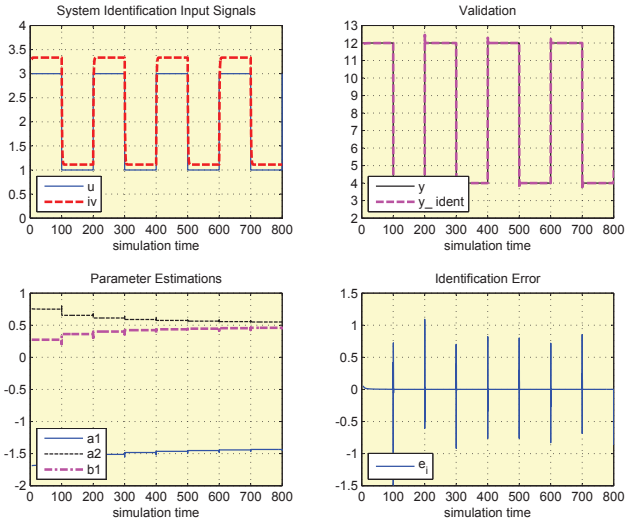

Figure A.5: Results of RIV identification applied on literature plant stimulated with square input signal

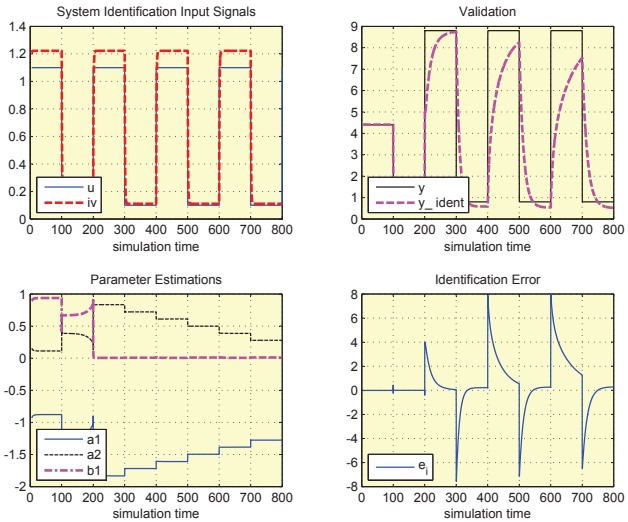

Figure A.6: Results of RIV identification applied on literature plant with changing parameters stimulated with square input signal

Table A.4: RIV tuning parameters

	n	λ	$\hat{\theta}_0$	$\overline{x}_0$	v_0	P_0
RIV	3	0.99	I_{31}	I_{31}	I_{31}	$1000 * I_3$

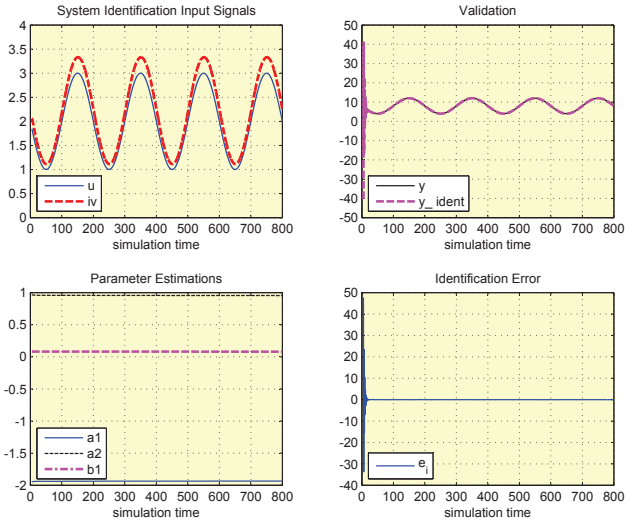

Figure A.7: Results of RIV identification applied on literature plant stimulated with sinusoidal input signal

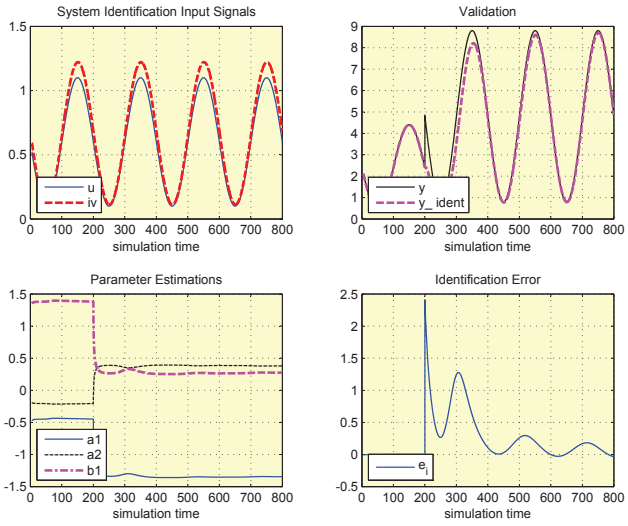

Figure A.8: Results of RIV identification applied on literature plant with changing parameters stimulated with sinusoidal input signal

Table A.5: SL tuning parameters

SL	n	γ_{sl}	$\hat{\theta}_0$	$\overline{x}_0$
	3	1	I_{31}	I_{31}

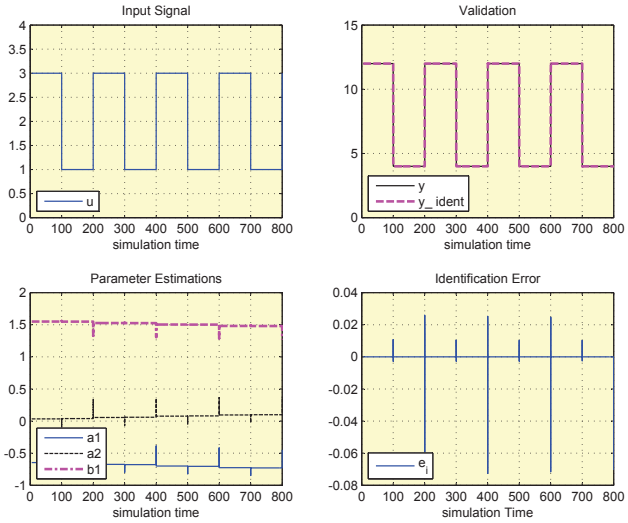

Figure A.9: Results of SL identification applied on literature plant stimulated with square input signal

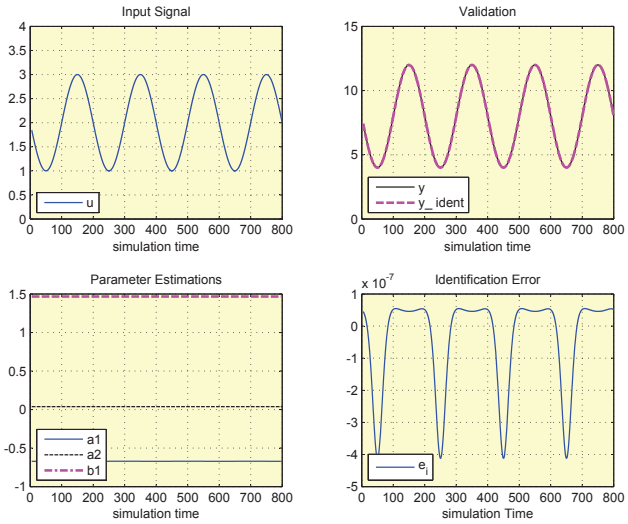

Figure A.10: Results of SL identification applied on literature plant stimulated with sinusoidal input signal

Table A.6: S.L tuning parameters

S.L	n	γ	$\hat{\theta}_0$	$\overline{x}_0$
	3	1	I_{31}	I_{31}

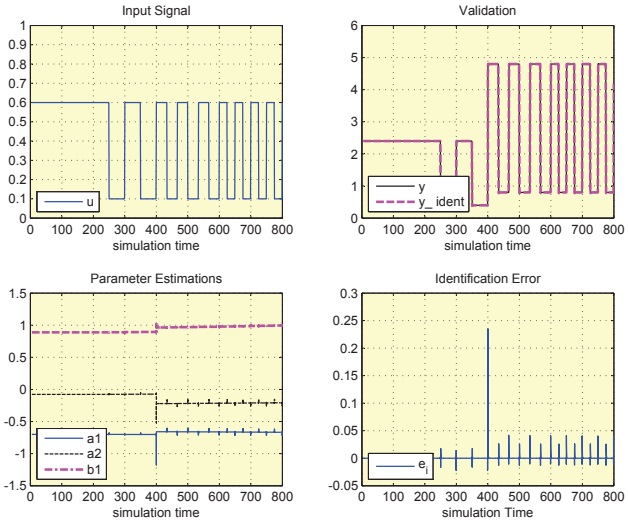

Figure A.11: Results of SL identification applied on literature plant with changing parameters stimulated with PRBS input signal

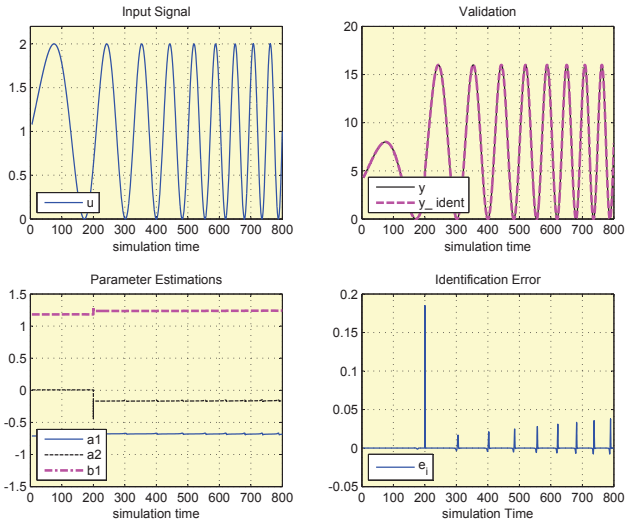

Figure A.12: Results of SL identification applied on literature plant with changing parameters stimulated with chirp input signal

Table A.7: RIV tuning parameters

	n	λ	$\hat{\theta}_0$	$\overline{x}_0$	v_0	P_0
RIV	2	0.99	I_{21}	I_{21}	I_{21}	$1000 * I_2$

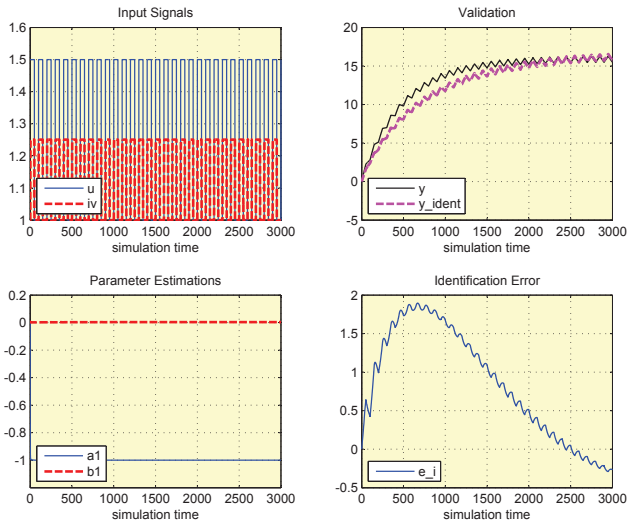

Figure A.13: Results of RIV identification applied on heat exchanger plant stimulated with square input signal of low frequency

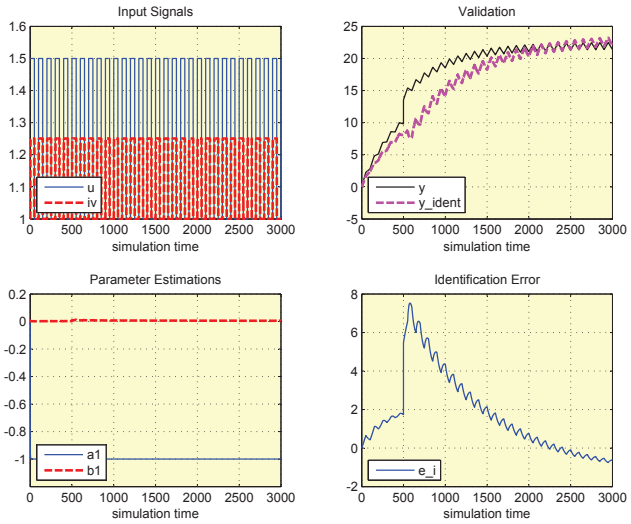

Figure A.14: Results of RIV identification applied on heat exchanger plant with changing parameters, stimulated with square input signal of low frequency

Table A.8: RIV tuning parameters

	n	λ	$\hat{\theta}_0$	$\overline{x}_0$	v_0	P_0
RIV	2	0.99	I_{21}	I_{21}	I_{21}	$1000 * I_2$

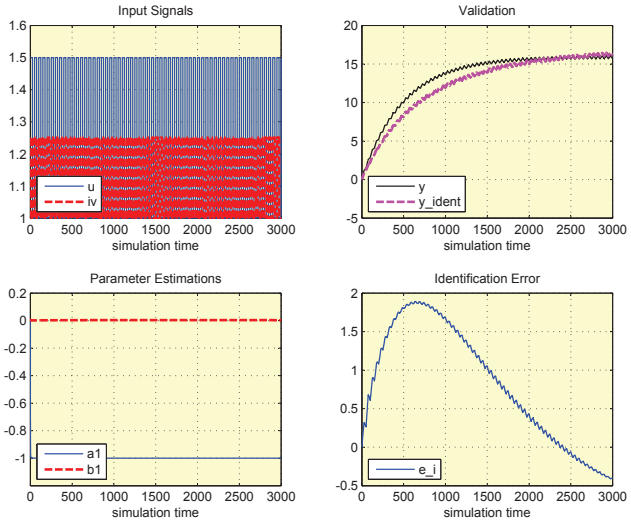

Figure A.15: Results of RIV identification applied on heat exchanger plant stimulated with square input signal of high frequency

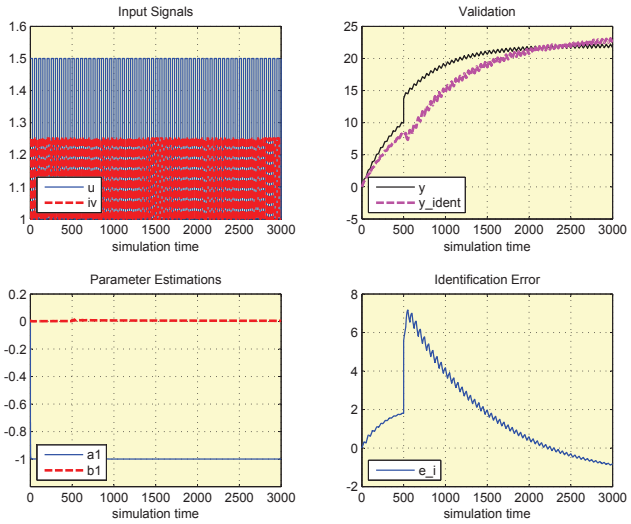

Figure A.16: Results of RIV identification applied on heat exchanger plant with changing parameters, stimulated with square input signal of high frequency

Table A.9: SL tuning parameters

	n	γ_{sl}	$\hat{\theta}_0$	$\overline{x}_0$
SL	2	1	I_{21}	I_{21}

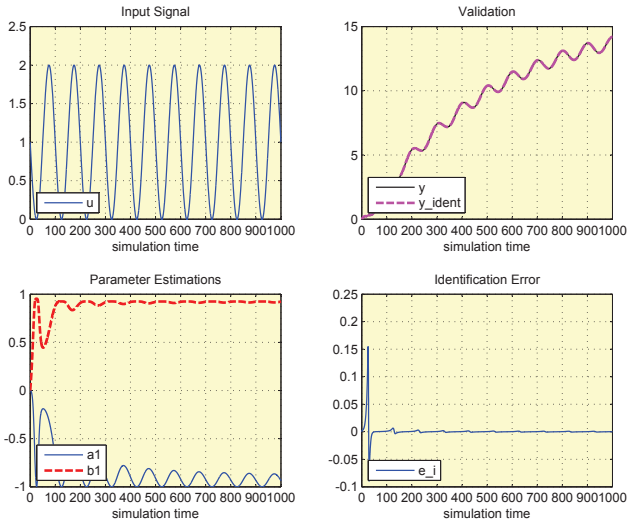

Figure A.17: Results of SL identification applied on heat exchanger plant stimulated with sinusoidal input signal of low frequency

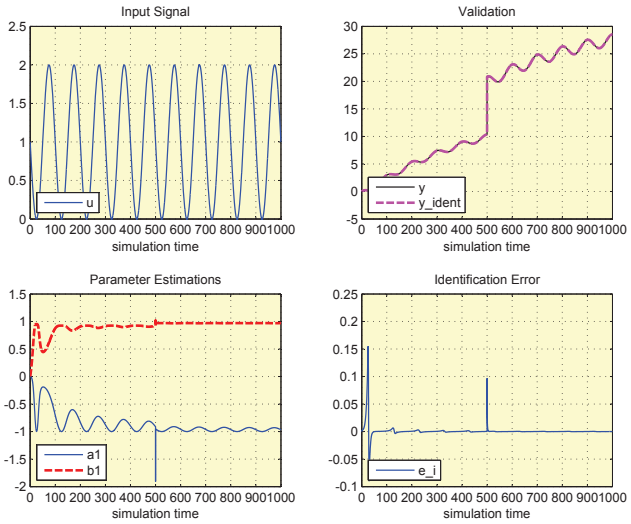

Figure A.18: Results of SL identification applied on heat exchanger plant with changing parameters, stimulated with sinusoidal input signal of low frequency

Table A.10: SL tuning parameters

SL	n	γ_{sl}	$\hat{\theta}_0$	$\overline{x}_0$
	2	1	I_{21}	I_{21}

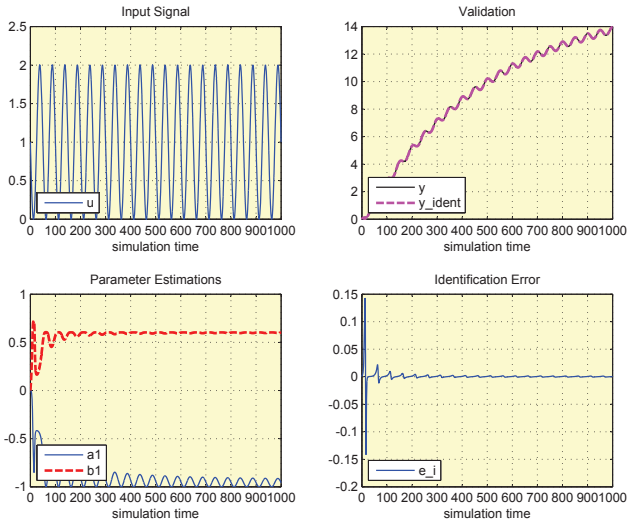

Figure A.19: Results of SL identification applied on heat exchanger plant stimulated with sinusoidal input signal of high frequency

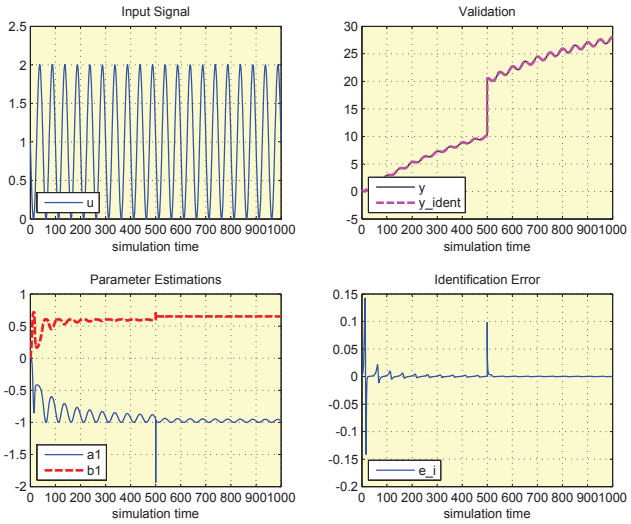

Figure A.20: Results of SL identification applied on heat exchanger plant with changing parameters, stimulated with sinusoidal input signal of high frequency

A.2 Experimental Results

Supplementary results of identification algorithms evaluation tests using heat exchanger experimental device (Figure 1.5) are presented in this section. The type of input signal, the plant parameters estimations, the identification error and the validation of estimated plant output signal are depicted in the following figures for each trial performed. Tables with each algorithm's tuning parameters are also depicted.

Table A.11: RLS tuning parameters

	n	λ	$\hat{\theta}_0$	$\overline{x}_0$	P_0
R.L.S	2	0.99	I_{21}	I_{21}	$1000 * I_2$

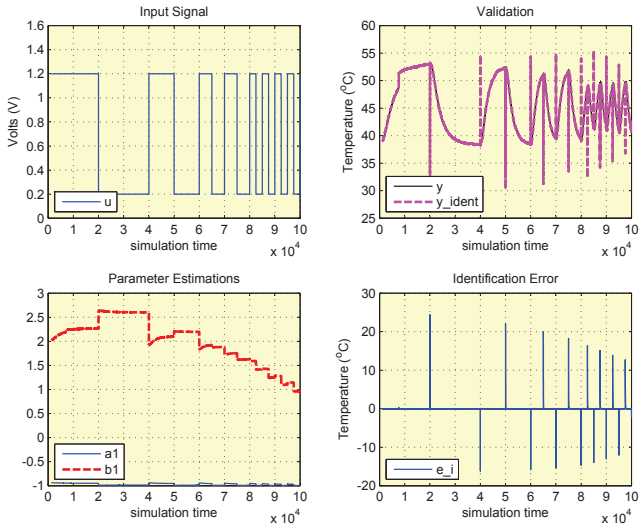

Figure A.21: Results of RLS identification applied on heat exchanger experimental device stimulated with P.R.B.S input signal

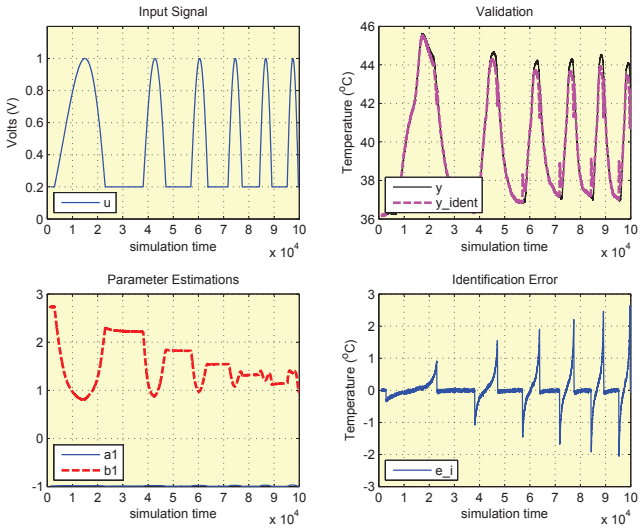

Figure A.22: Results of RLS identification applied on heat exchanger experimental device stimulated with chirp input signal

Table A.12: RIV tuning parameters

RIV	n	λ	$\hat{\theta}_0$	$\overline{x}_0$	v_0	P_0
	2	0.95	$[-0.1 - 0.1]^\top$	$[-0.1 - 0.1]^\top$	$[-0.1 - 0.1]^\top$	$1000 * I_2$

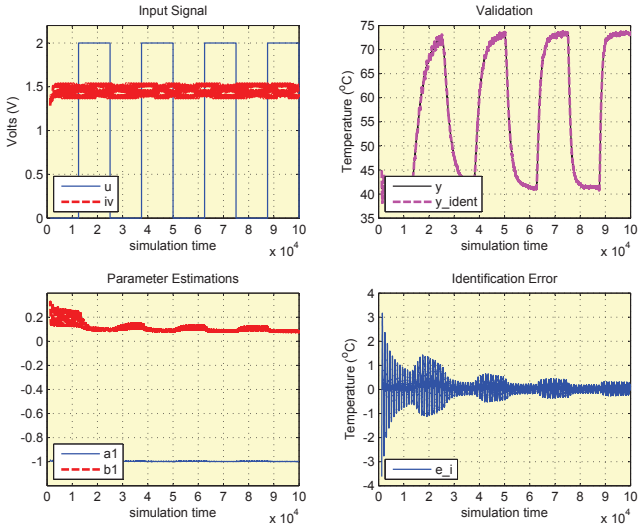

Figure A.23: Results of RIV identification applied on heat exchanger experimental device stimulated with square input signal

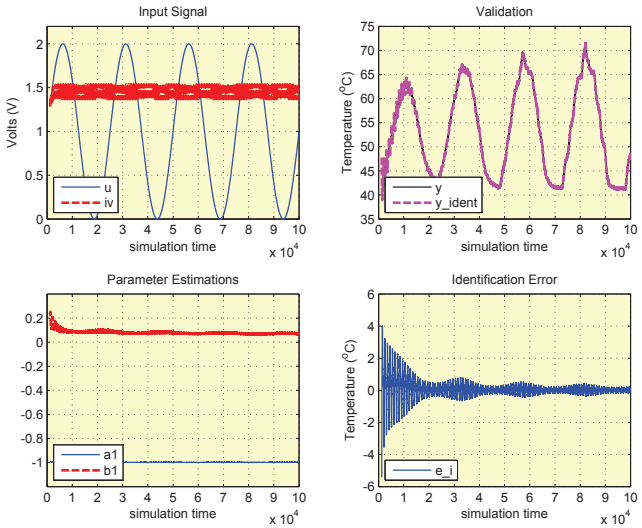

Figure A.24: Results of RIV identification applied on heat exchanger experimental device stimulated with sinusoidal input signal

Table A.13: S.L algorithm tuning parameters

S.L	n	γ	$\hat{\theta}_0$	$\overline{x}_0$
	2	1	I_{21}	I_{21}

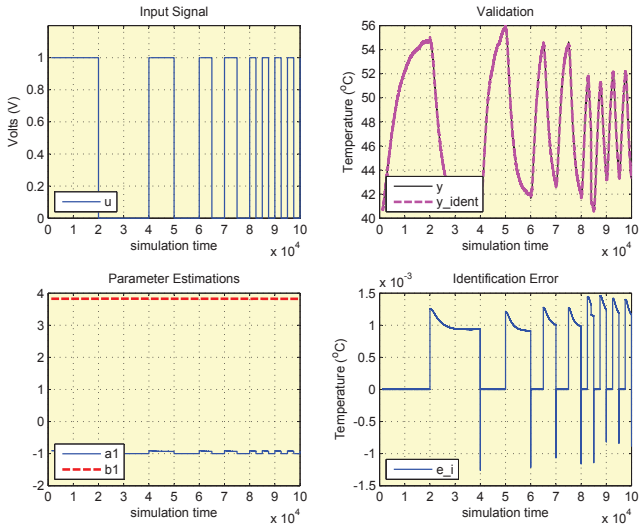

Figure A.25: Results of SL identification applied on heat exchanger experimental device stimulated with P.R.B.S input signal

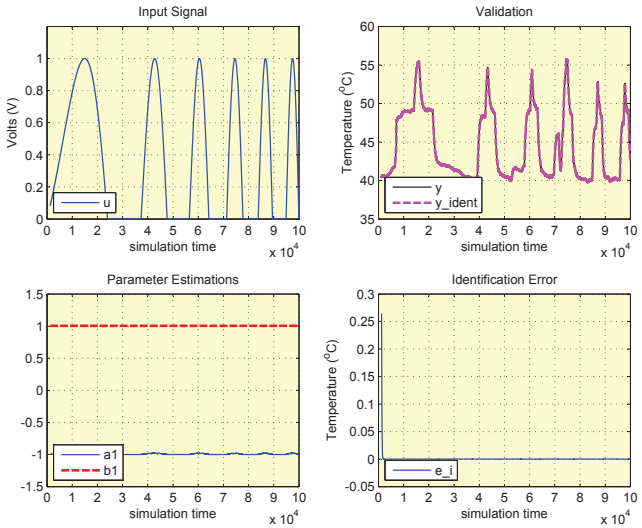

Figure A.26: Results of SL identification applied on heat exchanger experimental device stimulated with chirp input signal

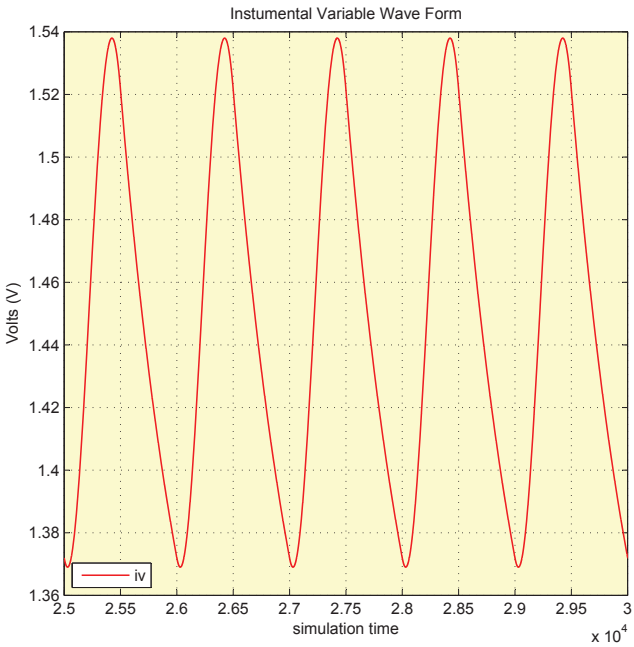

Figure A.27: Instrumental variable wave form used for instrumental variables system identification applied on heat exchanger experimental device

Appendix B

Evaluation of Control Algorithms

Supplementary results of control evaluation trials are presented in this chapter. The first section refers to results produced by making computer simulation trials. The second one refers to results from experimental evaluation trials using heat exchanger experimental device (Figure 1.5).

B.1 Computer Simulations Results

Figures B.1 to B.10 show results from computer simulations using the same literature plant with this used for the simulations presented in section 4.2.1. Figures B.14 to B.27 show results from computer simulations using the heat exchanger's first order discrete time mathematical model which was also used for the computer simulation trials of control algorithms presented in section 4.2.1 .

Except from figures depicting the values of control law, control parameter estimations and control error, there are figures depicting the trajectories of controller parameters, plant parameter errors and of closed-loop estimation errors. Tables with each controller's tuning parameters are also depicted.

Table B.1: MRAC tuning parameters

MRAC	γ
	100

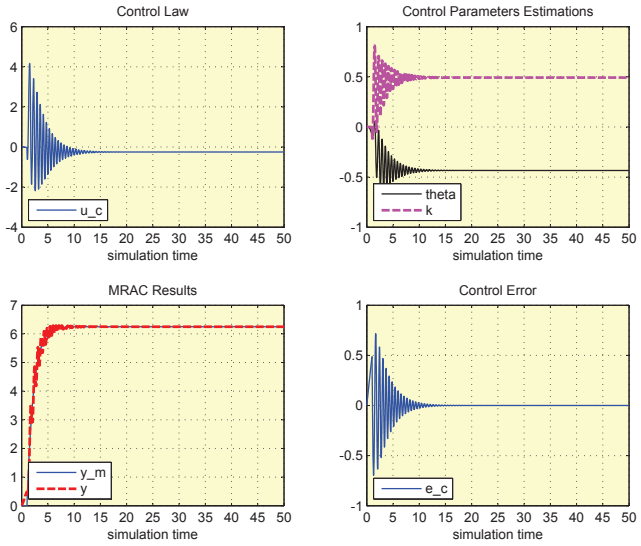

Figure B.1: MRAC of literature plant stimulated with step input signal

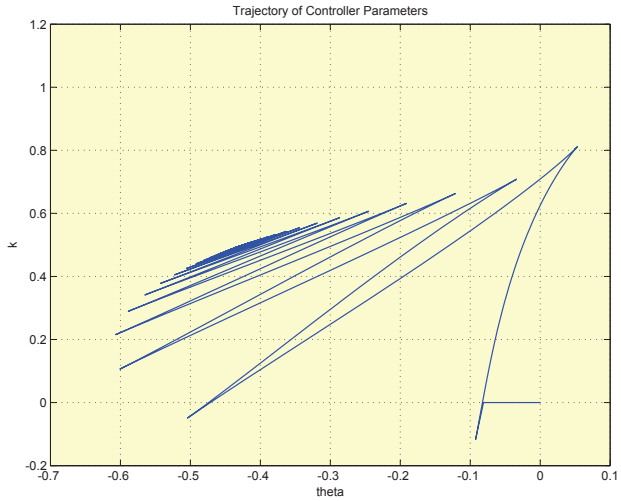

Figure B.2: Trajectory of controller parameters presented in figure B.1

Table B.2: MRAC tuning parameters

MRAC	γ
	100

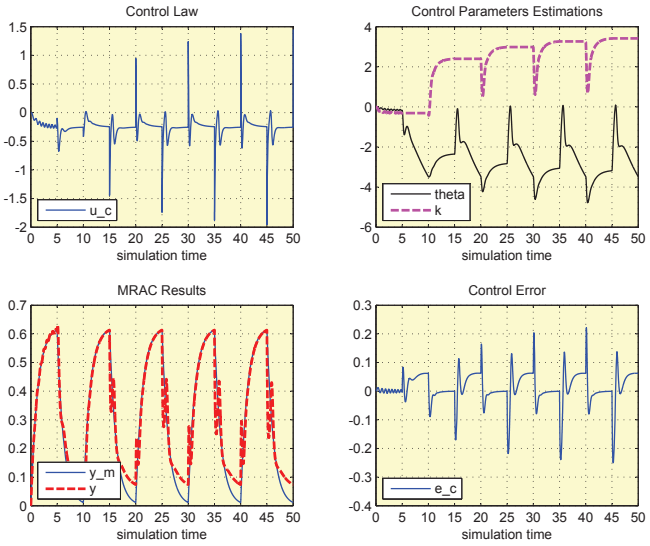

Figure B.3: MRAC of literature plant stimulated with square input signal

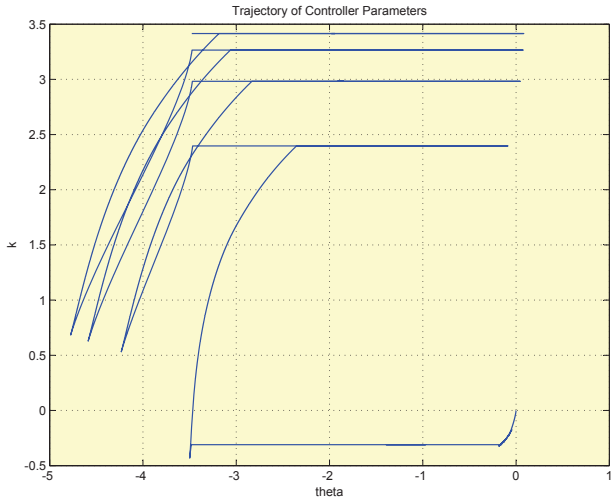

Figure B.4: Trajectory of controller parameters presented in figure B.3

Table B.3: CMRAC-RLS tuning parameters

CMRAC-RLS	γ	n	λ	$\hat{\theta}_0$	$\overline{x}_0$	P_0
	20	2	1	I_{21}	I_{21}	$1000 * I_2$

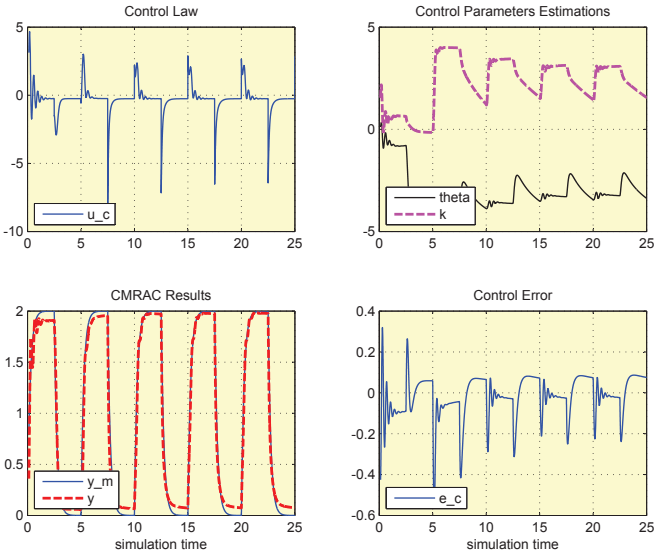

Figure B.5: CMRAC-RLS of literature plant stimulated with square input signal

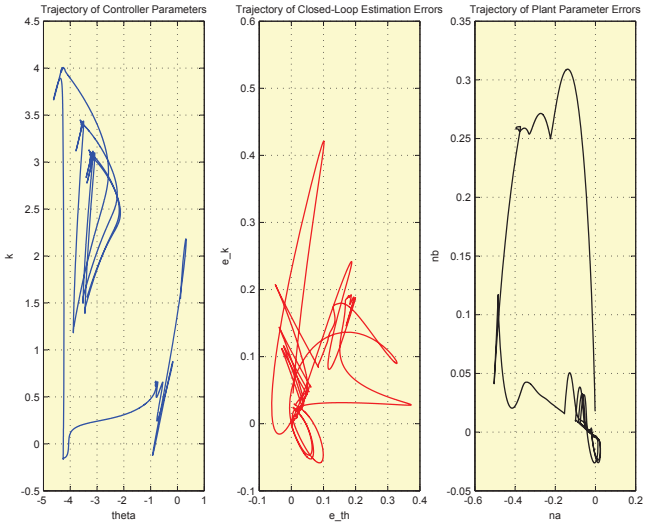

Figure B.6: Trajectories of closed-loop estimation errors, plant parameter errors and controller parameters presented in figure B.5

Table B.4: CMRAC-RIV tuning parameters

	γ	n	λ	$\hat{\theta}_0$	$\overline{x}_0$	v_0	P_0
CMRAC-RIV	100	2	1	$[0.01 \quad 0.01]^\top$	$[0.01 \quad 0.01]^\top$	$[0.01 \quad 0.01]^\top$	$1000 * I_2$

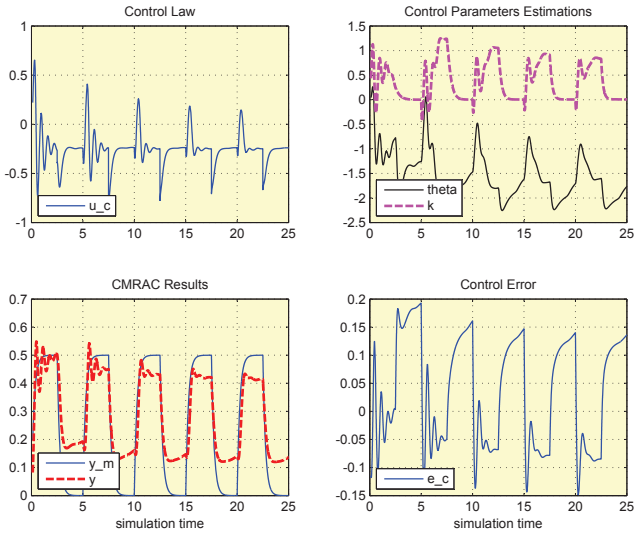

Figure B.7: CMRAC-RIV of literature plant stimulated with square input signal

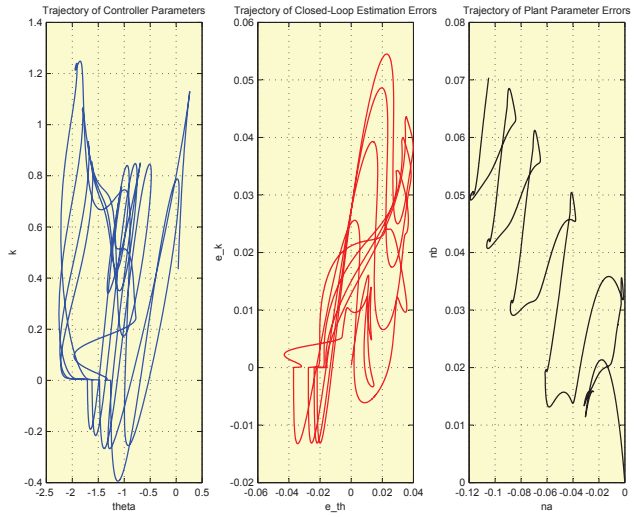

Figure B.8: Trajectories of closed-loop estimation errors, plant parameter errors and controller parameters presented in figure B.7

Table B.5: CMRAC-SL tuning parameters

	γ	n	γ_{sl}	$\hat{\theta}_0$	$\overline{x}_0$
CMRAC-SL	2	2	1	I_{21}	I_{21}

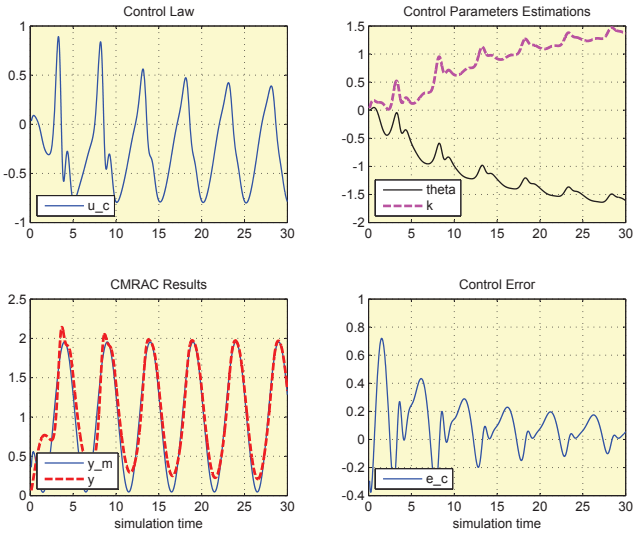

Figure B.9: CMRAC-SL of literature plant stimulated with sinusoidal input signal

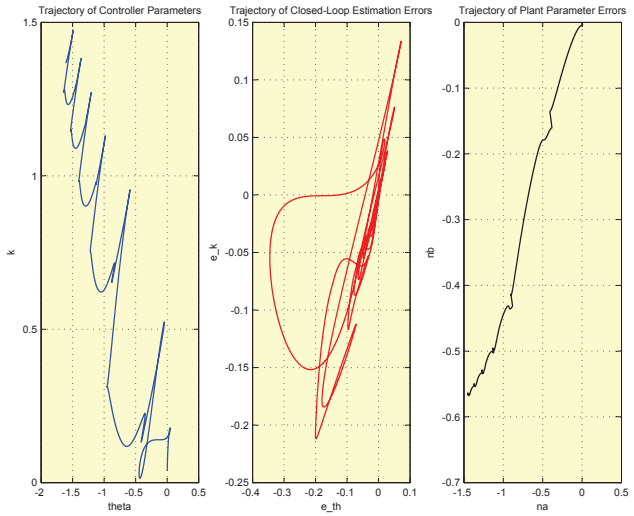

Figure B.10: Trajectories of closed-loop estimation errors, plant parameter errors and controller parameters presented in figure B.9

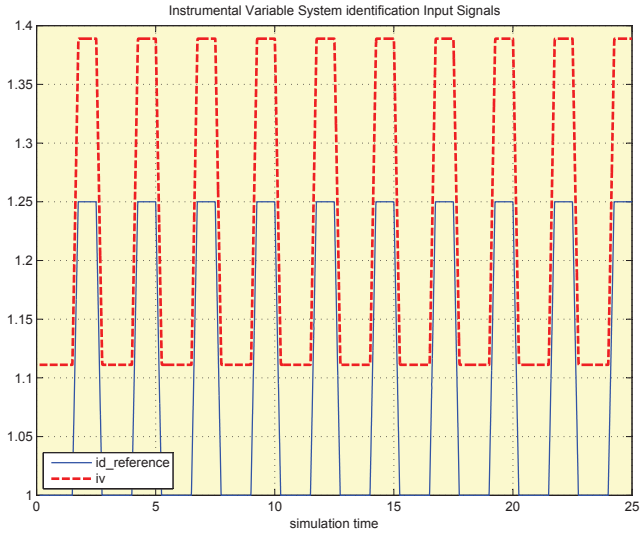

Figure B.11: Reference input and instrumental variable used for the implementation of evaluation trials presented in B.7

Table B.6: MRAC tuning parameters

MRAC	γ
	10^{-4}

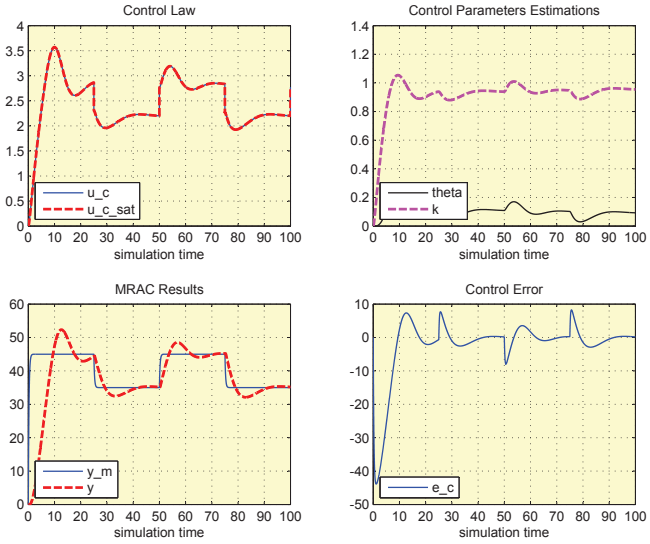

Figure B.12: MRAC of heat exchanger plant stimulated with square input signal

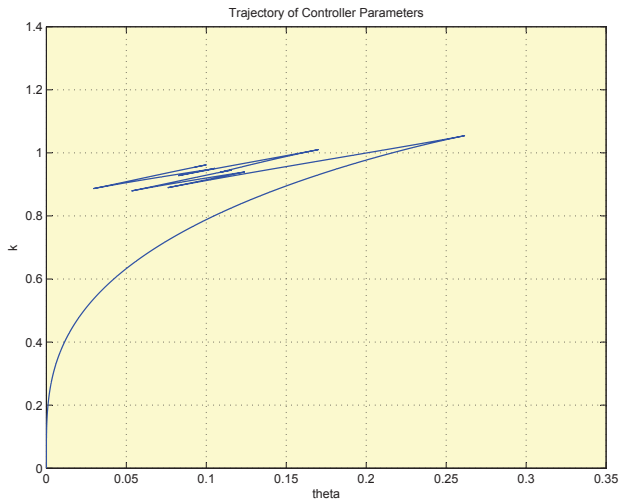

Figure B.13: Trajectory of controller parameters presented in figure B.12

Table B.7: CMRAC-RIV parameters

	γ	n	λ	$\hat{\theta}_0$	$\overline{x}_0$	v_0	P_0
CMRAC-RIV	10^{-4}	2	1	I_{21}	I_{21}	I_{21}	$1000 * I_2$

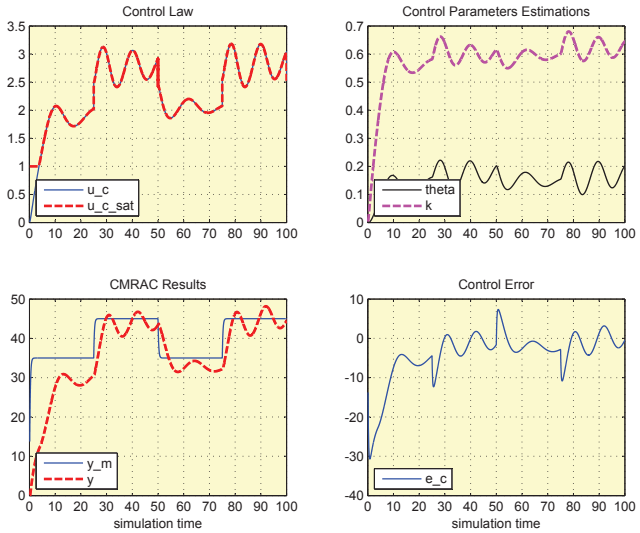

Figure B.14: CMRAC-RIV of heat exchanger plant stimulated with square input signal

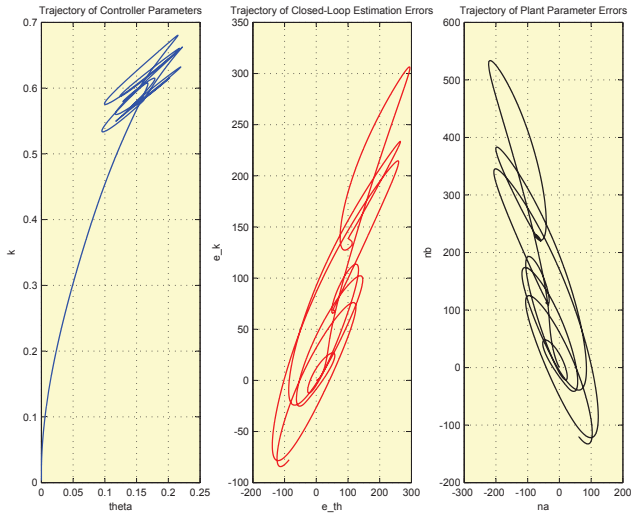

Figure B.15: Trajectories of closed-loop estimation errors, plant parameter errors and controller parameters presented in figure B.14

Table B.8: CMRAC-SL tuning parameters

	γ	n	γ_{sl}	$\hat{\theta}_0$	$\overline{x}_0$
CMRAC-SL	10^{-4}	2	1	I_{21}	I_{21}

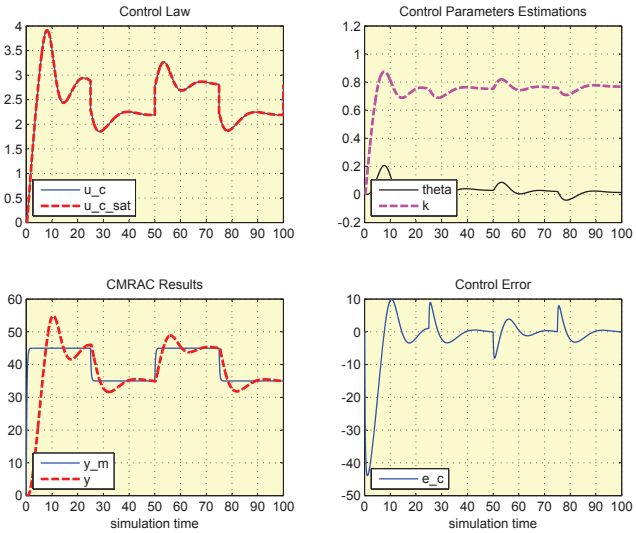

Figure B.16: CMRAC-SL of heat exchanger plant stimulated with square input signal

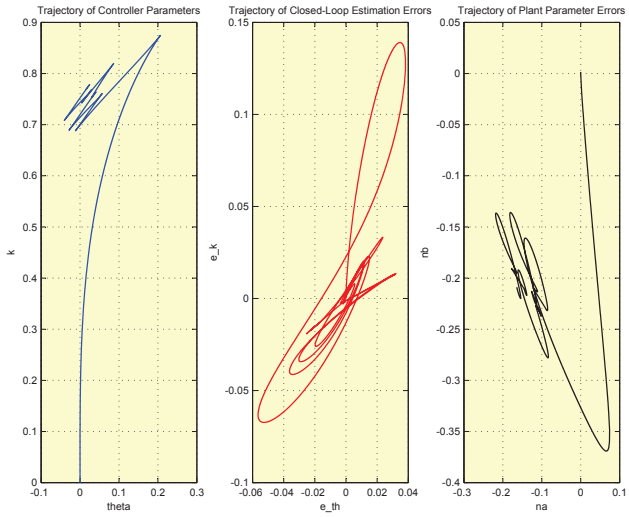

Figure B.17: Trajectories of closed-loop estimation errors, plant parameter errors and controller parameters presented in figure B.16

Table B.9: MRAC tuning parameters

MRAC	γ
	10^{-4}

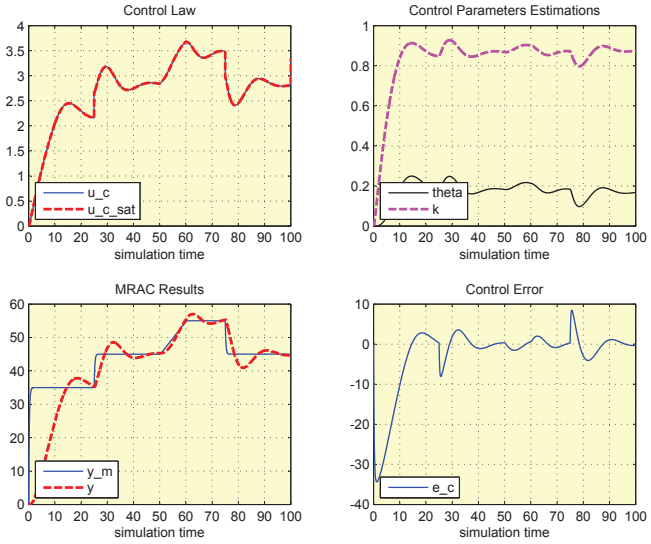

Figure B.18: MRAC of heat exchanger plant stimulated with square input signal of changing amplitude

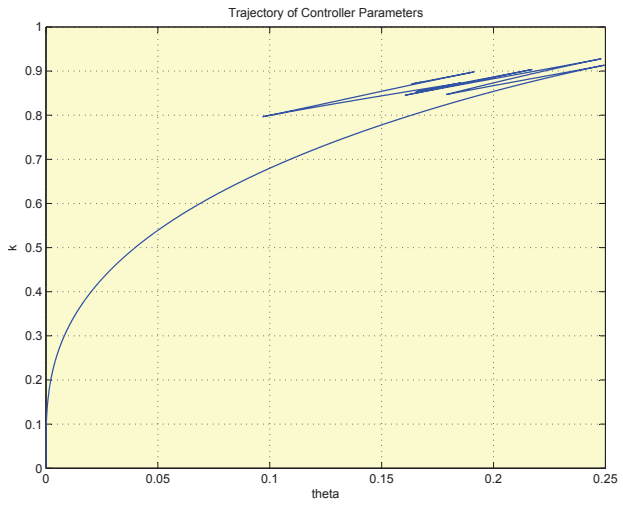

Figure B.19: Trajectory of controller parameters presented in figure B.18

Table B.10: CMRAC-RIV tuning parameters

CMRAC_ RIV	γ	n	λ	$\hat{\theta}_0$	$\overline{x}_0$	v_0	P_0
	10^{-4}	2	1	I_{21}	I_{21}	I_{21}	$1000 * I_2$

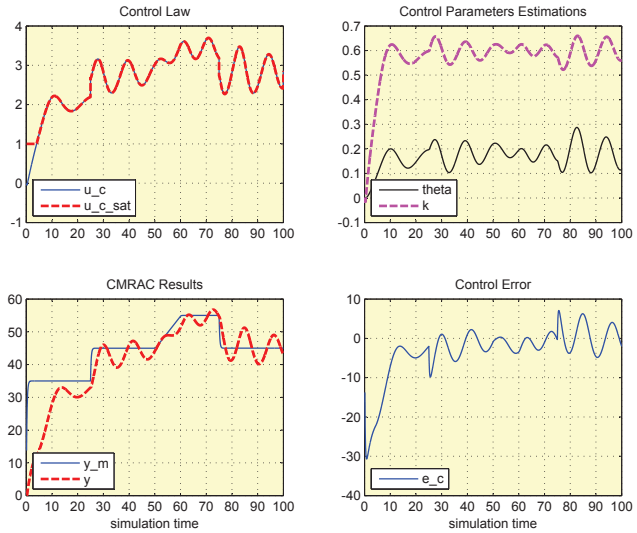

Figure B.20: CMRAC-RIV of heat exchanger plant stimulated with square input signal of changing amplitude

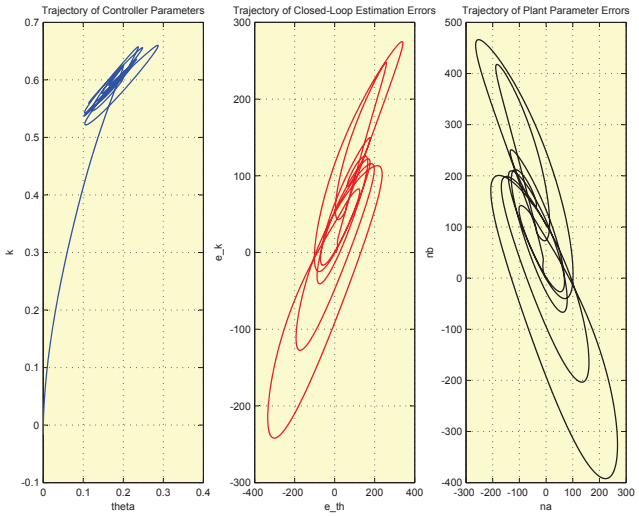

Figure B.21: Trajectories of closed-loop estimation errors, plant parameter errors and controller parameters presented in figure B.20

Table B.11: CMRAC-SL tuning parameters

CMRAC-SL	γ	n	γ_{sl}	$\hat{\theta}_0$	$\overline{x}_0$
	10^{-4}	2	1	I_{21}	I_{21}

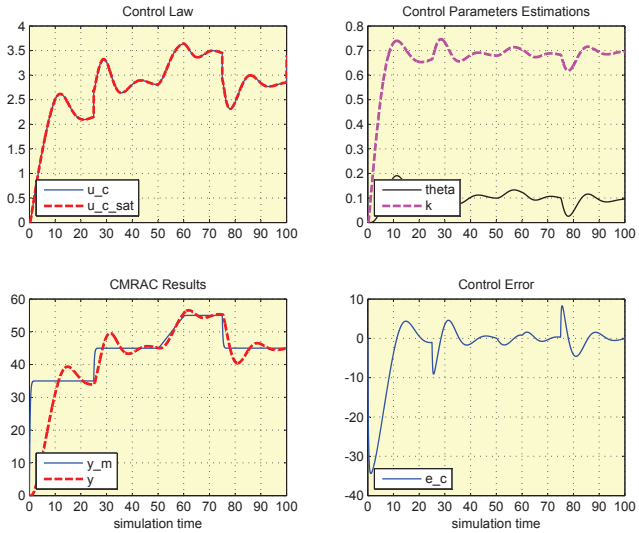

Figure B.22: CMRAC-SL of heat exchanger plant stimulated with square input signal of changing amplitude

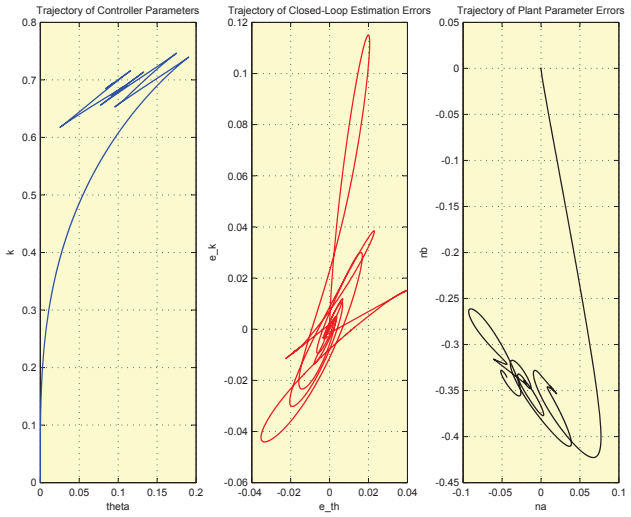

Figure B.23: Trajectories of closed-loop estimation errors, plant parameter errors and controller parameters presented in figure B.22

Table B.12: CMRAC-DZ-RIV tuning parameters

CMRAC_ RIV	γ	Δ	n	λ	$\hat{\theta}_0$	$\overline{x}_0$	v_0	P_0
	10^{-4}	0.5	2	1	I_{21}	I_{21}	I_{21}	$1000 * I_2$

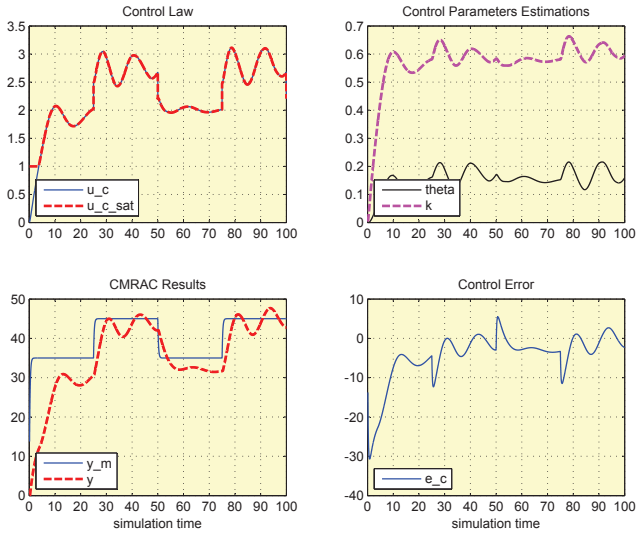

Figure B.24: CMRAC-RIV of heat exchanger plant stimulated with square input signal. Use of dead-zone

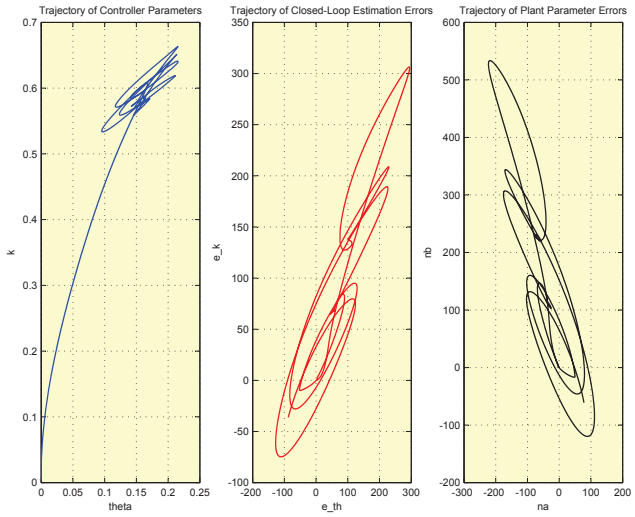

Figure B.25: Trajectories of closed-loop estimation errors, plant parameter errors and controller parameters presented in figure B.24

Table B.13: CMRAC-DZ-SL tuning parameters

S.L	γ	Δ	n	γ_{sl}	$\hat{\theta}_0$	$\overline{x}_0$
	10^{-4}	1	2	1	I_{21}	I_{21}

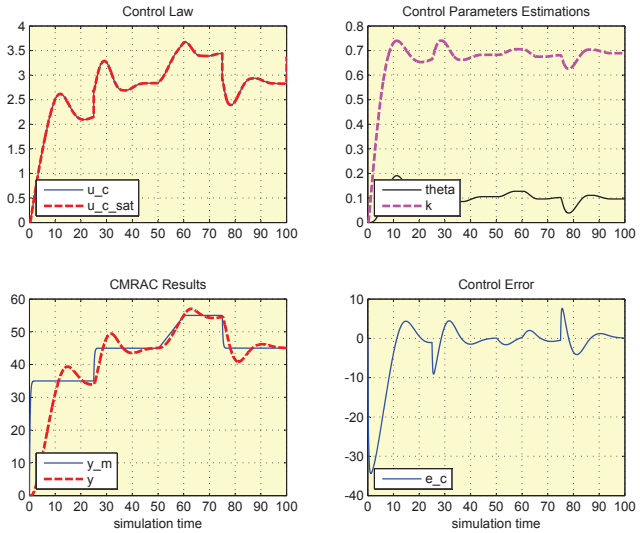

Figure B.26: CMRAC-SL of heat exchanger plant stimulated with square input signal of changing amplitude. Use of dead-zone

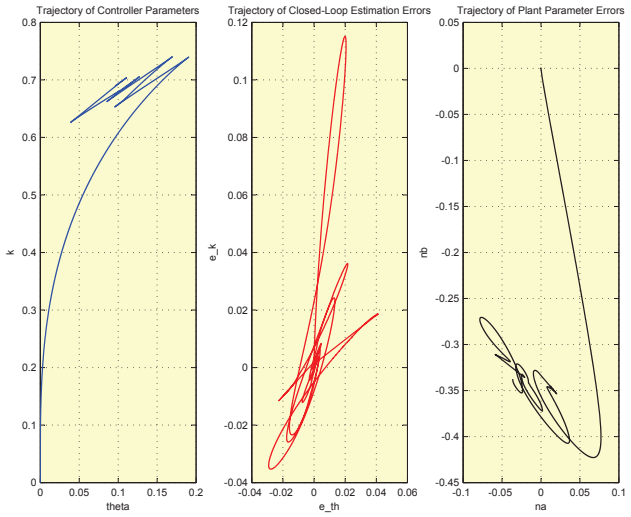

Figure B.27: Trajectories of closed-loop estimation errors, plant parameter errors and controller parameters presented in figure B.26

B.2 Experimental Results

Supplementary results of controllers' evaluation tests using heat exchanger experimental device (Figure 1.5) are presented in this section. Except from figures depicting the values of control law, control parameter estimations and control error, there are figures depicting the trajectories of controller parameters, plant parameter errors and of closed-loop estimation errors. Tables with each controller's tuning parameters are also depicted.

Table B.14: MRAC tuning parameters

	γ
MRAC	10^{-8}

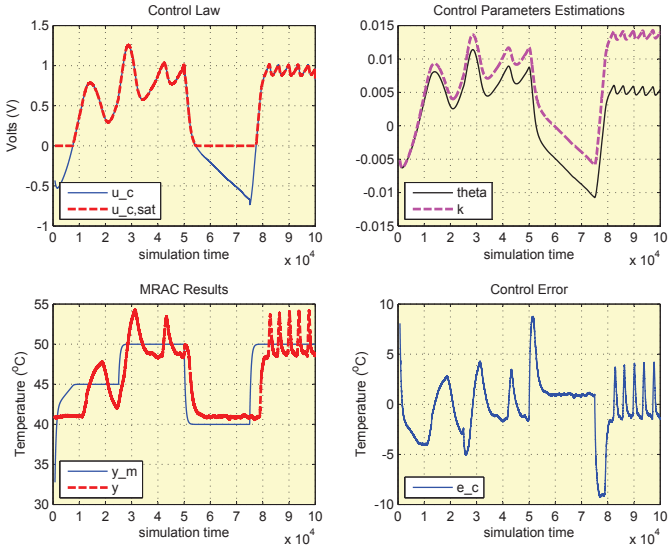

Figure B.28: MRAC of heat exchanger device stimulated with square input signal

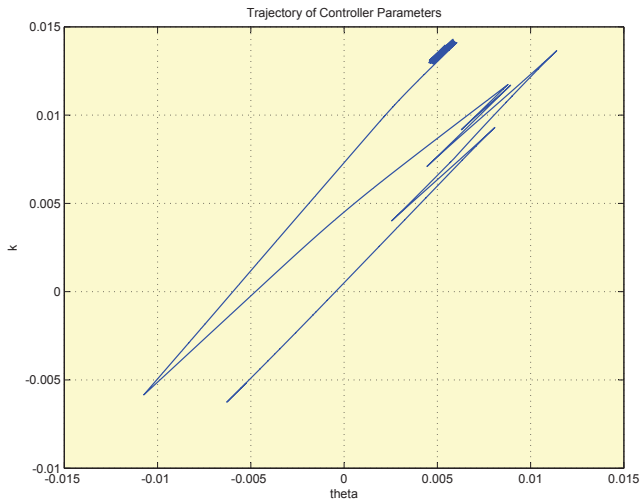

Figure B.29: Trajectory of controller parameters presented in Figure B.28

Table B.15: CMRAC-RLS tuning parameters

	γ	n	λ	$\hat{\theta}_0$	$\overline{x}_0$	P_0
CMRAC-RLS	$7 * 10^{-9}$	2	0.99	Z_{21}	Z_{21}	$1000 * I_2$

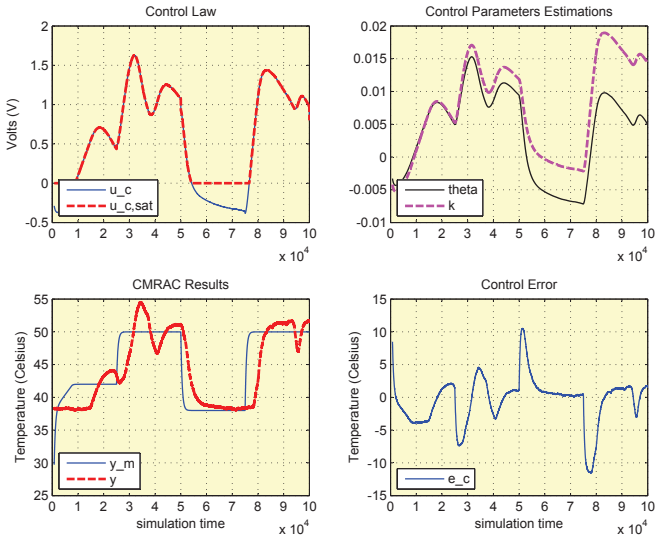

Figure B.30: CMRAC-RLS of heat exchanger device stimulated with square input signal

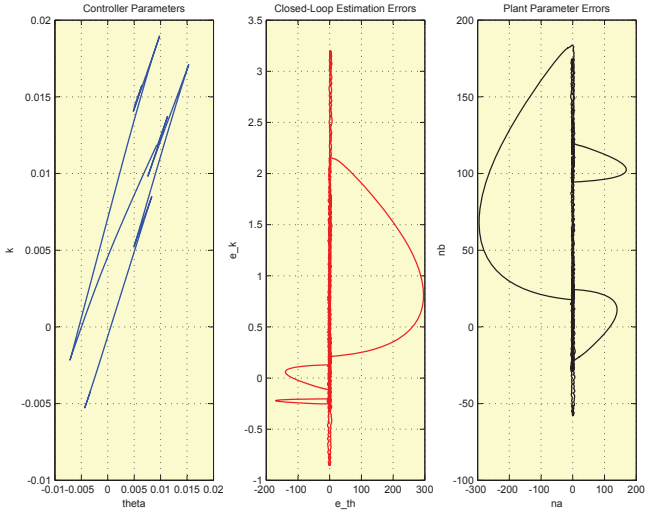

Figure B.31: Trajectories of closed-loop estimation errors, plant parameter errors and controller parameters presented in Figure B.30

Table B.16: CMRAC-RIV tuning parameters

	γ	n	λ	$\hat{\theta}_0$	$\overline{x}_0$	v_0	P_0
CMRAC-RIV	$5 * 10^{-9}$	2	0.95	$[-0.1 \quad -0.1]^\intercal$	$[-0.1 \quad -0.1]^\intercal$	$[-0.1 \quad -0.1]^\intercal$	$1000 * I_2$

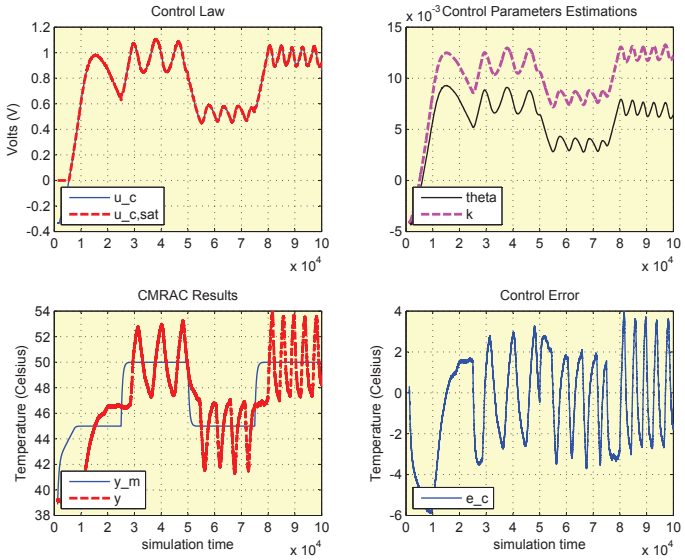

Figure B.32: CMRAC-RIV of heat exchanger device stimulated with square input signal

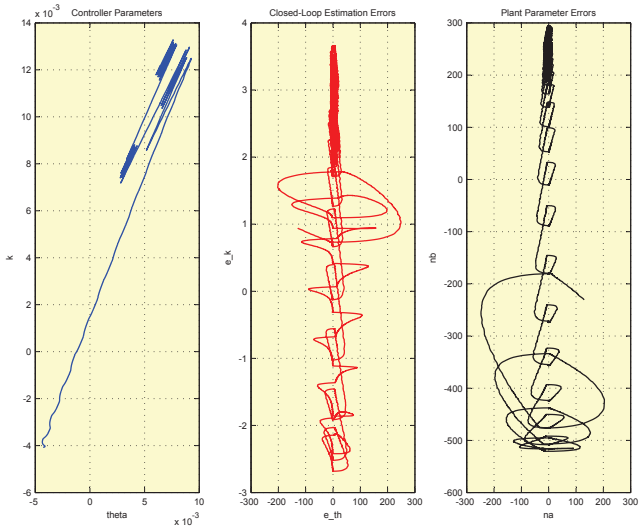

Figure B.33: Trajectories of closed-loop estimation errors, plant parameter errors and controller parameters presented in Figure B.32

Table B.17: CMRAC-SL tuning parameters

	γ	n	γ_{sl}	$\hat{\theta}_0$	$\overline{x}_0$
CMRAC-SL	$7 * 10^{-9}$	2	1	Z_{21}	Z_{21}

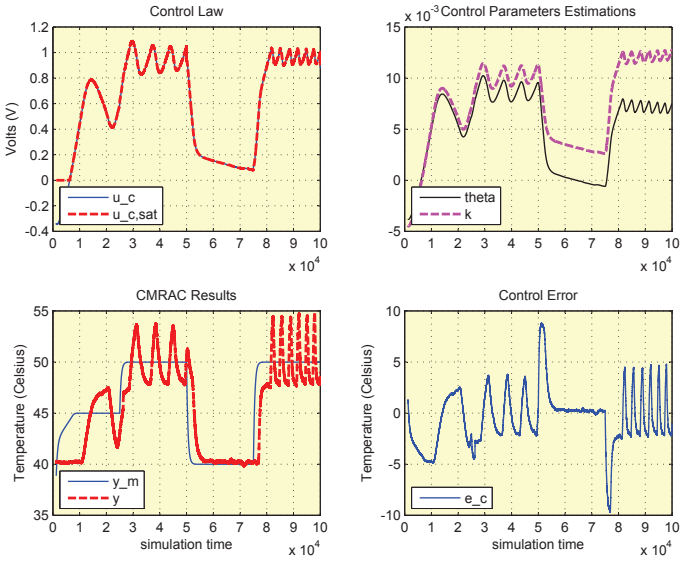

Figure B.34: CMRAC-SL of heat exchanger stimulated device with square input signal

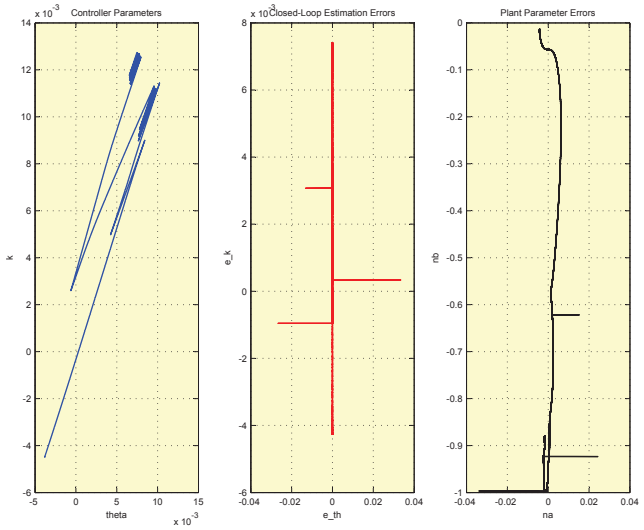

Figure B.35: Trajectories of closed-loop estimation errors, plant parameter errors and controller parameters presented in Figure B.34

Table B.18: MRAC tuning parameters

	γ
MRAC	10^{-8}

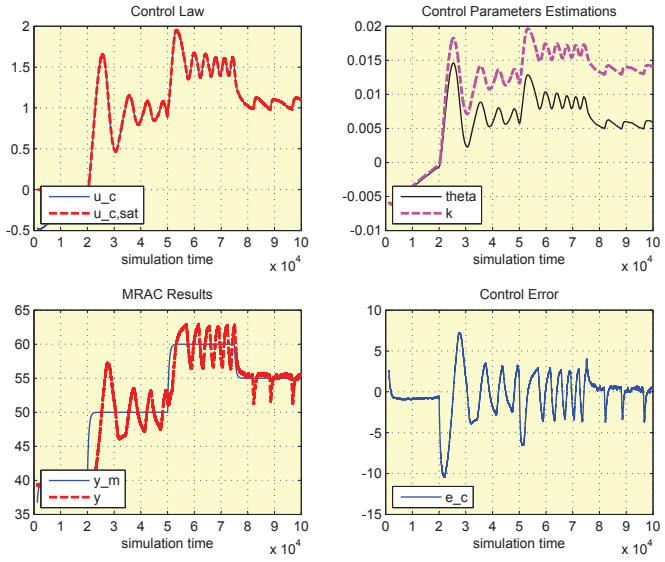

Figure B.36: MRAC of heat exchanger experimental device stimulated with square input signal of changing amplitude

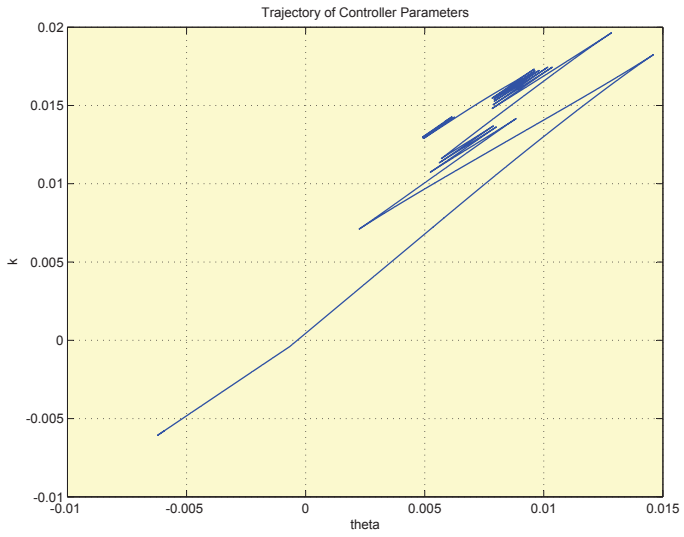

Figure B.37: Trajectory of controller parameters presented in Figure B.36

Table B.19: CMRAC-RLS tuning parameters

	γ	n	λ	$\hat{\theta}_0$	$\overline{x}_0$	P_0
CMRAC-RLS	$7 * 10^{-9}$	2	0.99	Z_{21}	Z_{21}	$1000 * I_2$

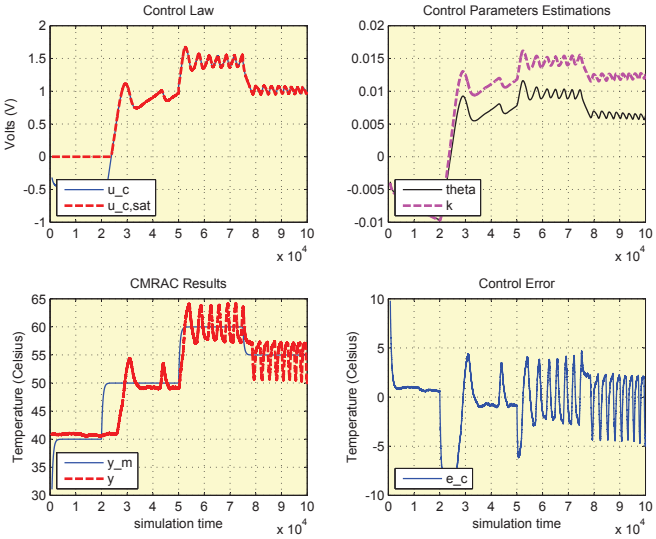

Figure B.38: CMRAC-RLS of heat exchanger experimental device stimulated with square input signal of changing amplitude

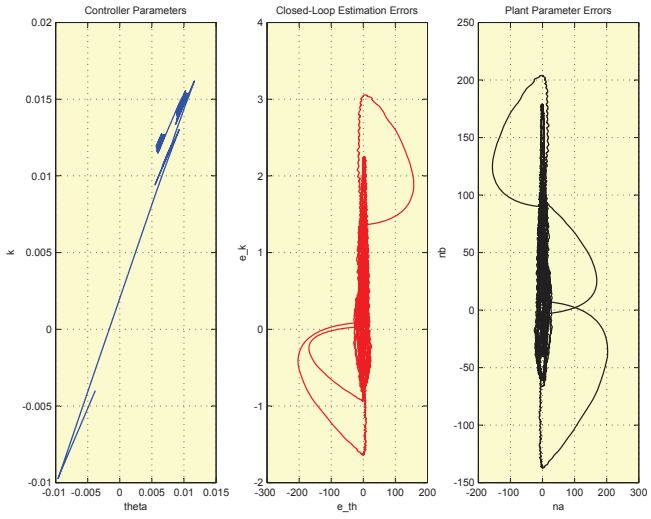

Figure B.39: Trajectories of closed-loop estimation errors, plant parameter errors and controller parameters presented in Figure B.38

Table B.20: CMRAC-RIV tuning parameters

	γ	n	λ	$\hat{\theta}_0$	$\overline{x}_0$	v_0	P_0
CMRAC-RIV	$5 * 10^{-9}$	2	0.95	$[-0.1 \quad -0.1]^\intercal$	$[-0.1 \quad -0.1]^\intercal$	$[-0.1 \quad -0.1]^\intercal$	$1000 * I_2$

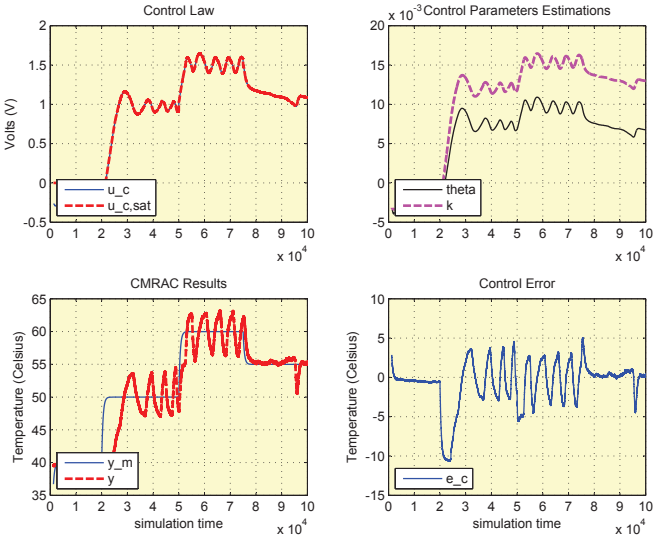

Figure B.40: CMRAC-RIV of heat exchanger experimental device stimulated with square input signal of changing amplitude

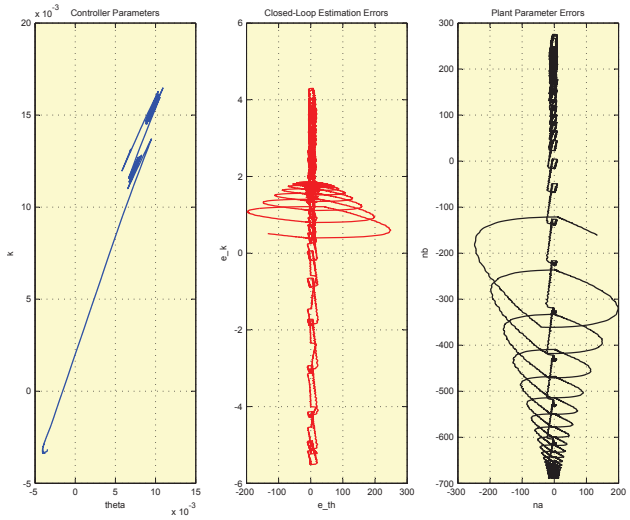

Figure B.41: Trajectories of closed-loop estimation errors, plant parameter errors and controller parameters presented in Figure B.40

Table B.21: CMRAC-SL tuning parameters

	γ	n	γ_{sl}	$\hat{\theta}_0$	$\overline{x}_0$
CMRAC-SL	$7 * 10^{-9}$	2	1	Z_{21}	Z_{21}

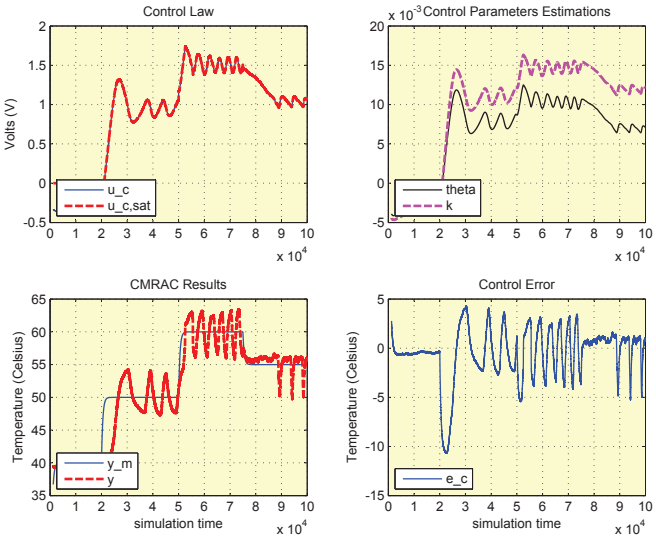

Figure B.42: CMRAC-SL of heat exchanger experimental device stimulated with square input signal of changing amplitude

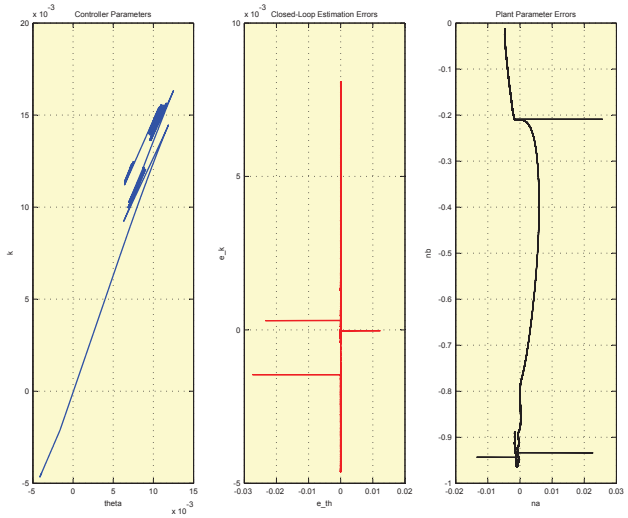

Figure B.43: Trajectories of closed-loop estimation errors, plant parameter errors and controller parameters presented in Figure B.42

Table B.22: MRAC tuning parameters

	γ	Δ
MRAC	10^{-8}	1

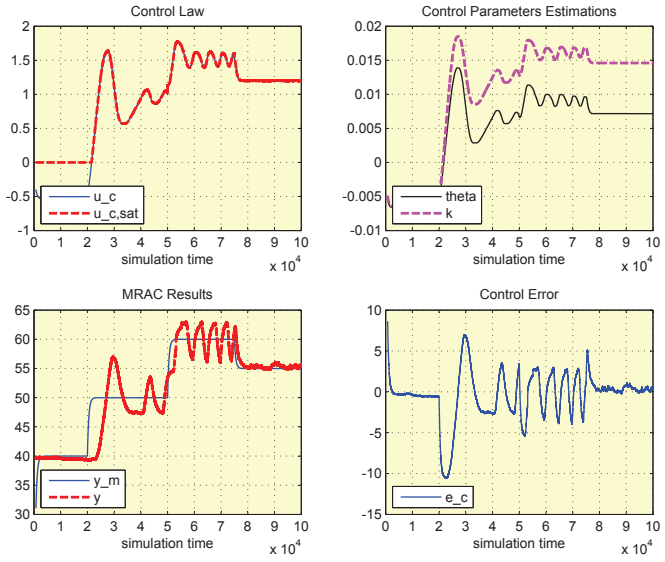

Figure B.44: MRAC of heat exchanger experimental device using dead-zone stimulated with square input signal of changing amplitude

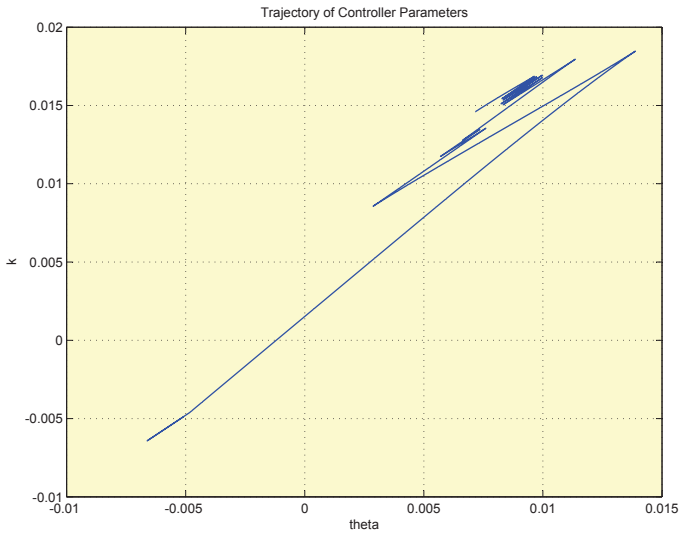

Figure B.45: Trajectory of controller parameters presented in Figure B.44

Table B.23: CMRAC-RLS tuning parameters

	γ	Δ	n	λ	$\hat{\theta}_0$	$\overline{x}_0$	P_0
CMRAC-RLS	$7.5 * 10^{-9}$	2	2	0.99	Z_{21}	Z_{21}	$1000 * I_2$

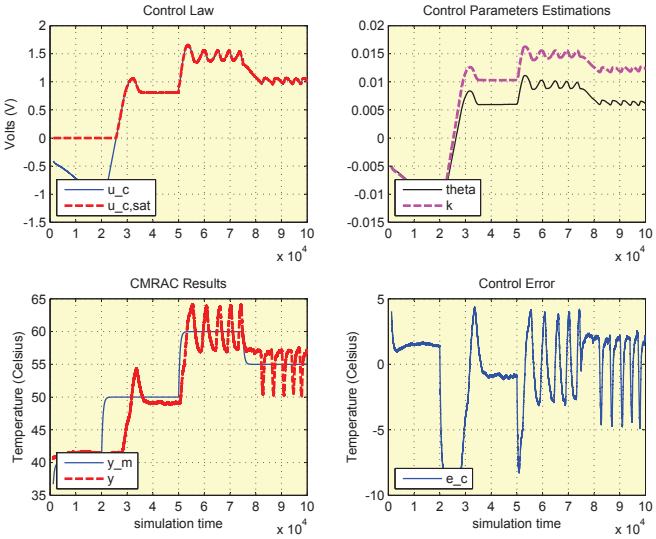

Figure B.46: CMRAC-RLS of heat exchanger experimental device using dead-zone stimulated with square input signal of changing amplitude

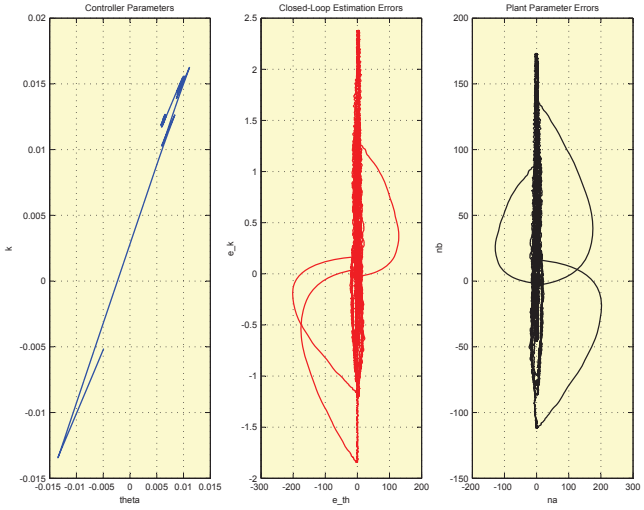

Figure B.47: Trajectories of closed-loop estimation errors, plant parameter errors and controller parameters presented in Figure B.46

Table B.24: CMRAC-RIV tuning parameters

	γ	Δ	n	λ	$\hat{\theta}_0$	$\overline{x}_0$	v_0	P_0
CMRAC-RIV	$6 * 10^{-9}$	1	2	0.95	$[-0.1 \quad -0.1]^\top$	$[-0.1 \quad -0.1]^\top$	$[-0.1 \quad -0.1]^\top$	$1000 * I_2$

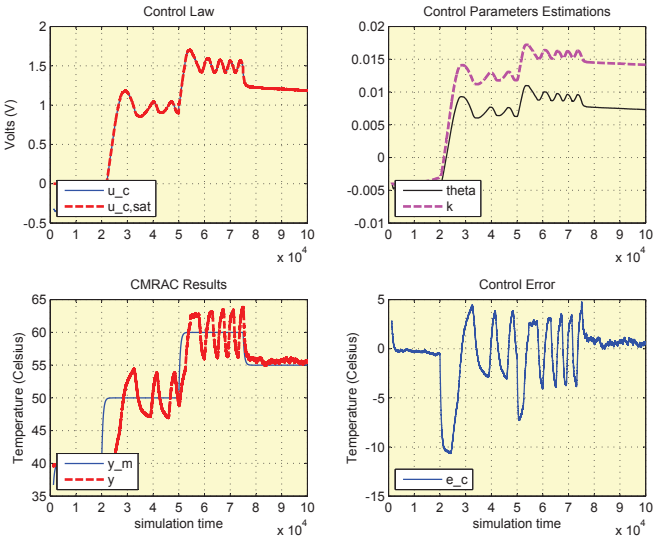

Figure B.48: CMRAC-RIV of heat exchanger experimental device using dead-zone stimulated with square input signal of changing amplitude

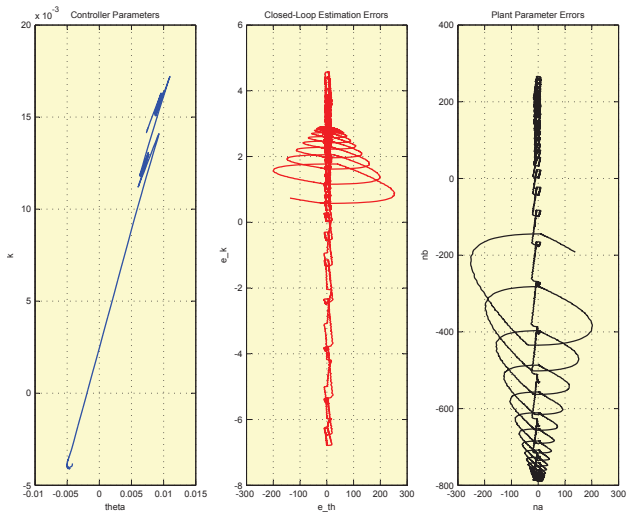

Figure B.49: Trajectories of closed-loop estimation errors, plant parameter errors and controller parameters presented in Figure B.48

Table B.25: CMRAC-SL tuning parameters

CMRAC-SL	γ	Δ	n	γ_{sl}	$\hat{\theta}_0$	$\overline{x}_0$
	$7 * 10^{-9}$	1	2	1	Z_{21}	Z_{21}

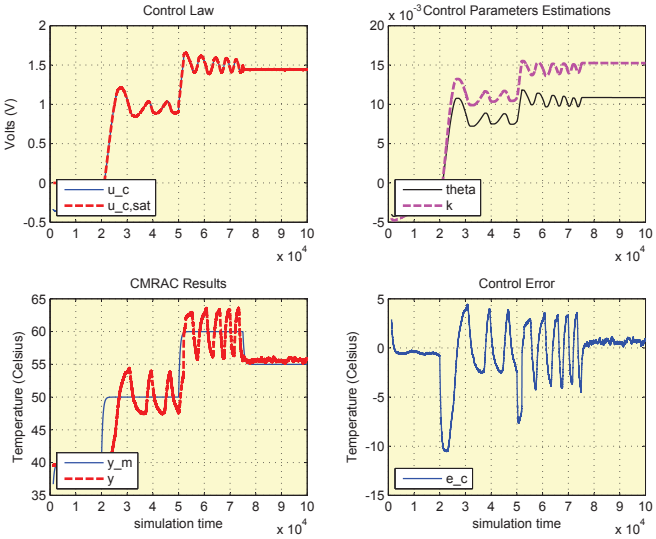

Figure B.50: CMRAC-SL of heat exchanger experimental device using dead-zone stimulated with square input signal of changing amplitude

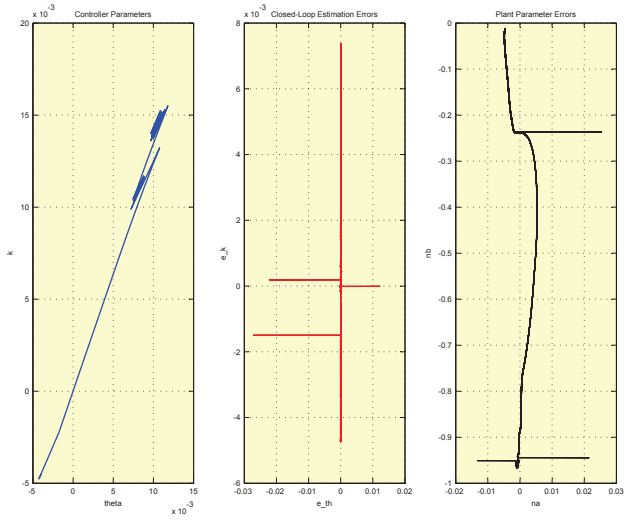

Figure B.51: Trajectories of closed-loop estimation errors, plant parameter errors and controller parameters presented in Figure B.50

Appendix C

Persistent Excitation

Persistent excitation term can be found in both system identification and adaptive control theory. It is a property characterizing signals used for producing parameter estimations and it is necessary for the effectiveness of the estimation mechanism.

In a system identification scheme, persistent excitation of the input signal of the system is a requirement for the convergence of the estimated plant parameters close to the values of the real plant parameters. In other words, how well and how fast plant parameters are estimated depends on two aspects

- The identification algorithm used and
- The information content (persistent excitation) of the input signal used

In a control scheme, persistent excitation of reference signal r and of system's output signal y is essential not only for the convergence of the estimated controller parameters but also for the robustness of the estimator. If the signals in the original design are not persistently exciting, parameters will not converge even in the absence of non-parametric uncertainties. In the presence of non-parametric uncertainties, the estimator may possibly become unstable even using persistently exciting signals. In this case, control designer may have to produce a more persistently exciting signal so as to obtain better parameter estimations. Therefore, it is clear that the Control Engineer should produce as much persistently exciting signals as allowed by the involved constraints so as to assure the best possible estimator performance.

Commonly used signals in parameter estimation are

- Square signal
- Sinusoidal signal
- Pseudo-Random Binary Sequence(PRBS)

- Chirp signal

To summarize, both in system identification and control design, the input signal used, except from being persistently exciting, should be designed with the appropriate frequency and amplitude level so as not to violate the linear operating range of the system or to excite system dynamics of higher order. Those are the requirements for the robust and satisfactory performance of the parameter estimation mechanism aiming to produce an approximate linear representation.

Bibliography

[1] K. Astrom and B. Wittenmark. *Adaptive Control*. Dover Publications, 1995.

[2] J. Perez Correa, F. Sepulveda, and M. Duarte. Adaptive control in a heating vessel: a comparative study. *International Journal of Adaptive Control and Signal Processing*, 1995.

[3] M. Duarte and K. Narendra. A new approach to model reference adaptive control. *International Journal of Adaptive Control and Signal Processing*, 1989.

[4] M. Duarte and R. Ponce. Discrete time combined model reference adaptive control. *International Journal of Adaptive Control and Signal Processing*, 1997.

[5] M. Duarte, F. Rojo, and R. Perez. Experimental evaluation of combined model reference adaptive controller in a ph regulation process. *International Journal of Adaptive Control and Signal Processing*, 2002.

[6] P. Hodgson. *Theoretical Model and Dynamic Simulation of Variable Fill Hydraulic Dynamometers*. PhD Thesis, University of Canterbury, 1991.

[7] P. Ioannou and J. Sun. *Robust Adaptive Control*. Prentice Hall, 1996.

[8] L. Ljung. *System Identification-Theory for the User(Second Edition)*. Prentice Hall, 1999.

[9] T. Passenbrunner, M. Sassano, H. Trogmann, L. del Re, M. Paulweber, M. Schmidt, and H. Kokal. Inverse torque control of hydrodynamic dyamometers for combustion engine test benches. *2011 American Control Conference. San Francisco, USA*, 1/7/2011.

[10] T. Passenbrunner, H. Trogmann, L. del Re, and H. Kokal. Speed control of hydrodynamic dyamometers for internal combustion engine test benches. *2012 American Control Conference. Montreal, Canada*, 29/6/2012.

[11] J. Raine and P. Hodgson. Computer simulation and test bed performance of a variable fill hydraulic dynamometer. *11th Australasian Fluid Mechanics Conference. University of Tasmania, Hobart, Australia*, 18/12/1992.

[12] S. Sastry and M. Bodson. *Adaptive control*. Prentice Hall, 1989.

[13] J-J Slotine and W. Li. *Applied Nonlinear Control*. Prentice Hall, 1991.

[14] M. Vetr, T. Passenbrunner, H. Trogmann, P. Ortner, H. Kokal, M. Schmidt, and M. Paulweber. Control oriented modeling of a water brake dynamometer. *2010 IEEE International Conference on Control Applications. Yokohama, Japan*, 8/10/2010.

[15] P. Wellstead. *Lectures on Signal Processing*. Control Systems Centre-UMIST, 1990.

[16] P. Wellstead and M. Zarrop. *Self-Tuning Systems*. John Wiley and Sons, 1991.

[17] T. Yu, R. Ortega, and R. Kelly. Adaptive control of a heat exchanger. *IEEE Control Systems Magazine*, 1987.